



National Library  
of Canada

Acquisitions and  
Bibliographic Services Branch

395 Wellington Street  
Ottawa, Ontario  
K1A 0N4

Bibliothèque nationale  
du Canada

Direction des acquisitions et  
des services bibliographiques

395, rue Wellington  
Ottawa (Ontario)  
K1A 0N4

*Your file* *Votre référence*

*Our file* *Notre référence*

## NOTICE

The quality of this microform is heavily dependent upon the quality of the original thesis submitted for microfilming. Every effort has been made to ensure the highest quality of reproduction possible.

If pages are missing, contact the university which granted the degree.

Some pages may have indistinct print especially if the original pages were typed with a poor typewriter ribbon or if the university sent us an inferior photocopy.

Reproduction in full or in part of this microform is governed by the Canadian Copyright Act, R.S.C. 1970, c. C-30, and subsequent amendments.

## AVIS

La qualité de cette microforme dépend grandement de la qualité de la thèse soumise au microfilmage. Nous avons tout fait pour assurer une qualité supérieure de reproduction.

S'il manque des pages, veuillez communiquer avec l'université qui a conféré le grade.

La qualité d'impression de certaines pages peut laisser à désirer, surtout si les pages originales ont été dactylographiées à l'aide d'un ruban usé ou si l'université nous a fait parvenir une photocopie de qualité inférieure.

La reproduction, même partielle, de cette microforme est soumise à la Loi canadienne sur le droit d'auteur, SRC 1970, c. C-30, et ses amendements subséquents.

TOPOCHEMICAL REACTIONS OF AMINES AND AMIDES  
WITH TITANIUM AND VANADIUM OXYCHLORIDES.

Irina Kargina



National Library  
of Canada

Acquisitions and  
Bibliographic Services Branch

395 Wellington Street  
Ottawa, Ontario  
K1A 0N4

Bibliothèque nationale  
du Canada

Direction des acquisitions et  
des services bibliographiques

395, rue Wellington  
Ottawa (Ontario)  
K1A 0N4

*Your file* *Voire référence*

*Our file* *Notre référence*

THE AUTHOR HAS GRANTED AN  
IRREVOCABLE NON-EXCLUSIVE  
LICENCE ALLOWING THE NATIONAL  
LIBRARY OF CANADA TO  
REPRODUCE, LOAN, DISTRIBUTE OR  
SELL COPIES OF HIS/HER THESIS BY  
ANY MEANS AND IN ANY FORM OR  
FORMAT, MAKING THIS THESIS  
AVAILABLE TO INTERESTED  
PERSONS.

L'AUTEUR A ACCORDE UNE LICENCE  
IRREVOCABLE ET NON EXCLUSIVE  
PERMETTANT A LA BIBLIOTHEQUE  
NATIONALE DU CANADA DE  
REPRODUIRE, PRETER, DISTRIBUER  
OU VENDRE DES COPIES DE SA  
THESE DE QUELQUE MANIERE ET  
SOUS QUELQUE FORME QUE CE SOIT  
POUR METTRE DES EXEMPLAIRES DE  
CETTE THESE A LA DISPOSITION DES  
PERSONNE INTERESSEES.

THE AUTHOR RETAINS OWNERSHIP  
OF THE COPYRIGHT IN HIS/HER  
THESIS. NEITHER THE THESIS NOR  
SUBSTANTIAL EXTRACTS FROM IT  
MAY BE PRINTED OR OTHERWISE  
REPRODUCED WITHOUT HIS/HER  
PERMISSION.

L'AUTEUR CONSERVE LA PROPRIETE  
DU DROIT D'AUTEUR QUI PROTEGE  
SA THESE. NI LA THESE NI DES  
EXTRAITS SUBSTANTIELS DE CELLE-  
CI NE DOIVENT ETRE IMPRIMES OU  
AUTREMENT REPRODUITS SANS SON  
AUTORISATION.

ISBN 0-612-04963-9

Canada



UNIVERSITÉ D'OTTAWA  
UNIVERSITY OF OTTAWA

## Abstract

The intercalation of primary, secondary, tertiary, and aromatic amines into layered TiOCl have been investigated by a variety of methods. The intercalation reaction does not appear to be a redox process. A key step for intercalation of amines into host TiOCl is proposed to be a coordination via nitrogen lone electron pair to  $Ti^{3+}$  metal centres.

Subsequent substitution of the interlayer chloride ions of TiOCl by the amine molecules is strongly dependent on the properties of the organic compounds and their ability to form ammonium salts. Based on X-ray diffraction, fluorescence, elemental analysis and thermal analysis, a model for the interaction of amines with TiOCl is proposed.

The intercalation of primary, secondary, and tertiary amides into TiOCl and VOCl have been studied. A redox intercalation process is ruled out by using variety of amides with a range of redox potentials. The proposed interaction of intercalated amides with the host is different from that of amines and may dominated by formation of hydrogen bonds between the amides protons and Cl ions of the host.

## **Acknowledgments**

I would like to thank my supervisor, Professor D. Richeson, for his help, advice, and support during the fulfillment of this research work.

I would also like to thank Professor S. Gambarotta and Professor C. Detellier for their fruitful suggestions throughout this work.

Also, I would like to thank my co-workers for their support.

## Table of Contents

<b>List of Tables</b>	IX
<b>List of Figures</b>	XII
<b>List of Abbreviations</b>	XV
<b>Introduction</b>	1
<b>Literature overview</b>	5
1. Graphite	5
2. Transition metal oxides	6
3. Transition metal dichalcogenides	8
4. Metal phosphorus trichalcogenides	13
5. Acid Salts of tetravalent metals	15
6. Clay minerals	17
7. Intercalation chemistry of Metal Oxychlorides	20
7.1 Structure and Synthesis of Metal Oxychlorides	20
7.1.1 Intercalation Chemistry of Metal Oxychlorides with the AlOCl structure	21
7.1.2 Metal Oxychlorides with the FeOCl structure	23
7.2 Topochemical Reactions of Metal Oxychlorides	26
7.2.1 Intercalation reactions	26
7.2.2 Topochemical substitution reactions	35
<b>Hypothesis</b>	39
<b>Experimental</b>	40
<b>Purification of starting materials</b>	40
<b>Instrumentation</b>	40
- Powder X-ray Diffraction	41

- Thermal Gravimetric Analysis	41
- FTIR Spectroscopy	41
- X-Ray Fluorescence	41
- Elemental analysis	42
<b>Reactions</b>	42
- Synthesis of TiOCl	42
- Synthesis of VOCl	42
- Reactions of TiOCl with pyridine	43
Reaction in a sealed tube at 250°C	43
Reaction in a Schlenk flask at 80°C	44
- Reactions of TiOCl with N,N,N',N'-tetramethylethylenediamine	44
Reaction at 100°C	44
Reaction at 170°C	45
- Reactions of TiOCl with N,N'-dimethylethylenediamine	45
Reaction in a sealed tube at 80°C	45
Reaction in a Schlenk flask at 80°C	45
Removal of $[\text{H}_2(\text{CH}_3)\text{NCH}_2\text{CH}_2\text{NH}_2(\text{CH}_3)]^{2+}\text{Cl}_2^-$ from the product	46
Synthesis of DMEN-salt	47
- Reactions of TiOCl with ethylenediamine	47
Reactions in a sealed tube at 160-170°C	47
Reaction in a Schlenk flask at 80°C for 5 days	48
Reaction in a Schlenk flask at 75°C for 9 hours	48
Reaction in a Schlenk flask at 75°C for 16 hours	48
Reaction in a Schlenk flask at 75°C for 4 days	49
Reaction in a Schlenk flask at 75°C for 7.5 days	49
Removal of $[\text{H}_3\text{NCH}_2\text{CH}_2\text{NH}_3]^{2+}\text{Cl}_2^-$ from the product	49

Synthesis of EN-salt	50
- Reaction of TiOCl with diethylenetriamine	50
- Reaction of TiOCl with N,N-dimethylacetamide	51
- Reaction of TiOCl with dimethylformamide	51
- Reaction of TiOCl with N-methylformamide	52
- Reaction of TiOCl with acetamide	52
- Reaction of VOCl with N,N-dimethylacetamide	53
- Reaction of VOCl with N-methylformamide	53
- Reaction of VOCl with acetamide	53
<b>Results and discussion</b>	54
<b>Preparation of starting materials</b>	54
- Synthesis of TiOCl	54
- Synthesis of VOCl	58
<b>Topochemical reactions of TiOCl and VOCl layered compounds</b>	63
- Reactions of TiOCl with amines	65
1. Reactions of TiOCl with N,N'-dimethylethylenediamine	66
1.1 Reaction in a sealed tube at 80°C	66
1.2 Reaction in a Schlenk flask at 80°C	70
1.3 DMEN-salt removal	80
1.4 Synthesis of DMEN-salt	88
2. Reactions of TiOCl with ethylenediamine	91
2.1 Reactions in a sealed tubes at 160-170°C	91
2.2 Reaction in a Schlenk flask at 80°C	91
2.3 Reaction in a Schlenk flask at 75°C for 9 hours	94
2.4 Reaction in a Schlenk flask at 75°C for 16 hours	98
2.5 Reaction in a Schlenk flask at 75°C for 4 days	98

2.6 Reaction in a Schlenk flask at 75°C for 7.5 days	101
2.7 Synthesis of EN-salt	116
3. Reaction of TiOCl with diethylenetriamine	120
4. Reactions of TiOCl with N,N,N',N'-tetramethylethylenediamine	124
5. Reactions of TiOCl with pyridine	127
5.1 Reaction in a sealed tube at 250°C	127
5.2 Reaction in a Schlenk flask at 80°C	131
- Proposed mechanism for topochemical reactions of TiOCl with amines	138
- Reactions of TiOCl and VOCl with amides	143
Reaction of TiOCl with N,N-dimethylacetamide	143
Reaction of TiOCl with dimethylformamide	146
Reaction of TiOCl with N-methylformamide	149
Reaction of TiOCl with acetamide	152
Reaction of VOCl with N,N-dimethylacetamide	156
Reaction of VOCl with N-methylformamide	158
Reaction of VOCl with acetamide	161
- Proposed mechanism for intercalation reactions of TiOCl and VOCl with amides	166
<b>Conclusions</b>	169
<b>References</b>	170

## List of Tables

<b>Table I</b>	Compounds with the Orthorhombic AlOCl structure	23
<b>Table II</b>	Unit - Cell parameters of selected compounds with the FeOCl structure	25
<b>Table III</b>	Metallocene Intercalates of MOCl	31
<b>Table IV</b>	Aromatic Amine Intercalates of FeOCl	33
<b>Table V</b>	Aromatic Amine Intercalates of VOCl	34
<b>Table VI</b>	Calculated and Experimental powder patterns for TiOCl	56
<b>Table VII</b>	Powder pattern of VOCl	61
<b>Table VIII</b>	Powder pattern of the product obtained during a sealed tube reaction of TiOCl with DMEN	68
<b>Table IX</b>	Powder pattern of the product obtained during a Schlenk flask reaction of TiOCl with DMEN	72
<b>Table X</b>	Powder pattern of the product obtained during a Schlenk flask reaction of TiOCl with DMEN and heated to 80°C for 4 days	76
<b>Table XI</b>	Powder pattern of the final product of the reaction of TiOCl with DMEN	82
<b>Table XII</b>	Summary of reactions of TiOCl with N,N'-dimethylethylenediamine	87
<b>Table XIII</b>	Powder pattern of $[H(H)(CH_3)NCH_2CH_2N(CH_3)(H)H]^{2+} + 2Cl^-$	90
<b>Table XIV</b>	EA results for $[H(H)(CH_3)N-CH_2-CH_2-N(CH_3)(H)H]^{2+} + 2Cl^-$	88
<b>Table XV</b>	Powder pattern of the product obtained during the reaction of TiOCl with EN in a Schlenk flask for 5 days at 80°C	93
<b>Table XVI</b>	Powder pattern of $TiOCl(C_2H_8N_2)_{0.4}$	96
<b>Table XVII</b>	EA results for $TiOCl(C_2H_8N_2)_{0.4}$	97
<b>Table XVIII</b>	Powder pattern of the product obtained from the reaction of TiOCl with EN in a Schlenk flask for 16 hours at 75°C	100
<b>Table XIX</b>	Powder pattern of the product obtained from the reaction of TiOCl with EN in a Schlenk flask at 75°C for 4 days	103

<b>Table XX</b>	Powder pattern of the product obtained from the reaction of TiOCl with EN at 75°C for 7.5 days	107
<b>Table XXI</b>	Powder pattern of $\text{TiOCl}_{0.5}(\text{C}_2\text{H}_7\text{N}_2)_{0.5}$	109
<b>Table XXII</b>	EA data for $\text{TiOCl}_{0.5}(\text{C}_2\text{H}_7\text{N}_2)_{0.5}$	109
<b>Table XXIII</b>	Summary of reactions of TiOCl with EN	114
<b>Table XXIV</b>	Powder pattern of EN-salt $[\text{H}_3\text{N}-\text{CH}_2-\text{CH}_2-\text{NH}_3]^{2+}2\text{Cl}^-$	118
<b>Table XXV</b>	EA data for $[\text{H}_3\text{N}-\text{CH}_2-\text{CH}_2-\text{NH}_3]^{2+}2\text{Cl}^-$	116
<b>Table XXVI</b>	Powder pattern of $\text{TiOCl}(\text{C}_4\text{H}_{13}\text{N}_3)_{0.15}$	122
<b>Table XXVII</b>	EA data for $\text{TiOCl}(\text{C}_4\text{H}_{13}\text{N}_3)_{0.15}$	123
<b>Table XXVIII</b>	Powder pattern of the product obtained during a sealed tube reaction of TiOCl with TMEDA	126
<b>Table XXIX</b>	Powder pattern of the grey product obtained from the sealed tube reaction of TiOCl with pyridine	129
<b>Table XXX</b>	EA data for $\text{TiOCl}(\text{py})_{0.2}$	132
<b>Table XXXI</b>	Powder pattern of the product obtained from the Schlenk flask reaction of TiOCl with pyridine	134
<b>Table XXXII</b>	EA data for $\text{TiOCl}(\text{py})_{0.38}$	132
<b>Table XXXIII</b>	Summary of reactions of TiOCl with pyridine	137
<b>Table XXXIV</b>	Powder pattern of the product obtained from the reaction of TiOCl with DMA	145
<b>Table XXXV</b>	Powder pattern of the product obtained from the reaction of TiOCl with DMF	148
<b>Table XXXVI</b>	Powder pattern of the product obtained from the reaction of TiOCl with NMF	151
<b>Table XXXVII</b>	EA results for $\text{TiOCl}(\text{HC}(\text{O})\text{N}(\text{H})\text{CH}_3)_{0.95}$	150

<b>Table XXXVIII</b>	Powder pattern of the product obtained from the reaction of TiOCl with acetamide	154
<b>Table XXXIX</b>	EA results for for TiOCl[(CH <sub>3</sub> )C(O)NH <sub>2</sub> ] <sub>0.03</sub>	153
<b>Table XL</b>	Summary of reactions of TiOCl with amides	155
<b>Table XLI</b>	Powder pattern of the product obtained from the reaction of VOCl with DMA	156
<b>Table XLII</b>	Powder pattern of the product of the reaction of VOCl and NMF	158
<b>Table XLIII</b>	EA data for VOCl(HC(O)N(CH <sub>3</sub> )H) <sub>1.0</sub>	160
<b>Table XLIV</b>	Powder pattern of the product obtained from the reaction of VOCl with acetamide	163
<b>Table XLV</b>	EA results for VOCl / (CH <sub>3</sub> C(O)NH <sub>2</sub> ) <sub>0.25</sub>	164
<b>Table XLVI</b>	Summary of reactions of VOCl with amides	165

## List of Figures

<b>Figure 1</b>	The MoO <sub>3</sub> structure	7
<b>Figure 2</b>	The WO <sub>3</sub> structure	7
<b>Figure 3</b>	The MX <sub>2</sub> structure	9
<b>Figure 4</b>	The Zr(PO <sub>4</sub> ) <sub>2</sub> H <sub>2</sub> •H <sub>2</sub> O Structure	16
<b>Figure 5</b>	Two layered and three layered variants of sheet silicates	18
<b>Figure 6</b>	The AlOCl structure	22
<b>Figure 7</b>	The TiOCl structure	24
<b>Figure 8</b>	Powder XRD spectrum of TiOCl	55
<b>Figure 9</b>	TGA curve of TiOCl	57
<b>Figure 10</b>	Powder XRD spectrum of VOCl	60
<b>Figure 11</b>	TGA of VOCl	62
<b>Figure 12</b>	PXRD spectrum of the product obtained during a sealed tube reaction of TiOCl with DMEN	67
<b>Figure 13</b>	TGA of the product obtained during a sealed tube reaction of TiOCl with DMEN	69
<b>Figure 14</b>	PXRD spectrum of the product obtained during a Schlenk flask reaction of TiOCl with DMEN	71
<b>Figure 15</b>	PXRD spectrum of the product obtained during a Schlenk flask reaction of TiOCl with DMEN and heated for 4 days at 80°C	75
<b>Figure 16</b>	TGA of the product obtained during a Schlenk flask reaction of TiOCl with DMEN and heated to 80°C for 4 days	79
<b>Figure 17</b>	PXRD of the final product of the reaction of TiOCl with DMEN	81
<b>Figure 18</b>	TGA of the final product of the reaction of TiOCl with DMEN	83
<b>Figure 19</b>	(a) An interlayer bridging model for TiOCl <sub>x</sub> (C <sub>4</sub> H <sub>11</sub> N <sub>2</sub> ) <sub>y</sub> (b) The intralayer bonding model for TiOCl <sub>x</sub> (C <sub>4</sub> H <sub>11</sub> N <sub>2</sub> ) <sub>y</sub>	85

	(c) Model structure of $\text{TiOCl}_x(\text{C}_4\text{H}_{11}\text{N}_2)_y$ represented by tilted guest molecules	
<b>Figure 20</b>	PXRD of the DMEN-salt $[\text{H}(\text{H})(\text{CH}_3)\text{N}-\text{CH}_2-\text{CH}_2-\text{N}(\text{CH}_3)(\text{H})\text{H}]^{2+}2\text{Cl}^-$	89
<b>Figure 21</b>	PXRD spectrum of the product obtained during the reaction of TiOCl with EN in a Schlenk flask for 5 days at 80°C	92
<b>Figure 22</b>	PXRD spectrum of $\text{TiOCl}(\text{C}_2\text{H}_8\text{N}_2)_{0.4}$	95
<b>Figure 23</b>	PXRD spectrum of the product obtained from the reaction of TiOCl with EN in a Schlenk flask at 75°C for 16 hours	99
<b>Figure 24</b>	PXRD spectrum of the product obtained from the reaction of TiOCl with EN in a Schlenk flask at 75°C for 4 days	102
<b>Figure 25</b>	PXRD spectrum of the product obtained from the reaction of TiOCl with EN at 75°C for 7.5 days	106
<b>Figure 26</b>	PXRD spectrum of $\text{TiOCl}_{0.5}(\text{C}_2\text{H}_7\text{N}_2)_{0.5}$	108
<b>Figure 27</b>	(a) Interlayer bridging model for $\text{TiOCl}_{0.5}(\text{C}_2\text{H}_7\text{N}_2)_{0.5}$ (b) Intralayer bonding model for $\text{TiOCl}_{0.5}(\text{C}_2\text{H}_7\text{N}_2)_{0.5}$ (c) Model structure of $\text{TiOCl}_{0.5}(\text{C}_2\text{H}_7\text{N}_2)_{0.5}$ represent hydrogen bonding (d) Model structure for $\text{TiOCl}_{0.5}(\text{C}_2\text{H}_7\text{N}_2)_{0.5}$ where EN molecules form a second layer	111 112
<b>Figure 28</b>	PXRD spectrum of EN-salt $[\text{NH}_3-\text{CH}_2-\text{CH}_2-\text{NH}_3]^{2+}2\text{Cl}^-$	117
<b>Figure 29</b>	PXRD spectrum of $\text{TiOCl}(\text{C}_4\text{H}_{13}\text{N}_3)_{0.15}$	121
<b>Figure 30</b>	PXRD spectrum of the product obtained during a sealed tube reaction of TiOCl with TMEDA	125
<b>Figure 31</b>	PXRD of the grey product obtained from the sealed tube reaction of TiOCl with pyridine	128
<b>Figure 32</b>	TGA of the grey product obtained from the sealed tube reaction of TiOCl with pyridine	130
<b>Figure 33</b>	PXRD of the product obtained from the Schlenk flask reaction of	

TiOCl with pyridine	133
<b>Figure 34</b> Structural model for pyridine intercalated compounds	136
<b>Figure 35</b> PXRD of the product obtained from the reaction of TiOCl with DMA	144
<b>Figure 36</b> PXRD of the product obtained from the reaction of TiOCl with DMF	147
<b>Figure 37</b> PXRD of the product obtained from the reaction of TiOCl with NMF	150
<b>Figure 38</b> PXRD of the product obtained from the reaction of TiOCl with acetamide	153
<b>Figure 39</b> PXRD of the product obtained from the reaction of VOCl with DMA	157
<b>Figure 40</b> PXRD spectrum of VOCl(NMF) <sub>1.0</sub>	159
<b>Figure 41</b> PXRD spectrum of the product obtained from the reaction of VOCl with acetamide	162
<b>Figure 42</b> (a) Interlayer bridging model for NMF intercalation into TiOCl and VOCl	167
(b) Structural model for acetamide intercalation into TiOCl and VOCl	

## List of Abbreviations

**Å** Angstrom

**AC** Acetamide

**DMEN** N,N'-dimethylethylenediamine

**DMA** N,N-dimethylacetamide

**DMF** N,N-dimethylformamide

**EA** Elemental Analysis

**EN** Ethylenediamine

**IR** Infrared Spectroscopy

**"3N"** Diethylenetriamine

**NMF** N-methylformamide

**PXRD** Powder X-Ray Diffraction

**py** Pyridine

**SCE** Saturated Calomel electrode

**TGA** Thermo Gravimetric analysis

**THF** Tetrahydrofuran

**TMEDA** N,N,N',N'-tetramethylethylenediamine

**XRF** X-Ray Fluorescence

## INTRODUCTION

The study of reactions between guest molecules or ions and solid host lattices has been an active research topic for more than 150 years. The first report concerning the intercalation of graphite by sulfate ions appeared in 1841 by Schaufautl. However, interest in intercalation chemistry began to grow significantly and to extend into many scientific disciplines only in the 1960s.

Since the sixties, the number of host lattices has been expanded significantly to now include investigations with natural aluminosilicates and layered synthetic materials.

Intercalation chemistry has become an increasingly interesting topic over the last 30 - 40 years. Areas of major interest have been the intercalation of ions and molecules into layered inorganic lattices with the ultimate goal of preparing materials for high-density energy storage devices (e.g.,  $\text{Li}_x\text{TS}_2$ ;  $\text{Li}_x\text{V}_3\text{O}_8$ ), heterogeneous catalysis (e.g.,  $\text{Co}_x\text{MoS}_2$ ;  $\text{Ni}_x\text{WS}_2$ ), and shape - selective adsorption/ catalysis.<sup>1</sup> Compounds prepared by intercalation reactions may also exhibit unusual physical properties such as enhanced electronic conductivity, fast ion conductivity, and even superconductivity.<sup>1</sup>

Traditional solid state synthesis requires high temperatures and long reaction times. One of the distinctive features of intercalation reactions is that they may take place under mild conditions and are, therefore, often called easy solid state reactions.

A variety of inorganic layered compounds are able to undergo intercalation reactions that involve the reversible insertion of guest species between two - dimensional layers of the

host. In the case of expandable layered compounds, the interlayer region of the host expands to accommodate the guest, and interlayer host - host interactions are replaced by host - guest and guest - guest interactions often leading to the preferred orientation of the guest species.

Previous research work has shown that organic molecules containing at least one functional group can be used as guest molecules. Typical representatives are amines, alcohols, organophosphonates, thia - compounds, and heterocyclic compounds. Also, some large organic molecules including metallocenes and their derivatives and molecules with a very long carbon chains ( $C_{20}$ ) can penetrate between the layers of the host lattice. Inorganic species such as ammonia, water, and some inorganic acids or their anions can play the role of a guest molecules as well.

From a thermodynamic standpoint a major consideration in the driving force for intercalation reactions is the interaction of the guest with the host lattice. It is possible to pick out several types of interaction between the guest molecules and the host lattice.<sup>2</sup>

1. Binding of the guest can be realized by the formation of a coordination bond to a lattice site. In this case the guest molecule will be an electron donor.
2. The formation of hydrogen bond between the oxygen atom of the oxo-anion of the host and the hydrogen atom of the guest species. Frequently only part of the molecules can be held by the hydrogen bond.
3. An electron transfer from the guest molecule to the host lattice can take place. This electron transfer leads to the oxidation of the guest and reduction of the host.

4. A proton transfer from the hydroxyl group of a layered material to the guest molecule. The result is a guest molecule that has become positively charged and the layers of the host now bear a negative charge.
5. Weak van der Waals forces between the layers of the host can trap the guest molecule inside layers.

A fundamental problem of all intercalation reactions is the effect of the host on the guest and the guest on the host. Which forces or mechanisms are involved into the intercalation process and keep the guest molecule inside of the host? How do the properties of the guest and of the host layered compound change? What is the orientation of the guest inside the host lattice? Is it possible to effect on the rate of the intercalation process? All these questions are the central questions of intercalation chemistry.

Different layered materials can be used as a host lattices. The most thoroughly investigated layered materials for intercalation reactions are:

- Graphite
- Transition metal oxides
- Transition metal dichalcogenides
- Metal phosphorus trichalcogenides
- Acid salts of tetravalent metals
- Clay minerals
- Metal oxyhalides

The present research work is devoted to study of topochemical reactions of layered metal oxychlorides  $TiOCl$  and  $VOCl$ .

In the following section, an overview of related literature is presented. This overview consists of a brief description of different classes of layered compounds that may undergo intercalation reactions and more detailed description of synthesis, properties, and structures of metal oxyhalides and their chemical reactivity in terms of ability to undergo topochemical reactions.

## LITERATURE OVERVIEW.

There are several classes of layered materials that can be used as host lattices for topotactic chemical reactions.

### 1. Graphite

Graphite is unique in its ability to intercalate both electron donors and acceptors. Intercalation with reduction of the graphite layers can occur with alkali metals.<sup>3a</sup> Alkali metal intercalates can be divided into two classes. The heavier metals such as K, Rb and Cs react easily with graphite at 200<sup>0</sup>C or less. Lithium reacts only at higher temperatures or pressures. The sodium compound is difficult to make directly and is poorly characterised. The distinction between the two groups ( K, Rb, Cs and Li, Na ) has generated speculation that the ionization potentials of the gaseous atoms provide the basis for distinction between the two classes. The ionization potentials (in eV) of K (4.34), Rb (4.18), and Cs (3.89) lie below the electron affinity of graphite (4.6), whereas those of Li (5.39) and Na (5.14) lie above this value.

The first ionization energies of alkaline earth metals ( Ca, Ba, Sr ) and lanthanides ( Eu, Yb, Sm, Tm ) lie above the electron affinity of graphite. Therefore the conditions of synthesis of the alkaline earth and lanthanide intercalates parallel the conditions for Li - intercalation (several weeks at 500 - 600<sup>0</sup>C).

Graphite forms compounds with electron acceptors such as bromine and Lewis acid molecules. Many metal fluorides, such as  $\text{TiF}_4$ ,  $\text{SbF}_5$ ,  $\text{UF}_6$  and  $\text{XeF}_6$  can be easily incorporated into the graphite structure.<sup>3a</sup>

## 2. Transition metal oxides.

A number of metal oxides with layered structures exist (e.g.,  $\text{V}_2\text{O}_5$ ,  $\text{MoO}_3$ ,  $\text{WO}_3$ ). These materials fall into two classes: those with layered host lattices and those formed from oxides containing tunnel networks. The first class is represented by  $\text{MoO}_3$  and  $\text{V}_2\text{O}_5$ , in which the interlayer spacing can be increased to accommodate a guest species (Figure 1). An example of another class is  $\text{WO}_3$ , which has an interpenetrating three - dimensional network of tunnels (Figure 2). In this case there is a limit to the size of the insertion atom that can be incorporated without breaking bonds in the host oxide matrix, and only guests with a small atomic radius, such as H and Li, have been inserted.

Intercalation of transition metal oxides is of broad interest in the synthesis of new materials. It is known that  $\text{MoO}_3$  is an important component of many industrial catalysts, but molybdena - based systems suffer from the disadvantage of a very low surface area. Intercalation of layered  $\text{MoO}_3$  may lead to a new materials with catalytic properties and with high surface area.<sup>4</sup> Pillared crystals of  $\text{MoO}_3$  may combine the catalytic and conducting properties that can lead to a new type of sensors.<sup>4</sup>

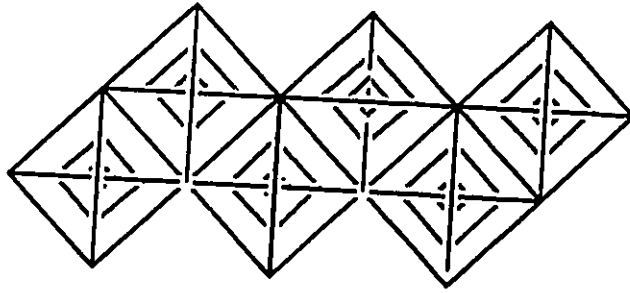


Figure 1 The MoO<sub>3</sub> structure.

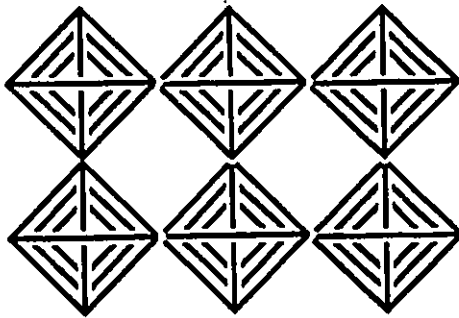


Figure 2 The WO<sub>3</sub> structure.

Several different polyoxycations have been introduced as pillaring agents into highly crystalline  $\text{MoO}_3$ . The most widely used has been  $[\text{AlO}_4\text{Al}_{12}(\text{OH})_{24}(\text{H}_2\text{O})_{12}]^{7+}$ . Lerf, Lalik and co-workers reported successful insertion of  $[\text{AlO}_4\text{Al}_{12}(\text{OH})_{24}(\text{H}_2\text{O})_{12}]^{7+}$  and  $[\text{Bi}_6(\text{OH})_{12}]^{6+}$  into layered  $\text{MoO}_3$  by ion exchange with sodium forms of hydrated layered compounds.<sup>4</sup> The insertion of a gallium analogue  $[\text{GaO}_4\text{Ga}_{12}(\text{OH})_{24}(\text{H}_2\text{O})_{12}]^{7+}$ , and a mixed  $[\text{GaO}_4\text{Al}_{12}(\text{OH})_{24}(\text{H}_2\text{O})_{12}]^{7+}$  polyoxycation were reported in 1991.<sup>5,6</sup>

Intercalation of electroactive polymers poly(pyrrole), poly(aniline) and poly(thiophene) has been achieved in layered  $\text{V}_2\text{O}_5$  and  $\text{MoO}_3$ .<sup>7</sup> Poly(ethylene oxide)(PEO) has been intercalated into  $\text{V}_2\text{O}_5$ <sup>8</sup> and the product material has a promising application as cathodes for high - energy batteries.

### 3. Transition metal dichalcogenides

Layered metal chalcogenides of the type  $\text{MX}_2$  ( M = metal, X = S, Se, Te ) are found for transition elements of group IVb ( Ti, Zr, Hf ), Vb ( V, Nb, Ta ), VIb ( Mo, W ), VIIb ( Tc, Re ), and VIIIb ( Pt ) and for the main group elements Sn and Pb.

The  $\text{MX}_2$  layers consist of two anion sheets with a sheet of metal atoms in the central plane. There is strong ( partially covalent) bonding between the interlayer atoms M and X. Two varieties of coordination of the metal between the anions are known (octahedral or trigonal prismatic) (Figure 3).<sup>3b</sup>

The electronic properties of these materials range from semiconducting to metallic behavior depending on the metal, the chalcogen, the coordination of the metal to the

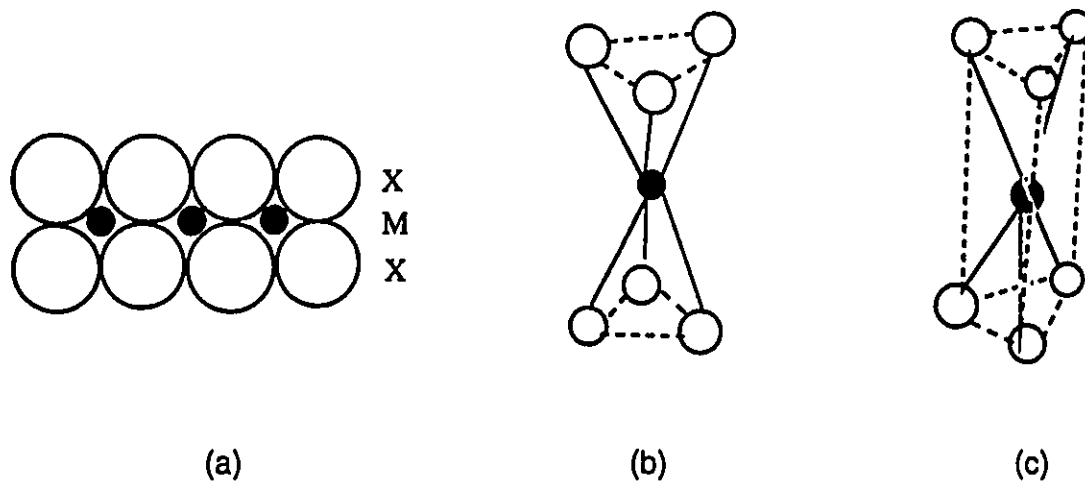


**Figure 3** The  $MX_2$  structure.

- (a) Single layer;
- (b) Octahedral coordination;
- (c) Trigonal prismatic coordination of M.

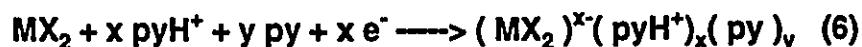
chalcogen atoms, and on the mode of stacking of the  $\text{MX}_2$  layers. Transition - metal dichalcogenides have been extensively investigated for their interesting electrical properties and their application as cathode materials for rechargeable high - energy - density lithium batteries.<sup>9</sup>

In 1965 Rudorff first observed alkali metal intercalation into dichalcogenides and proposed an ionic structure model.<sup>13,14</sup> Compounds with Lewis base molecules were prepared originally by Weiss and Ruthardt.<sup>13</sup> Recent investigations of the mechanism of direct Lewis base intercalation established that these reactions are correlated with redox process. Such intercalation reactions are usually accompanied by oxidation of the guest species coupled with electron transfer to the host.<sup>15</sup> This concept is supported by studies on the mechanism of intercalation of  $\text{NH}_3$ .<sup>16</sup> An investigation on the mechanism of  $\text{NH}_3$  intercalation into  $\text{TaS}_2$  demonstrated this reaction involves the oxidation of the guest molecules with formation of  $\text{N}_2$ . The electrons are transferred to the  $\text{TaS}_2$  layers, while the protons are accepted by  $\text{NH}_3$  molecules.



It was shown<sup>19</sup> that in the case of pyridine intercalation in  $\text{NbS}_2$ ,  $\text{TaS}_2$ , etc., the orientation of pyridine molecules in their van der Waals gap prohibits any direct interaction

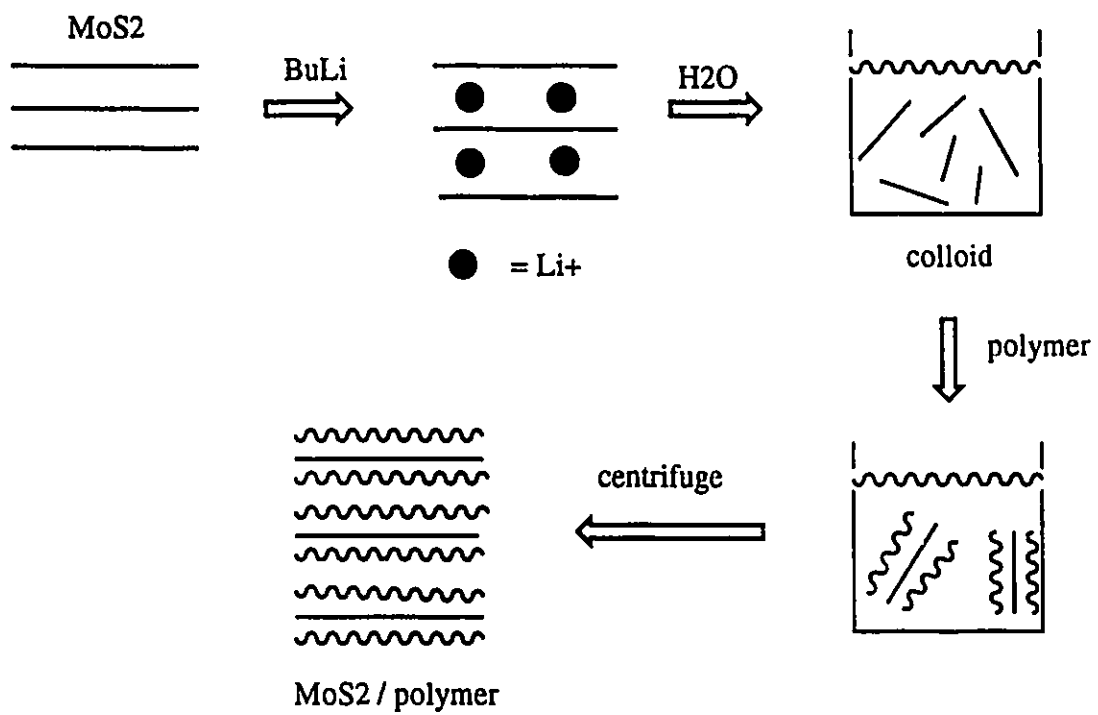
between the nitrogen lone pair and the host lattice. The mechanism of pyridine (py) intercalation into  $\text{MX}_2$  can be described by the Schöllhorn model.<sup>20</sup> The key step in this model is the condensation of two pyridine molecules to give 4,4'-bipyridyl with the loss of two protons and two electrons. These two electrons are transferred to the host lattice. The condensation reaction provides the source of protons for the formation of pyridinium ions ( $\text{pyH}^+$ ) (equations 4,5,6).



The stability of the intercalated compounds in this model is provided by the electrostatic interaction between the negatively charged lattice and pyridinium ions. The pyridinium ions in this model are solvated by neutral pyridine.

The intercalation of organometallic species into layered compounds was first demonstrated for transition metal dichalcogenides by Dines in 1975 and appeared to be redox process.<sup>51</sup>

The intercalation of conjugated and saturated polymers in layered transition metal dichalcogenides is of interest because resulting organic / inorganic structures can possess new electrical, structural, and mechanical properties.<sup>10</sup> Incorporation of polyethers<sup>11</sup>, polyaniline<sup>10</sup>, and polystyrene<sup>12</sup> into layered  $\text{MoS}_2$  has been achieved recently by different



**Scheme 1** Preparative route to MoS<sub>2</sub> / polymer material.

research groups. It was observed that intercalation into  $\text{MoS}_2$  is possible only with strong reducing agents such as alkali metals. Reaction of  $\text{Li}_x\text{MoS}_2$  with water produces single layers of  $\text{MoS}_2$ . These single layers adsorb a polymer forming a layered nano-composite material containing well-ordered alternating monolayers of polymer and  $\text{MoS}_2$ .<sup>10,11</sup> (Scheme 1).

#### 4. Metal phosphorus trichalcogenides

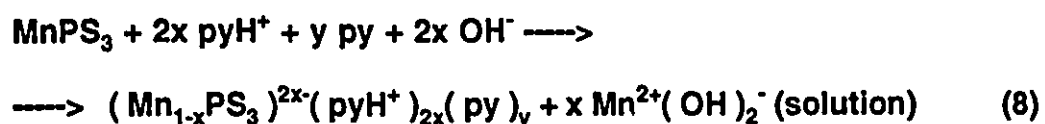
Metal phosphorus trichalcogenides of the formula  $\text{M}^{\text{II}}\text{PX}_3$ , where M stands for a metal in the  $\text{II}^+$  oxidation state ( $\text{M} = \text{Cd}, \text{Ni}, \text{Zn}, \text{Mn}, \text{Fe}, \text{Mg}, \text{Ca}, \text{V}, \text{Co}, \text{Pd}, \text{In}, \text{Sn}, \text{Pb}, \text{Hg}$ ) and X is S or Se, form a family of layered materials, structurally similar to the layered dichalcogenides. These solids are best described as two-dimensional arrays of  $\text{M}^{2+}$  ions assembled by  $\text{P}_2\text{S}_6^{4-}$  bridging ligands.

Several  $\text{MPS}_3$  compounds display a unique reactivity, as they take up cations from a solution and discharge interlamellar  $\text{M}^{2+}$  cations into the solution.<sup>18</sup> These results imply that the M-S bonds are quite labile.<sup>17</sup>

The intercalation chemistry of the metal phosphorus trichalcogenides can be divided into three classes according to the nature of the guest molecule. The first reported intercalation reactions were the reactions with organic amines, followed by a great deal of work on alkali metal intercalates. More recently, organometallic intercalation have been investigated.

Very interesting results have been achieved with  $\text{MPS}_3$ , using the Lewis base pyridine as a guest species. Much of this work was performed before the Schöllhorn model mechanism of pyridine intercalation into transition metal dichalcogenides was described. An extension of the Schöllhorn model to the  $\text{MPS}_3$  compounds would require the transition metals to be reduced from their stable  $\text{II}^+$  state. Alternatively, intercalation may proceed by reduction of a site other than the metal, e.g., either the P - P or P - S linkages, or it may proceed by a totally different mechanism.

Joy and Vasudevah<sup>19</sup> have shown in the case of  $\text{MnPS}_3$ ,  $\text{FePS}_3$  and  $\text{NiPS}_3$  materials that the intercalated species were, indeed, pyridinium ions solvated by neutral pyridine molecules, and intercalation mechanism is not an electron transfer to the host lattice but a novel ion - exchange/ intercalation process in which charge neutrality is maintained by a loss of  $\text{M}^{2+}$  ions. The proton originates from trace amounts of water present in the starting pyridine and it is unlikely to be from bipyridyl formation. This was confirmed by the observation that intercalation of rigorously dried pyridine was extremely difficult. The reaction scheme can be described by equations 7 and 8:

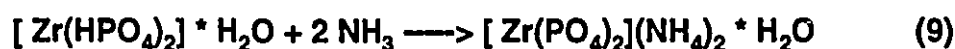


A similar intercalation mechanism was observed for intercalation of organometallic cations.<sup>19,21</sup> and alkali metal cations<sup>21</sup> into  $\text{MPS}_3$  materials. The most direct method for

organometallic cation intercalation is through ion - exchange with previously intercalated alkali metals and ammonium cations.<sup>21</sup>

### 5. Acid Salts of Tetravalent Metals

These compounds, whose structures are schematically represented in Figure 4, have the general formula  $M^{IV}(HXO_4)_2 \cdot nH_2O$ , where  $M = Zr, Ti, Sn$  and  $X = P, As$ . Owing to the presence of  $\equiv P - OH$  acidic groups between the layers, strong interactions are especially obtained with polar guest molecules that are Brønsted bases. In the case of  $[Zr(PO_4)_2] \cdot H_2O$ , it has been found that one molecule of  $NH_3$  for each  $\equiv P - OH$  group is taken up, even from very dilute aqueous solutions of ammonia.<sup>22</sup> This intercalation into  $[Zr(PO_4)_2] \cdot H_2O$  occurs via protonation of  $NH_3$  and formation of the diammonium form, according to equation 9.



The uptake of  $NH_3$  by zirconium phosphate was successfully employed in kidney machines for the removal of  $NH_3$  and  $NH_4^+$  from human blood after previous catalytic decomposition of the urea to  $NH_3$  and  $CO_2$ .<sup>22</sup>

The intercalation of n - alkylamines in  $M^{IV}(PO_4)_2 \cdot H_2O$  can be represented by the equation 10<sup>23</sup>:

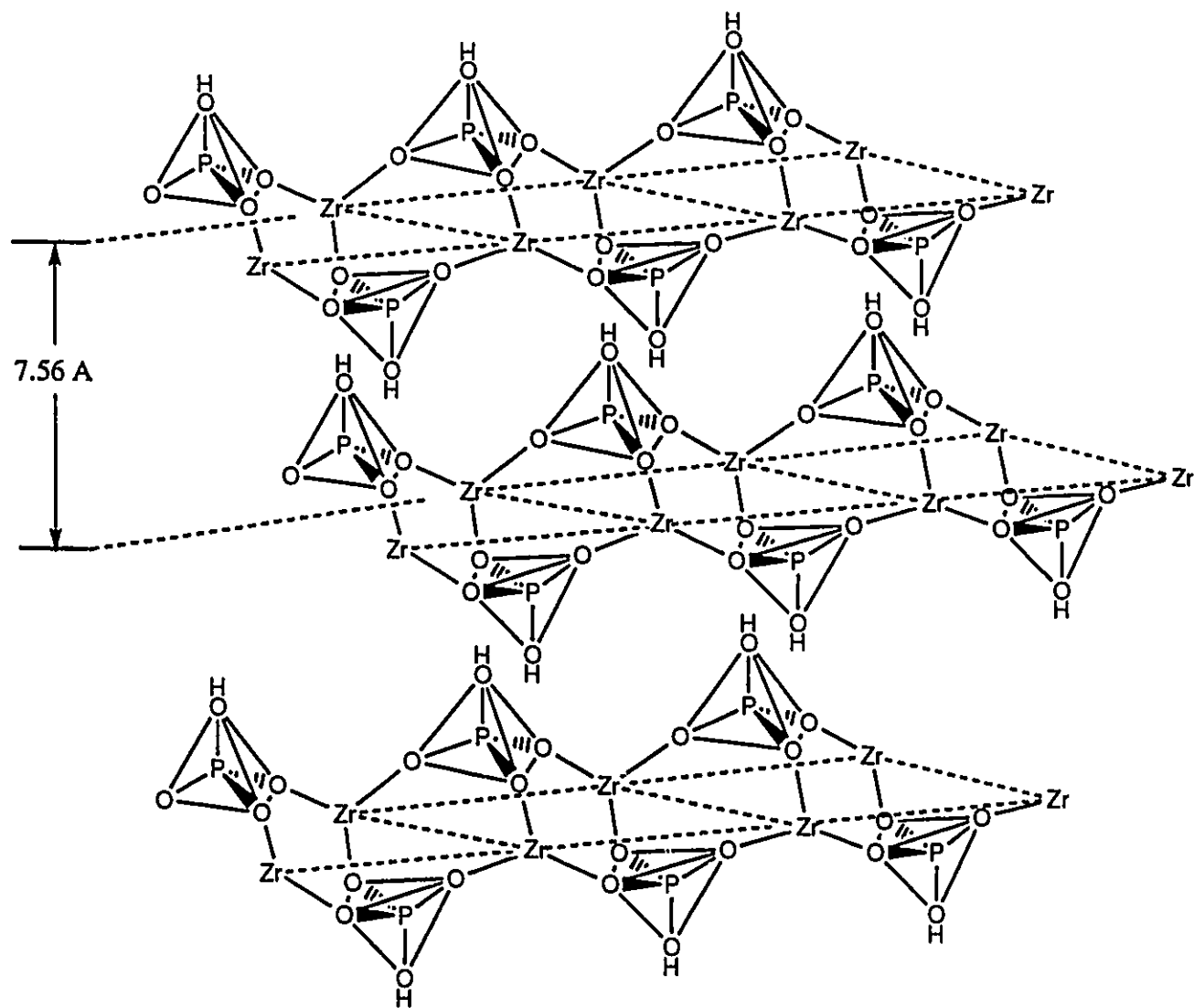
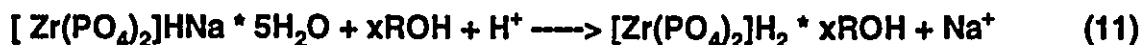


Figure 4 The  $[Zr(PO_4)_2] \cdot H_2O$  structure.



The topotactic acid - base reaction between the layered acid and basic guest affects all acid groups of the solid material.

Alcohols are much weaker proton acceptors than are amines, and the strength of their interactions with the acid  $\equiv \text{P} - \text{OH}$  groups of layered acid salts is also expected to be weaker. Due to this fact, alcohol intercalates are not obtained. Intercalation of alcohols has been achieved, however, by using salt forms of zirconium phosphate, e.g.,  $[\text{Zr}(\text{PO}_4)_2]\text{HNa} \cdot 5\text{H}_2\text{O}$ .<sup>22</sup> The salt form is contacted with pure alcohols previously acidified with a strong mineral acid, so that the metal ions are exchanged and the reaction can be described by the following equation:



The intercalation of glycols may also be easily achieved by such a procedure.

## 6. Clay minerals

Clay materials are a class of naturally occurring sheet silicates that are well known to form intercalates with guest organic molecules.

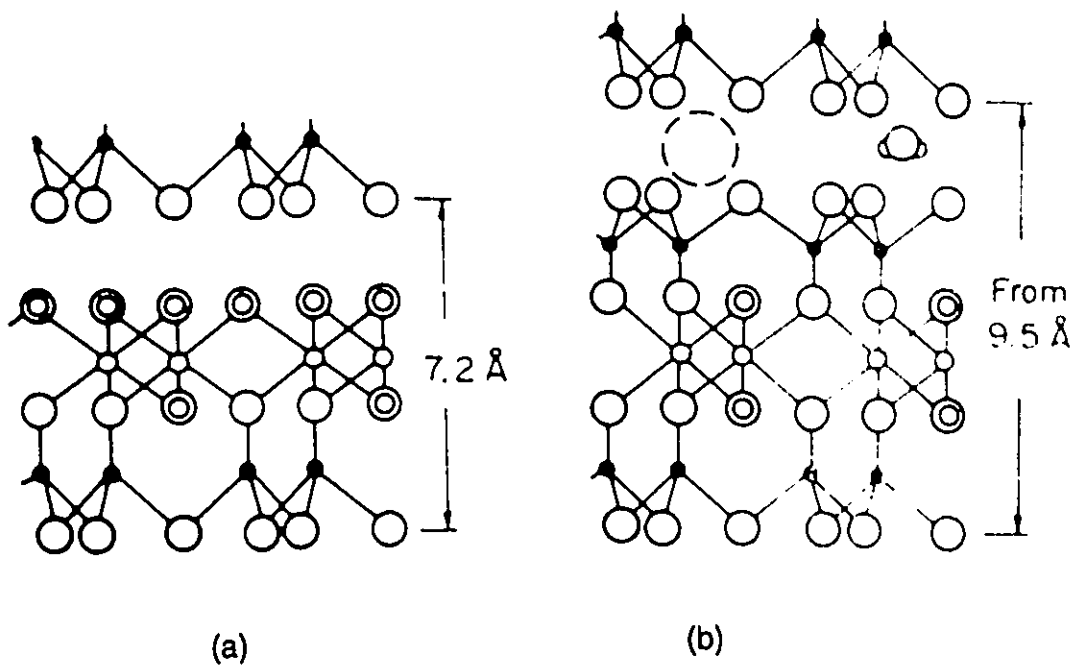
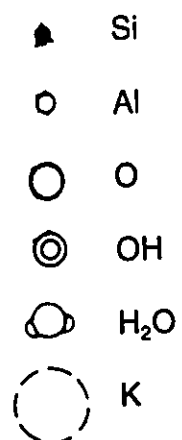


**Figure 5** Two - layered (a) and three - layered (b) variants of sheet silicates.



There are two main structural types of sheet silicates ( Figure 5):

- two - layered sheets ( kaolinite and dickite )
- three - layered sheets ( smectites, vermiculites and micas )

A clay sheets can be made up of two or three layers which are linked together. The first is a layer of corner - linked tetrahedra, and the second is a layer of edge - linked octahedra. The tetrahedral layer is composed of  $\text{Si}^{4+}$  cations in tetrahedral coordination with oxygen. The octahedral layer consists of two planes of closest - packed oxygen or hydroxyl ions with  $\text{Al}^{3+}$  or  $\text{Mg}^{2+}$  cations occupying the resulting octahedral sites between the two planes.

All of the kaolin minerals are made up of nearly identical  $7.2\text{\AA}$  sheets of composition  $\text{Al}_2\text{Si}_2\text{O}_5(\text{OH})_4$  and can be intercalated ( directly or indirectly ) by different organic compounds. The direct intercalation involves the direct reaction of the mineral with the organic compound. The compounds that can be directly intercalated into clay minerals have certain common properties such as high dipole moments and a tendency to form strong hydrogen bonding. Direct organokaolinite intercalates were obtained with  $\text{DMSO}^{24,25}$  ,  $\text{NMF}^{25}$  , formamide<sup>25,26</sup> , potassium acetate<sup>27</sup>, ammonium acetate, and hydrazine.<sup>28</sup> Organokaolinite intercalation compounds may be formed indirectly by the replacement of a previously intercalated molecule with another molecule. A wide range of alkali, alkaline halides, and amino acids have been intercalated into clay minerals by using either hydrazine or ammonium acetate as an agent to first open up the layers, followed by its displacement with the desired compound<sup>28</sup>.

## 7. Intercalation chemistry of Metal Oxyhalides

Metal chalcogenohalides are known for all of the group IIIA ( Al, Ga, In, Tl ) and IIIB ( Sc, Y, La, Ac ) metals, for the first row transition metals up to and including iron ( Ti, V, Cr and Fe ), for antimony and bismuth, and for nearly all the lanthanides and actinides.

Nearly 250 metal chalcogenohalides of formula  $MXY$  are known, where  $M$  = metal,  $X = O, S, Se$  and  $Y = Cl, Br, I$ . Despite this wide range of existence, only a small number of metal chalcogenohalides have been reported to undergo topochemical reactions. Among the whole class of  $MXY$  only the oxyhalides with  $M = Ti, V, Cr, Fe$  and  $Al$  and the thio- and selenohalides with  $M = Al$  are known to act as a hosts for this kind of reaction.

### **7.1. Structure and synthesis of Metal Oxyhalides**

Layered metal oxyhalides can be broken down into four structural types based on the radius ratio of  $M^{3+}$  to  $O^{2-}$ .<sup>29</sup>

- The smallest metal ions (  $R_{M^{3+}} / R_{O^{2-}}$  between 0.35 and 0.44 ) give the  $AlOCl$  structure, in which the  $M^{3+}$  ion is four - coordinate.
- Metal ions of intermediate size (  $R_{M^{3+}} / R_{O^{2-}}$  between 0.46 and 0.58 ) give the  $FeOCl$  structure, in which the  $M^{3+}$  ion is six - coordinate.
- Slightly larger metal ions (  $R_{M^{3+}} / R_{O^{2-}}$  between 0.66 and 0.69 ) give the  $SmSI$  structure, in which the  $M^{3+}$  ion is seven - coordinate.

- The largest metal ions (  $R_{M^{3+}} / R_{O^{2-}}$  between 0.69 and 0.86 ) give the PbFCI structure, in which the  $M^{3+}$  ion is nine - coordinate.

Topochemical reactions are known only for materials with the AlOCl and FeOCl structures, none has been reported for compounds in the PbFCI or SmSI structural class.<sup>29</sup>

### 7.1.1. Intercalation chemistry of Metal Oxyhalides with the AlOCl structure

There are four known members of this group : AlOX with X = Cl, Br or I, and GaOCl. None of these compounds has been obtained in the form of single crystals suitable for X-ray diffraction. All conclusions about structure and lattice parameters were done on the basis of X-ray powder studies.<sup>30a,b</sup> Analysis of X-ray powder diffraction spectra allowed the conclusion that these compounds have an orthorhombic structure, the space group is  $Pca2_1$ , with four MOCl per unit cell. Each metal ion is tetrahedrally coordinated to three  $O^{2-}$  ions and one  $Cl^-$  ion (Figure 6). The  $O^{2-}$  of the tetrahedra are linked together to form layers perpendicular to the b axis. The  $Cl^-$  vertices are perpendicular to the Al-O-Al network bonding to the Al center along the c direction. The unit - cell parameters of the orthorhombic AlOCl structure are listed in Table I.

Schafer and co - workers were the first to investigate synthetic routes to this class of compounds.<sup>31a,b</sup> AlOCl was prepared using a sealed - tube reaction of  $AlCl_3$  with a wide variety of metal oxides. The best result was obtained in the sealed tube reaction of

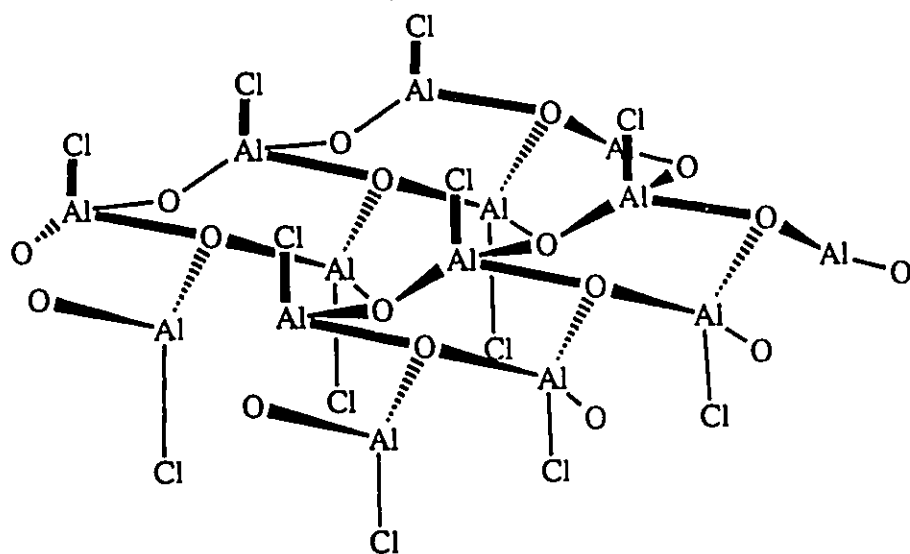


Figure 6 The AlOCl structure.

excess  $\text{AlCl}_3$  with  $\text{As}_2\text{O}_3$  at  $250^\circ\text{C}$ .  $\text{AsCl}_3$  and unreacted  $\text{AlCl}_3$  can be separated from the colorless, microcrystalline product by sublimation or by washing with the proper organic solvents.  $\text{AlOBr}$ ,  $\text{AlOI}$  and  $\text{GaOCl}$  have been prepared by similar methods.<sup>30a,32,33,34</sup>

**Table I**

Compounds with the Orthorhombic  $\text{AlOCl}$  structure

Compound	a(Å)	b(Å)	c(Å)	References
$\text{AlOCl}$	5.50	8.24	4.92	30a
$\text{AlOBr}$	6.73	10.02	4.92	30a
$\text{AlOI}$	6.86	11.03	4.92	30a
$\text{GaOCl}$	5.65	8.33	5.08	30b

### 7.1.2. Metal Oxyhalides with the $\text{FeOCl}$ structure

This structural class of compounds consists of  $\text{MOCl}$  and  $\text{MOBr}$  ( $\text{M} = \text{Ti}, \text{V}, \text{Cr}, \text{Fe}$  and  $\text{In}$ ), and  $\text{InOI}$ .

Goldsztaub first determined the structure of  $\text{FeOCl}$ , the parent structure of this class of compounds, in 1934.<sup>35</sup>  $\text{FeOCl}$  crystallizes in the orthorhombic space group  $\text{Pmmn}$  (Figure 7). Each metal is coordinated to four  $\text{O}^{2-}$  and two  $\text{Cl}^-$  ions. All chlorides are bridging with the  $\text{Cl}^-$  vertices perpendicular to the  $\text{M-O-M}$  bonding of the layers. The unit -

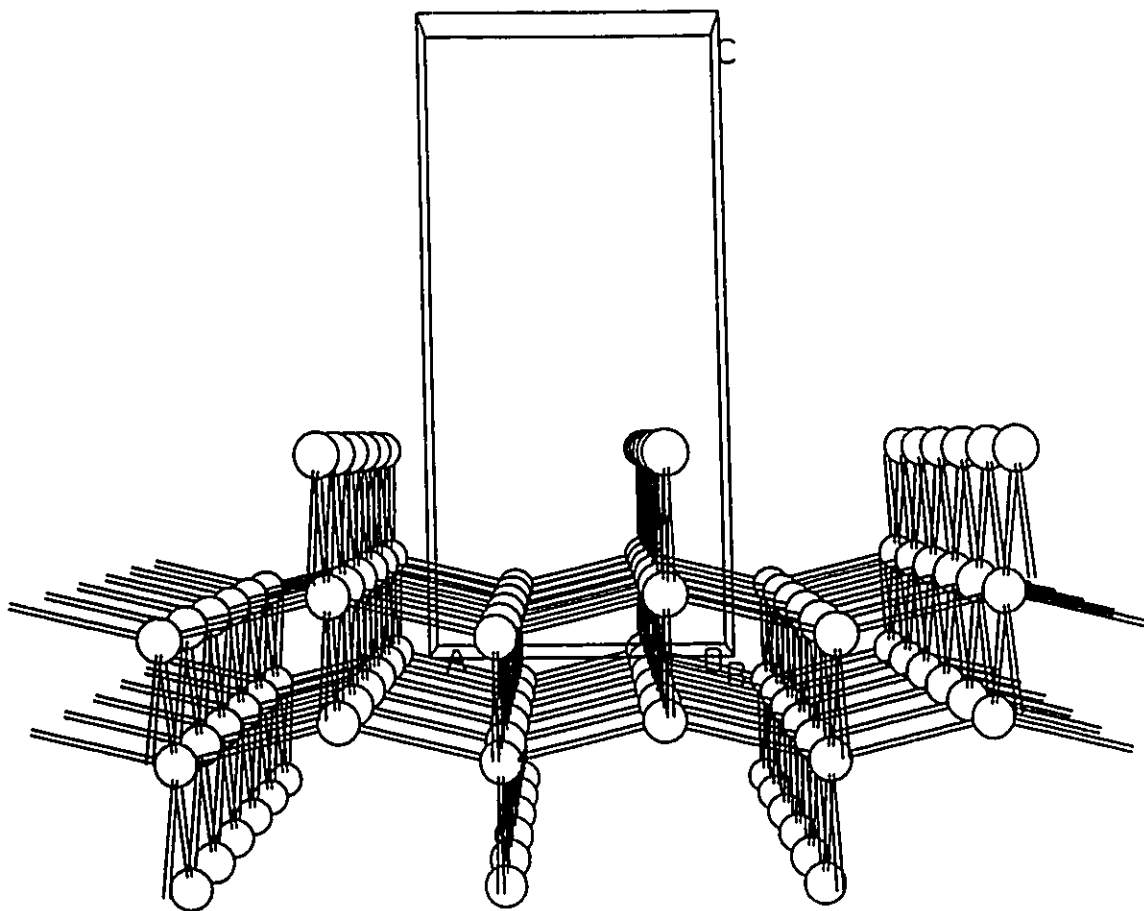


**Figure 7** One layer of the TiOCl structure

cell parameters of selected compounds with the FeOCl structure are listed in Table II.

**Table II**

Unit - Cell parameters of selected compounds with the FeOCl structure

Compound	a(Å)	b(Å)	c(Å)	References
TiOCl	3.79	8.03	3.38	38
VOCl	3.77	7.93	3.29	37
FeOCl	3.78	7.92	3.3	36

Methods of TiOCl synthesis have been reported by Schafer et al.<sup>38</sup> in 1958 and include the high - temperature sealed - tube reaction of TiCl<sub>3</sub> and TiO<sub>2</sub>. The best procedure appears to be the sealed - tube reaction of excess TiCl<sub>3</sub> with TiO<sub>2</sub> in a temperature gradient 650° - 550°C. The product is a reflective yellow - brown crystalline solid which is stable in moist air but converts slowly to TiO<sub>2</sub> in boiling H<sub>2</sub>O. In an N<sub>2</sub> steam, TiOCl decomposes to TiCl<sub>3</sub> and Ti<sub>2</sub>O<sub>3</sub> above 700°C.

The only reported synthesis of TiOBr involves the sealed - tube reaction of Ti, TiO<sub>2</sub> and Br<sub>2</sub> in a temperature gradient 650° - 550°C.<sup>39</sup> The product is a reflective, red - brown flat needles.

Many synthetic approaches have been reported for the synthesis of VOCl. The best synthetic pathway involves the sealed - tube reaction of excess VCl<sub>3</sub> with V<sub>2</sub>O<sub>3</sub> in a

temperature gradient  $720^{\circ} - 620^{\circ}\text{C}$ .<sup>40</sup>  $\text{VOCl}$  is red - brown flat crystals which are stable in air.

The synthesis of  $\text{VOBr}$  employed sealed tube reactions of excess  $\text{VBr}_3$  with several oxides have been carried out.<sup>41</sup> The best result came from the reaction with  $\text{As}_2\text{O}_3$  at  $400^{\circ}\text{C}$ . The product is obtained as a small violet crystals.

Several synthetic procedures to yield  $\text{FeOCl}$  are known. The most commonly employed method involves the sealed - tube reaction of  $\text{FeCl}_3$  and  $\text{Fe}_2\text{O}_3$  at  $370^{\circ}\text{C}$ .<sup>42</sup>  $\text{FeOCl}$  is obtained as shiny dark violet crystals.

## **7.2. Topochemical reactions of Metal Oxychlorides**

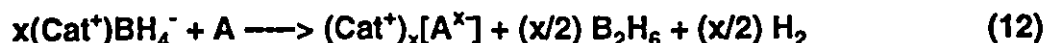
It is well known from the literature that metal oxychlorides can undergo topochemical reactions. These reactions can be divided into two general types: intercalation reactions and topochemical substitution reactions.

### **7.2.1. Intercalation reactions**

Intercalation reactions fall into five broad categories:

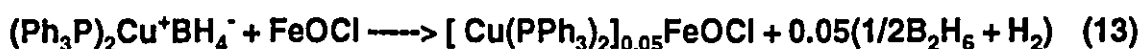
- A. Intercalation of cationic molecules using tetrahydroborate reagents and  $n\text{BuLi}$
- B. Intercalation of organosulphorus compounds
- C. Intercalation of conducting polymers
- D. Organometallic intercalation
- E. Intercalation of amines

A variety of cationic molecules can be intercalated into FeOCl matrix using tetrahydroborate reagents (equation 12).



In this reaction, the  $\text{BH}_4^-$  anion acts as the reducing agent, and cation intercalation occurs with generation of two gases -  $\text{B}_2\text{H}_6$  and  $\text{H}_2$ .<sup>43</sup> Results concerning intercalation of different cationic guests using this  $\text{BH}_4^-$  method were reported only for FeOCl.

FeOCl is a very susceptible matrix for different cationic guests intercalation. Alkali metal ions (e.g.  $\text{Li}^+$ ,  $\text{K}^+$ ,  $\text{Na}^+$ ) can be incorporated into FeOCl very rapidly, even within two hours at room temperature ( $25^\circ\text{C}$ ).<sup>43</sup> The ease with which the FeOCl lattice can be intercalated is also demonstrated by the introduction of the large cationic transition - metal complex  $(\text{Ph}_3\text{P})_2\text{Cu}^+$  by this remarkable reaction<sup>43</sup> (equation 13).



Intercalation of lithium cations guests into layered MOCl can also be achieved both chemically and electrochemically giving  $\text{Li}_x\text{MOCl}$  product.<sup>44</sup> Chemical and electrochemical intercalation of lithium was performed for FeOCl, VOCl and CrOCl host lattices ( nothing was reported for TiOCl). In all these cases lithium intercalation corresponds to the reduction of  $\text{M}^{3+}$  to  $\text{M}^{2+}$ . It is very interesting to note that lithium can be washed out of  $\text{Li}_x\text{FeOCl}$  with water to yield the original structure. This reaction gives convincing evidence

of the stability of the FeOCl host lattice. In contrast to the iron derivative,  $\text{Li}_x\text{CrOCl}$  as well as  $\text{Li}_x\text{VOCl}$ , are decomposed by water to give mainly lithium chloride and the transition metal oxides.

From our point of view, the result obtained with FeOCl host lattice seems a bit strange. It is known that FeOCl in dry air is stable, but, in air saturated with  $\text{H}_2\text{O}$  completely decomposes into  $\text{FeO}(\text{OH})$  and then to  $\text{Fe}_2\text{O}_3$ . The product of hydrolysis appears amorphous to X-rays and could be easily missed by the authors of the article.

Intercalation of planar electron donors has been investigated for FeOCl and results in the formation of new inorganic / organic conducting materials.<sup>45</sup>

A new intercalation compound,  $\text{FeOCl}(\text{ET})_{1/4}$ , where ET = bis(ethylenedithio)tetrathiafulvalene, was prepared by treating FeOCl with a solution of ET.<sup>45</sup> Structural and electronic studies showed that the new material contains stacks of partially oxidized ET molecules in the interlayer region.

The powder X-ray diffraction pattern of the intercalate showed that the FeOCl interlayer spacing expands by  $14.43\text{\AA}$  upon intercalation of ET. A structural model for  $\text{FeOCl}(\text{ET})_{1/4}$  was proposed on the base of calculated atomic distances in which ET molecules are canted at an angle of ca.  $10^\circ$  from the perpendicular with respect to the anion sheets. These materials exhibited high electrical conductivity presumably due to the intercalated electron donors.

FeOCl is one of the most convenient redox - intercalation hosts for a variety of

organic molecules including organic polymers. The resulting intercalation compounds are very interesting systems of theoretical and practical interest. In general, they are composed of monolayers of positively charged conductive polymer and negatively charged FeOCl.<sup>46</sup>

Wu and co-workers<sup>46</sup> studied the intercalation of furan, terfuran and tetrafulan into FeOCl layered host. These species are known to oxidatively polymerize chemically or electrochemically to yield polyfuran. The results of intercalation reactions showed that furan itself did not intercalate in FeOCl because of its high oxidation potential. The redox potentials of terfuran and tetrafulan are 1.3 and 1.0 Volts vs. SCE respectively. These values are low enough to be suitable for redox intercalation reaction with FeOCl. Reaction of terfuran with FeOCl proceeded in a sealed tube at 100°C. The product exhibited an interlayer expansion of 7.7Å to accommodate the intercalated polyfuran species.

Tetrafulan partially intercalated FeOCl under sealed tube conditions. The authors assume that the kinetics of tetrafulan intercalation were slow due to the large size of this monomer.

Kanatzidis and colleagues reported the successful oxidative intercalation of aniline<sup>47a</sup>, pyrrole<sup>48</sup>, and 2,2'-bithiophene<sup>47b</sup> into FeOCl using the same technique. X-ray studies showed that these new materials are highly crystalline and the FeOCl interlayer spacing expands by more than 5Å. Elaboration and characterisation of such materials is continuing.

The layered transition metal oxyhalides FeOCl, VOCl, and TiOCl has been found

to undergo direct intercalation of organometallic compounds. In 1975, Dines<sup>49</sup> first demonstrated the intercalation of organometallic species into layered transition metal dichalcogenides. After additional studies Davies<sup>50</sup> et al. have identified that for direct intercalation in metal dichalcogenides the organometallic compounds first ionization potential must lie below 6.2 eV.

Halbert and Scanlon<sup>52</sup> discovered that ferrocene with its first ionization potential of 6.88 eV can be successfully intercalated into FeOCl. This fact illustrated that FeOCl permits a broad range of organometallic intercalates to be prepared.

Metallocene intercalates,  $(Cp_2M^*)_x(MOCl)^x$ , prepared by direct reaction of the electron - rich metallocenes with the hosts FeOCl, VOCl and TiOCl are listed in Table III.

The electronic nature of the ferrocene and cobaltocene intercalates of FeOCl has been probed by Mössbauer spectroscopy and magnetic susceptibility.<sup>51</sup> On the basis of the electronic studies of metallocene intercalates it was assumed that the electron - rich metallocenes are oxidized upon intercalation, and the electrons donated to the layers are essentially localized on metal sites in the host lattice.

The more recent Mössbauer and conductivity studies<sup>51</sup> suggest delocalization of the transferred electron density in the host lattice.

Detailed examination of the mechanism of organometallic intercalation and the nature of the products have only been performed for the FeOCl host lattice. No details of characterisation other than layer expansion have been given for intercalation of  $Cp_2Co$  into VOCl and TiOCl.

Table III.

## Metallocene Intercalates of MOCl

Metallocene*	x	MOCl	d-space(Å)	References
NiCp <sub>2</sub>		FeOCl		53
FeCp <sub>2</sub>	0.16	FeOCl	5.13	52
MnCp <sub>2</sub>		FeOCl		53
VCp <sub>2</sub>		FeOCl		53
CoCp <sub>2</sub>	0.16	FeOCl	4.94	51, 52
CoCp <sub>2</sub>	0.16	VOCl	4.86	51
CoCp <sub>2</sub>	0.16	TiOCl	5.12	51

\*Cp = cyclopentadienyl

The intercalation of transition metal oxyhalides by ammonia and n - alkylamines was first recognized by Hagenmuller and co - workers in 1967.<sup>54</sup> In the extension of the above work, the reactions of many aliphatic and aromatic amines with MOX, especially with FeOCl, has been widely studied.

The intercalation of C<sub>n</sub>H<sub>2n+1</sub>NH<sub>2</sub> ( n = 10, 12, 14, 16, 18 ) was achieved with FeOCl as the host material.<sup>55</sup> The intercalates were obtained by direct reaction between

FeOCl and anhydrous amine. X-ray studies showed that the interlayer distance at room temperature increase gradually with the increase of chain length.

Choy and colleagues<sup>56</sup> studied the intercalation of  $C_nH_{2n+1}NH_2$  ( $n = 2, 6, 8, 10, 12$ ) into VOCl host lattice. X-ray studies showed that the d-spacing ( distance between layers) of n-ethylamine intercalate is only slightly higher than that of ammonia - derivative, indicating the axes C - C - N lie parallel rather than perpendicular to the VOCl sheets. The d-spacing increases significantly if the intercalated amine contains six or more carbon atoms per alkyl chain. Comparison of the obtained d-values with calculated ones ( the calculated d-spacings were obtained by assuming that alkyl chains are perpendicular to VOCl layers) showed that alkyl chains have an orientation of 40-60° to the VOCl plane.

The proposed mechanism for the alkylamine intercalation reactions is a charge transfer between the amine guest and MOCl host lattice resulting in a weak bonding between host and guest.<sup>56</sup>

The intercalation of aromatic amines into FeOCl and VOCl seems to be the most thoroughly studied reaction from point of view orientation, bonding and structure.

On the basis of X-ray powder diffraction data, Koizumi<sup>67</sup> et al. proposed a uniform model in which the neutral amine molecules lie in the van der Waals gap with their aromatic rings perpendicular to the host layers and their nitrogen lone pairs bonding to the layers. This research group studied the intercalation of pyridine (py), 4-aminopyridine (4-Apy), and 2,4,6-trimethylpyridine (2,4,6-TMpy) into the layered FeOCl matrix and proposed a mechanism for this reaction based on a Lewis acid and base reaction with

partial transfer of the pyridine electrons to the host FeOCl layers.

**Table IV.**

**Aromatic Amine Intercalates of FeOCl**

Compound	d-space(Å)	layered expansion (Å)	References
FeOCl(py) <sub>1/4</sub>	13.27	5.35	57
FeOCl(4 - Apy) <sub>1/4</sub>	13.57	5.65	57
FeOCl(2,4,6 - Tmpy) <sub>1/4</sub>	11.9	3.87	57

The interlayer spacings for the intercalated compounds are summarized in Table IV. According to Table IV, the layered expansion of FeOCl in the case of pyridine intercalation is bigger than that in the case of 2,4,6-trimethylpyridine. This layered expansion data is not consistent with Koizumi's model.

Venien and co - workers<sup>58</sup> proposed that in VOCl the pyridine axis ( defined in the plane of the ring through the nitrogen atom and para carbon ) is inclined to the layers. This model was consistent with experimental data for a series of methyl substituted pyridines intercalated into VOCl. The results are listed in Table V.

X-ray powder diffraction suggests that the intercalated molecules lie in the van der Waals gap of VOCl with the molecular axis tilted at angles at about 50° relative to the normal to the layers.

Table V.

## Aromatic Amine Intercalates of VOCl

Guest molecules	d-space (Å)	layered expansion (Å)	dimensions of molecules (Å)
pyridine	13.35	5.45	6.8; 6.6; 3.0
o-methylpyridine	13.39	5.49	6.8; 7.5; 3.4
m-methylpyridine	13.20	5.27	6.8; 7.5; 3.4
p-methylpyridine	13.95	6.02	7.7; 6.6; 3.4
p-ethylpyridine	12.02	4.09	8.7; 6.6; 4.4

### 7.2.2. Topochemical Substitution Reactions

In section 7.1 it was pointed out that, in general, the structure of layered metal oxyhalides consist of strongly interacting central M - O sheets with more weakly bound interlayer halides. The interlayer halides form a two dimensional array on each side of the M - O layer and this structure should be an ideal for topochemical substitution reactions involving the substitution of chloride ions by the organic molecule without the reconstruction of the other part of the layers.

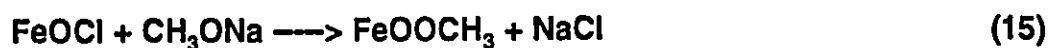
The literature contains some brief reports concerning the use of ethylene glycol (C<sub>2</sub>H<sub>4</sub>(OH)<sub>2</sub>), methanol and ammonia in substitution reactions of MOCl layered hosts.

Koizumi and co - workers<sup>59</sup> reported the preparation of the new compound FeOOCH<sub>3</sub> by two different methods. The first method involves the reaction of the intercalated compound FeOCl(4-aminopyridine)<sub>1/4</sub> with methanol (14).



This new compound was not obtained by direct reaction between FeOCl and CH<sub>3</sub>OH.

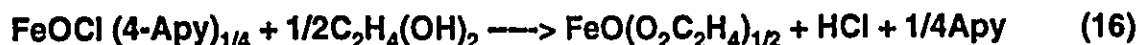
Second method for the preparation of FeOOCH<sub>3</sub> involves the direct reaction of FeOCl with sodium methoxide (15).



In both cases, the compound was identified to be  $\text{FeOOCH}_3$  by chemical, IR, X-ray diffraction, and differential thermogravimetric analysis ( TGA ). X-ray diffraction data showed the presence of NaCl. The new compound was found to have the d-spacing of  $10\text{\AA}$ . Thermal analysis data of  $\text{FeOOCH}_3$  showed that the compound decomposes at  $300^\circ\text{C}$  associated with a 19% weight loss.

Attempts to prepare  $\text{VOOCH}_3$  from  $\text{VOCl}$  and  $\text{CH}_3\text{ONa}$  by the same method were unsuccessful. In spite of the similarity between the  $\text{VOCl}$  and  $\text{FeOCl}$  structures, and the ability of both of them to form intercalated compounds with pyridine molecules, the product  $\text{VOOCH}_3$  was not obtained. This interesting phenomenon has not been explained.

Another substituted product<sup>60</sup> was prepared by the reaction of the intercalation compound  $\text{FeOCl} (4\text{-aminopyridine})_{1/4}$  with ethylene glycol  $\text{C}_2\text{H}_4(\text{OH})_2$  (16).



The reaction product  $\text{FeO}(\text{O}_2\text{C}_2\text{H}_4)_{1/2}$  was examined by X-ray diffractometry, IR, chemical and TGA analysis.

The interlayer distance of the wet product was  $14.5\text{\AA}$ , however, after the product was washed with acetone, in order to remove free ethylene glycol, the d-spacing decreased to  $10.89\text{\AA}$ . The thermal behavior of  $\text{FeO}(\text{O}_2\text{C}_2\text{H}_4)_{1/2}$  is very similar to that of the methoxide derivative  $\text{FeOOCH}_3$ . A weight loss was observed at  $300^\circ\text{C}$  which corresponds to 22% of the starting mass. Mössbauer spectrum studies of  $\text{FeO}(\text{O}_2\text{C}_2\text{H}_4)_{1/2}$  concluded that the new material had a crystal structure derived from that of  $\text{FeOCl}$ ; i.e.

the  $\text{Fe}^{3+}$  ions are octahedrally coordinated by oxygens. Two model structures have been proposed for the product. In both cases, the ethylene glycol (EG) is directly bonded to the iron in the FeO double layers. The first model involves interlayer bridging with the EG molecules coordinated to Fe ions of two parallel FeO layers. The interlayer distance for this bridging model is estimated to be below  $8.2\text{\AA}$  even if the molecules have an all trans configuration (the longest possible molecular length). In contrast, the second model proposes the EG molecules coordinate to two  $\text{Fe}^{\text{III}}$  ions in the same layer. This gives an estimated interlayer distance of approximately  $11.0\text{\AA}$  based on methylene groups belonging to upper and lower layers contacting each other at a distance of twice their van der Waals radii. The observed interlamellar distance was  $10.89\text{\AA}$ . Thus, the interlayer bonding model was taken to be more probable. The collapse of the interlayer spacing from  $14.5\text{\AA}$  to  $10.89\text{\AA}$  when the sample was washed with acetone was explained by the fact that before being washed with acetone, the new product  $\text{FeO}(\text{O}_2\text{C}_2\text{H}_4)_{1/2}$  contained an excess amount of EG molecules lying parallel to the layers. The difference of  $3.6\text{\AA}$  corresponds to almost twice the van der Waals radius of the methylene group.

Exposure of  $\text{AlOCl}$  and  $\text{FeOCl}$  to gaseous ammonia results in the uptake of ammonia over a period of 48 hours for  $\text{AlOCl}$ , and several months for  $\text{FeOCl}$  at  $25^\circ\text{C}$ <sup>54</sup>. Powder X-ray diffraction indicated the presence of  $\text{NH}_4\text{Cl}$ , which can be removed from the product through washing with liquid  $\text{NH}_3$  to leave amorphous solids  $\text{AlO}(\text{NH}_2)$  and  $\text{FeO}(\text{NH}_2)$  respectively. Infrared spectrum showed signals at  $3300$ ,  $3200$ , and  $1600\text{ cm}^{-1}$  that were assigned to  $-\text{NH}_2$  - related vibrations.

The reaction of  $\text{VOCl}$  with  $\text{NH}_3$ <sup>61</sup> is similar to that of  $\text{FeOCl}$ . Two equivalents of  $\text{NH}_3$  are absorbed at  $25^\circ\text{C}$  over a period of one month. The final black amorphous product  $\text{VO}(\text{NH}_2)$  was analysed by IR and TGA. Infrared spectrum showed absorptions at  $3200$  and  $1630\text{ cm}^{-1}$  that have been assigned to the  $-\text{NH}_2$  group. A band at  $420\text{ cm}^{-1}$  assigned to  $\text{V-Cl}$  stretching disappears in the product. TGA studies showed that  $\text{VO}(\text{NH}_2)$  decomposes at  $160^\circ\text{C}$  to give  $\text{V}_2\text{O}_3$  and  $\text{V}(\text{NH}_2)_3$ ;  $\text{V}(\text{NH}_2)_3$  decomposes further at  $260^\circ\text{C}$  to give  $\text{VN}$  and  $2\text{NH}_3$ .

## HYPOTHESIS

The existing literature completely supports the idea that metal oxychlorides can undergo topochemical reactions. The features that control the intercalation process are complicated and not completely clear. Among the intercalation reactions of metal oxychlorides, FeOCl has been the major host lattice that has been studied, and it is quite clear that many intercalation reactions involving FeOCl and a variety of substrates proceed via redox processes. It is of our interest to probe the features that control the intercalation of both amines and amides into TiOCl and VOCl host lattices.

We believe that redox potential may be important feature in the thermodynamics of intercalation of organic molecules into MOX. Furthermore, based on the literature review, the presence of reactive protons may provide an additional driving force for these reactions. Therefore, amines and amides that have a range of oxidation potentials, that have different number of reactive protons, and various molecular sizes and shapes were chosen as the guest molecules. From these studies we hoped to gain information about the mechanism for the intercalation of amines and amides, the possibility of substituting of interlayer Cl ions of the host by the amine or amide molecule, the driving force for the substitution process, and an idea about the orientation of the guest molecules inside the host.

## EXPERIMENTAL

The purification of starting materials and the following reactions were performed in the absence of air and water using standard Schlenk techniques, a vacuum line or a nitrogen - filled glovebox.

### Purification of starting materials:

Ethylenediamine, N,N'- dimethylethylenediamine, N,N,N',N'- tetramethylethylenediamine, diethylenetriamine, and pyridine were dried by reflux for 12 hours with sodium and then distilled under nitrogen. tert - Butylamine was dried with  $\text{CaH}_2$  and then distilled under  $\text{N}_2$ . N,N - Dimethylformamide ( DMF ) was dried with  $\text{CaSO}_4$  and then distilled under  $\text{N}_2$ . N - Methylformamide ( NMF ) was dried with molecular sieves for 2 days followed by distillation under  $\text{N}_2$ . Acetamide was purified by sublimation in vacuo. N,N - Dimethylacetamide ( DMA ) was shaken with BaO, then refluxed for one hour followed by distillation under  $\text{N}_2$ .

$\text{TiCl}_3$ ,  $\text{TiO}_2$ ,  $\text{V}_2\text{O}_3$ , and  $\text{VCl}_3$  were purchased from Aldrich and used without further purification.

### Instrumentation.

**Powder X - Ray Diffraction ( PXRD )**

Diffraction patterns were collected with a Phillips PW 3710 based Xpert system. The powder patterns for the air sensitive samples were obtained using a brass air - tight holder assembled in the dry box while the air - stable samples were analysed using a no background spinning Si holder. In both cases the powder patterns were collected using  $\text{Cu}_{k\alpha}$  radiation ( wavelength 1.54060 ).

**Thermal Gravimetric Analysis ( TGA ).**

Thermal analysis for all samples was done on a Polymer Laboratories simultaneous DSC/TGA STA 1500H ( Differential Scanning Calorimetry / ThermoGravimetric Analysis) instrument. A heating rate of 20°C/min was found to be an ideal for both sample and curve quality purposes. All measurements were done in an alumina pan under nitrogen flow at a rate of 40 - 60 cm<sup>3</sup>/s.

**FTIR Spectroscopy ( IR ).**

All IR spectra were recorded using Nujol mull between NaCl plates on either a Mattson 3000 or Bomem Michelson Series 100 FTIR systems.

**X - Ray Fluorescence ( XRF ).**

Fluorescence spectra were measured with a Philips PW 2400 X-ray spectrometer.

**Elemental analysis ( EA ).**

EA of all the samples was obtained on Perkin Elmer 2400 Series 2 CHN Analyzer.

**Reactions****Synthesis of TiOCl.**

Titanium(III) oxychloride was prepared by sealing a mixture of 1.8g (0.01 moles)  $\text{TiCl}_3$  and 0.3g (0.003 moles)  $\text{TiO}_2$  in a Quartz ( or Vycor ) glass tube 20cm long and 2cm in diameter. The glass tube was heated in an oven in a temperature gradient of 550°C to 650°C for 3.5 days. The glass tube was opened in air and the product was washed with DMF, ethanol and ether to remove starting materials (excess of  $\text{TiCl}_3$ ) or by products ( $\text{TiCl}_4$ ) formed during the reaction. Dark brown flat shiny crystals of TiOCl were obtained and stored in a vial. Our experience showed that TiOCl is not moisture or air sensitive. TiOCl was not obtained in the form of single crystal suitable for X-ray diffraction. TiOCl was characterised through thermal analysis, powder X-ray diffraction and X-ray fluorescence.

TGA showed one weight loss at 755°C that corresponds to 44.6% of the sample weight. X-ray powder pattern: d-value (Å) (relative intensity): 7.96 (100); 4.00 (0.2); 3.41 (0.3); 2.67 (2.9); 2.57 (0.4). XRF showed the ratio Ti/Cl equal to 1.

**Synthesis of VOCl.**

VOCl was prepared by heating a mixture of 1.8g (0.01 mol)  $\text{VCl}_3$  and 1.0g (0.006

mol)  $V_2O_3$  in a temperature gradient of  $580^\circ\text{C}$  to  $620^\circ\text{C}$  in an evacuated sealed Quartz ( or Vycor ) tube for 3 days. The solid thus obtained was washed with DMF, ethanol and ether in air to remove unreacted starting materials. After this procedure, the compound was dried and stored in a vial. Brown - red flat VOCl crystals were not suitable for single crystal X-ray crystallography and the compound was characterised by TGA, PXRD and XRF.

Powder X-ray diffraction data: d-value ( $\text{\AA}$ ) (relative intensity) : 7.80 (100); 3.38 (10.9); 2.63 (2.1); 2.52 (13.8); 2.36 (2.5). TGA: two weight losses at  $730^\circ\text{C}$  (23%), and at  $880^\circ\text{C}$  (15%)

XRF: The ratio V/Cl = 1.

### Reactions of TiOCl with pyridine ( $C_5H_5N$ ).

#### Reaction in a sealed tube at $250^\circ\text{C}$ :

0.5g of TiOCl and 5ml of pyridine were mixed together in a heavy walled glass tube. The tube was sealed under vacuum and heated for 2 days at  $250^\circ\text{C}$ . The product appeared as shiny grey crystals that were analysed by PXRD, thermal analysis and EA. PXRD pattern: d-value ( $\text{\AA}$ ) (relative intensity): 11.85 (100); 7.99 (66.0); 5.96 (12.8); 4.00 (0.3); 3.41 (2.0); 2.98 (0.7); 2.67 (1.1); 2.57 (0.8); 2.39 (0.3); 2.01 (5.6); 1.61 (2.0). The TGA showed two weight losses . The first one takes place before  $70^\circ\text{C}$  (4% of the original mass). The second weight loss occurs between  $150^\circ\text{C}$  and  $300^\circ\text{C}$  (9% of the original mass). The compound remaining in a pan after TGA run was confirmed to be

TiOCl by PXRD. The 9% weight loss in the TGA measurement corresponds to an intercalation compound with the formula  $\text{TiOCl}(\text{py})_{0.11}$ .

Elemental analysis: Calculated values for  $\text{TiOCl}(\text{py})_{0.2}$ : %C (10.4); %H (0.8); %N (2.4)

Experimental values: %C (10.1); %H (1.05); %N (2.0)

#### Reaction in a Schlenk flask at 80°C:

5ml of pyridine and 0.5g of TiOCl were mixed in a Schlenk flask and vigorously stirred at 80°C for 2 weeks. A dark grey crystalline solid was isolated by filtration.

PXRD pattern: d-value (Å) (relative intensity) : 12.72 (8.3); 7.95 (100); 6.45 (1.2); 4.00 (0.4); 2.67 (5.4); 2.57(0.1)

Elemental analysis: Calculated values for  $\text{TiOCl}(\text{py})_{0.38}$ : %C (17.61); %H (1.46); %N (4.1)

Experimental values: %C (17.53); %H (2.28); %N (4.50)

#### **Reactions of TiOCl with N,N,N',N',- tetramethylethylenediamine (TMEDA)**



#### Reaction at 100°C:

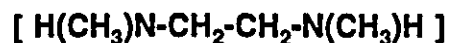
0.5g of TiOCl and 5ml of TMEDA were mixed together inside a teflon lined acid digestion bomb. The bomb was heated at 100°C for 1.5 days. The brown product was analysed by PXRD.

d-value (Å) (relative intensity): 7.98 (100); 3.88 (1.6); 3.4 (1.0).

Reaction at 170°C:

0.5g TiOCl and 5ml TMEDA were mixed in a heavy walled tube. The tube was sealed evacuated and heated to 170°C for 4.5 days. The resultant solid looked the same as starting material. The reaction mixture was allowed to stay in the sealed tube for 18 months. A brown crystalline product was isolated by filtration.

PXRD: d-value (Å) (relative intensity): 13.18 (1.9); 7.93 (100); 3.4 (5.1); 2.67 (1.7); 2.57 (5.8); 2.39 (0.9).

**Reaction of TiOCl with N,N'-dimethylethylenediamine (DMEN)**Reaction in a sealed tube at 80°C:

A mixture of TiOCl (0.5g) and DMEN (5ml) was sealed in an evacuated heavy walled glass tube. The tube was heated to 80°C for 2 days. A dark blue product was obtained after the DMEN solution was removed under vacuum.

PXRD : d-value (Å) (relative intensity): 11.25 (100); 7.92 (12.8); 5.71 (6.9); 4.00 (1.4); 3.73(0.5); 3.41 (0.4); 2.88 (2.0); 2.55 (0.4)

TGA: One weight loss at 283.5°C (26.3%) and consistent with a formulation  $\text{TiOCl}(\text{C}_4\text{N}_2\text{H}_{12})_{0.44}$

Reaction in a Schlenk flask at 80°C:

DMEN (5ml) was vacuum transferred into a Schlenk flask containing 0.5g of TiOCl.

The reaction mixture was maintained under N<sub>2</sub> flow for 2 weeks at 80°C. The DMEN solution was removed under vacuum and the resulting dark blue - grey product was isolated.

PXRD: d-value (Å) (relative intensity): 14.27 (17.9); 11.4 (100); 7.92 (23.6); 5.8 (10.9); 4.34 (1.9); 3.89 (1.2); 3.74 (3.3); 3.48 (4.5); 3.4 (9.5); 3.18 (3.3); 2.92 (5.9); 2.67 (1.6); 2.56 (1.1)

The dark blue - grey product was heated in a tube under N<sub>2</sub> for 4 days at 80°C in the absence of solution.

PXRD: d-value (Å) (relative intensity): 14.57 (100); 8.60 (6.3); 7.91 (34.0); 7.38 (8.1); 5.01 (8.1); 4.34 (15.6); 3.65 (4.1); 3.58 (8.3); 3.4 (10.3); 3.25 (4.0); 3.01 (1.6); 2.87 (1.1); 2.79 (0.5); 2.72 (1.0); 2.67 (1.2); 2.54 (1.0)

TGA of the compound after 4 days heating: Three weight losses: 310°C(25%); 504°C(10%) and 700°C(10.87%)

IR spectrum of the compound obtained after 4 days heating at 80°C showed absorption bands at 2449; 2360; 1716; 1261; 1022 and 721 cm<sup>-1</sup>.

Removal of [H(H)(CH<sub>3</sub>)N-CH<sub>2</sub>-CH<sub>2</sub>-N(CH<sub>3</sub>)(H)H]<sup>2+</sup>2Cl<sup>-</sup> (DMEN-salt) from the reaction mixture:

The compound obtained after 4 days of heating was heated to 360°C under N<sub>2</sub> flow inside of the TGA instrument. A shiny grey product was obtained.

PXRD : d-value (Å) (relative intensity) : 10.12 (7.9); 7.95 (100); 3.40 (0.8); 3.37(0.8); 2.67 (5.4)

IR of the shiny grey product showed an absorption bands at 1718; 1261 and 721  $\text{cm}^{-1}$ .

TGA: Two weight losses: the first weight loss was observed at 506°C (13.2% of the original mass) and the second weight loss was taking place at 703°C (12.03% of the original mass).

XRF showed the ratio Ti/Cl = 4.

EA (experimental values): %C (3.09); %H (1.26); %N(0.76).

#### Synthesis of $[\text{H}(\text{H})(\text{CH}_3)\text{N}-\text{CH}_2-\text{CH}_2-\text{N}(\text{CH}_3)(\text{H})\text{H}]^{2+}2\text{Cl}^-$

DMEN - salt was synthesised by adding HCl to DMEN. The white crystalline product was isolated and dried.

PXRD: d-value (Å) (relative intensity): 8.64 (32.1); 4.35 (100); 3.85 (3.0); 3.58 (5.6); 3.29 (1.9); 3.17 (4.8); 2.87 (5.1); 2.84 (3.9); 2.79 (1.9); 2.74 (1.6); 2.54 (0.8); 2.42 (0.4).

TGA: One weight loss at 327°C (100% of the original mass).

EA: Calculated values for  $\text{C}_4\text{H}_{14}\text{N}_2\text{Cl}_2$ : %C (29.81); %H (8.69); %N (17.39)

Experimental values: %C (29.83); %H (9.08); N (17.33)

#### **Reactions of $\text{TiOCl}$ with ethylenediamine (EN) $[\text{H}_2\text{N}-\text{CH}_2-\text{CH}_2-\text{NH}_2]$ .**

##### Reactions in a sealed tubes at 160° - 170°C.

$\text{TiOCl}$  (0.5g) and 5ml of EN were mixed together in a heavy walled glass tube. The tube was then evacuated, sealed, and heated in the oven at 160°-170°C for 2; 2.5 and 4 days. The dark grey products were isolated by vacuum and analysed by PXRD.

Reaction in a Schlenk flask at 80°C for 5 days.

0.2g TiOCl and 2ml EN were mixed in a Schlenk flask and heated to 80°C for 5 days. The EN solution was removed under vacuum and a dark blue - grey crystalline product was isolated.

PXRD: d-value (Å) (relative intensity): 11.24 (100); 5.69 (7.6); 2.87 (2.3); 2.51 (0.6); 2.29 (0.2).

Reaction in a Schlenk flask at 75°C for 9 hours:

0.5g TiOCl and 0.5ml EN were allowed to react in a Schlenk flask with vigorous stirring for 9 hours at 75°C. In approximately 7 hours a colour change of the solid from dark brown to dark blue - grey was observed. After an additional 2 hours, the EN solution was removed under vacuum and a dark blue - grey crystalline product was isolated.

PXRD: d-value (Å) (relative intensity): 11.39 (100); 5.73 (14.0); 3.83 (0.6); 2.88 (5.0); 2.28 (0.5).

EA: Calculated values for  $\text{TiOCl}(\text{C}_2\text{N}_2\text{H}_8)_{0.4}$ : %C (7.80); %H (2.68); %N (9.18).  
Experimental values: %C (7.80); %H (2.81); %N (7.97).

Reaction in a Schlenk flask at 75°C for 16 hours:

A mixture of 0.5g of TiOCl and 5ml of EN was stirred vigorously for 16 hours at 75°C in a Schlenk flask. The EN solution was removed by vacuum and a dark blue - grey solid was obtained.

PXRD: d-value (Å) (relative intensity): 13.42 (5.4); 11.31 (100); 5.65 (25.4); 3.77 (0.5);

2.83 (17.2); 2.27 (2.2).

Reaction in a Schlenk flask at 75°C for 4 days:

The dark blue - grey product obtained in the previous reaction and 5ml of EN were mixed together in a Schlenk flask. The mixture was heated for 3 days at 75°C under vigorous stirring. EN solution was removed by vacuum and the product appeared as a mixture of dark blue - grey and yellowish - white solids.

PXRD: d-value (Å) (relative intensity): 13.80 (22.6); 11.31 (100); 5.69 (6.5); 3.71 (0.2); 3.61 (0.3); 3.45 (1.1); 3.33 (0.7); 3.24 (2.1); 2.98 (1.4); 2.94 (0.5); 2.85 (1.9); 2.71 (0.4); 2.62 (0.7); 2.51 (0.2); 2.39 (0.2); 2.33 (0.2); 2.28 (0.2)

Reaction in a Schlenk flask at 75°C for 7.5 days:

The dark blue - grey product obtained in the previous reaction and 5ml of EN were mixed together in a Schlenk flask. The mixture was heated for 3.5 days at 75°C. The EN solution was removed by vacuum and the product appeared as a mixture of dark blue - grey and yellowish - white solids.

PXRD: d-value (Å) (relative intensity): 13.16 (100); 4.92 (27.3); 3.62 (22.2); 3.51 (14.5); 3.33 (7.0); 3.25 (14.5); 2.98 (21.6)

Removal of  $[\text{H}_3\text{N-CH}_2\text{-CH}_2\text{-NH}_3]^{2+}2\text{Cl}^-$  (EN-salt) from the reaction mixture:

A mixture of dark blue -grey and yellowish - white solids was washed with EN, dried with ether, and heated at 80°C for 1 hour.

PXRD : d-value (Å) (relative intensity): 14.52 (100); 7.13 (5.5); 4.88 (2.1)

EA: Calculated for  $\text{TiOCl}_{0.5}(\text{C}_2\text{N}_2\text{H}_7)_{0.5}$ : %C (10.6); %H (3.5); %N (12.4)

Experimental values: %C (10.24); %H (3.52); %N (10.14)

IR showed an absorption bands at 1716, 1261, and 721  $\text{cm}^{-1}$

XRF : the ratio Ti/Cl = 1.9

#### Synthesis of $[\text{H}_2\text{N-CH}_2\text{-CH}_2\text{-NH}_3]^{2+}2\text{Cl}^-$ :

EN-salt was synthesised by adding HCl to EN solution. The yellowish - white product was isolated and dried.

PXRD: d-value (Å) (relative intensity): 7.50 (30.9); 3.86 (20.6); 3.70 (14.7); 3.45 (100); 3.33 (70.3); 3.24 (62.7); 3.18 (5.1); 2.97 (81.3); 2.94 (45.2); 2.82 (5.2); 2.73 (91.9); 2.71 (20.7); 2.62 (43.7); 2.49 (4.9); 2.44 (9.6); 2.39 (10.2); 2.33 (10.4).

TGA : One weight loss at 311.7°C (100% of the sample weight).

EA: Calculated values for  $\text{C}_2\text{N}_2\text{H}_{10}\text{Cl}_2$ : %C (18.0); %H (7.52); %N (21.05)

Experimental values: %C (19.35); %H (7.81); %N (21.08)

#### **Reaction of TiOCl with diethylenetriamine $[\text{H}_2\text{N-CH}_2\text{-CH}_2\text{-N(H)-CH}_2\text{-CH}_2\text{-NH}_2]$ ("3N")**

5ml of "3N" was vacuum transferred to a Schlenk flask containing 0.5g of TiOCl. The reaction mixture was heated for 5 days at 90°C under vigorous stirring. Excess "3N" was removed by filtration and the dark grey product was washed with THF in order to remove residual "3N".

PXRD : d-value (Å) (relative intensity): 12.01 (100); 6.02 (25.0); 4.03 (2.0); 3.03 (5.6);

2.41 (0.9).

EA: Calculated values for  $\text{TiOCl}(\text{C}_4\text{N}_3\text{H}_{13})_{0.15}$ : %C (6.30); %H (1.96); %N (5.50) ;

Experimental values: %C (6.31); %H (2.14); %N (5.29).

IR showed an absorption bands at 1718, 1081, 800, and  $721\text{cm}^{-1}$

#### **Reaction of TiOCl with N,N - Dimethylacetamide ( DMA ) $[\text{CH}_3\text{C}(\text{O})\text{N}(\text{CH}_3)_2]$ .**

TiOCl (0.5g) and 5ml of DMA were sealed in an evacuated glass tube. The tube was heated to  $60^\circ\text{C}$  for 10 days. The mixture was filtered and the solid was dried under vacuum to yield a brown product.

PXRD: d-value (Å) (relative intensity): 7.91 (100); 3.99 (0.2); 3.40 (0.3); 2.67 (2.6); 2.57 (0.4).

IR spectrum did not show the presence of DMA.

#### **Reaction of TiOCl with Dimethylformamide ( DMF ) $[\text{HC}(\text{O})\text{N}(\text{CH}_3)_2]$ .**

0.5g of TiOCl and 5ml of DMA were mixed together in a Schlenk flask and allowed to react for 1 week at  $80^\circ\text{C}$  with vigorous stirring. The DMF was removed by filtration and the product was dried under vacuum to yield a brown solid.

PXRD: d-value (Å) (relative intensity): 16.01 (0.5); 7.88 (100); 3.99 (0.2); 3.40 (0.4); 2.67 (2.2); 2.57 (0.8)

IR spectrum did not have characteristic absorption bands for DMF.

**Reaction of TiOCl with N - Methylformamide ( NMF ) [HC(O)N(CH<sub>3</sub>)H].**

0.5g of TiOCl and 5ml of NMF were sealed in an evacuated glass tube and heated to 100° - 110°C for 8 days. The NMF was removed by filtration and the solid was dried under vacuum to yield a grey - blue crystalline product.

PXRD: d-value (Å) (relative intensity): 15.35 (2.7); 7.87 (100); 3.97 (0.2); 3.39 (4.2); 2.66 (2.3); 2.56 (2.0); 2.39 (0.2)

IR spectrum showed an absorption bands at 3300, 1670, 1570, and 721 cm<sup>-1</sup>

EA: Calculated values for TiOCl(HC(O)N(CH<sub>3</sub>)H)<sub>0.95</sub>: %C (14.67); %H (3.05); %N (8.5);

Experimental values: %C (14.53); %H (3.34); %N (9.5)

**Reaction of TiOCl with acetamide [CH<sub>3</sub>C(O)NH<sub>2</sub>].**

TiOCl (0.5g) and 2.0g of acetamide were sealed in an evacuated glass tube. The mixture was heated to 100° - 110°C ( the melting point of acetamide is 81°C ) for 9 days. A dark brown/purple product was washed with ethanol and dried under vacuum.

PXRD: d-value (Å) (relative intensity): 14.21 (0.3); 11.63 (0.3); 7.92 (100); 5.69 (0.3); 3.99 (0.3); 3.41 (0.1); 2.86 (0.0); 2.67 (3.9); 2.57 (0.1)

IR: 721 cm<sup>-1</sup>.

EA: Calculated values for TiOCl(CH<sub>3</sub>C(O)NH<sub>2</sub>)<sub>0.03</sub>: %C (0.71); %H (0.14); %N (0.41);

Experimental values: %C (0.80); %H (0.12); %N (0.38)

**Reaction of VOCl with N,N - dimethylacetamide.**

VOCl (0.5g) and 5ml of DMA were mixed together in a Schlenk flask. The mixture

was heated to 80°C for 10 days with vigorous stirring. The DMA was removed by filtration and the dark brown product was dried under vacuum.

PXRD: d-value (Å) (relative intensity): 7.87 (100); 3.39 (0.4); 2.63 (2.2); 2.53 (0.7).

IR spectrum did not show any presence of DMA.

#### **Reaction of VOCl with N - Methylformamide.**

0.5g of VOCl and 5ml of NMF were sealed in an evacuated glass tube and heated to 100° - 110°C for 8 days. The NMF was removed by vacuum, the solid was dried to yield a dark brown product.

PXRD: d-value (Å) (relative intensity): 12.84 (100); 6.49 (21.2); 3.31 (6.2); 2.70 (1.9)

IR spectrum showed an absorption bands at 1710, 1645, and 723 cm<sup>-1</sup>.

EA: Calculated values for VOCl(HC(O)N(CH<sub>3</sub>)H)<sub>1,0</sub>: %C (14.86); %H (3.09); %N (8.6)

Experimental values: %C (14.56); %H (3.28); %N (7.12)

#### **Reaction of VOCl with Acetamide.**

0.5g of VOCl and 2g of acetamide were sealed in an evacuated heavy walled glass tube. The mixture was heated to 100° - 110°C for 9 days. A dark brown product was washed with ethanol and dried under vacuum.

PXRD: d-value (Å) (relative intensity): 11.77 (100); 8.57 (21.5); 3.94 (6.6); 2.95 (4.3)

IR spectrum showed signals at 1714, 1658 and 723 cm<sup>-1</sup>.

EA: Calculated values for VOCl / (CH<sub>3</sub>C(O)NH<sub>2</sub>)<sub>0,25</sub>: %C (5.1); %H (1.07); %N (2.9) ;

Experimental values: %C (4.91); %H (1.20); %N (1.55)

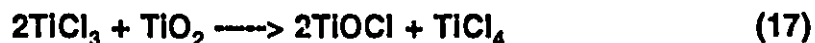
## RESULTS AND DISCUSSION

### Preparation of starting materials

#### 1. Synthesis of TiOCl.

The solid state preparation of TiOCl crystals has been reported by Schafer<sup>38</sup> who suggested a sealed quartz tube reaction of TiCl<sub>3</sub> (1.8g; 0.01moles) and TiO<sub>2</sub> (0.3g; 0.003moles) mixture in a temperature gradient of 550°C - 650°C. We used the same synthetic procedure and were completely satisfied with the product in terms of purity, quality and quantity.

This synthetic method proceeds by the redox reaction described by the following equation (17):



TiCl<sub>4</sub> and an excess of TiCl<sub>3</sub> can be easily removed by washing the sample with dimethylformamide, ethanol, and ether. Pure TiOCl is a large flat brown shiny crystals which are hard to break and not moisture or air sensitive.

All characterisations of the product were done by PXRD, TGA and XRF. The powder pattern of TiOCl is shown in Figure 8. The comparison of calculated and experimentally obtained powder patterns is presented in Table VI. Powder XRD shows that obtained TiOCl crystals are pure and not contaminated by unreacted starting materials.

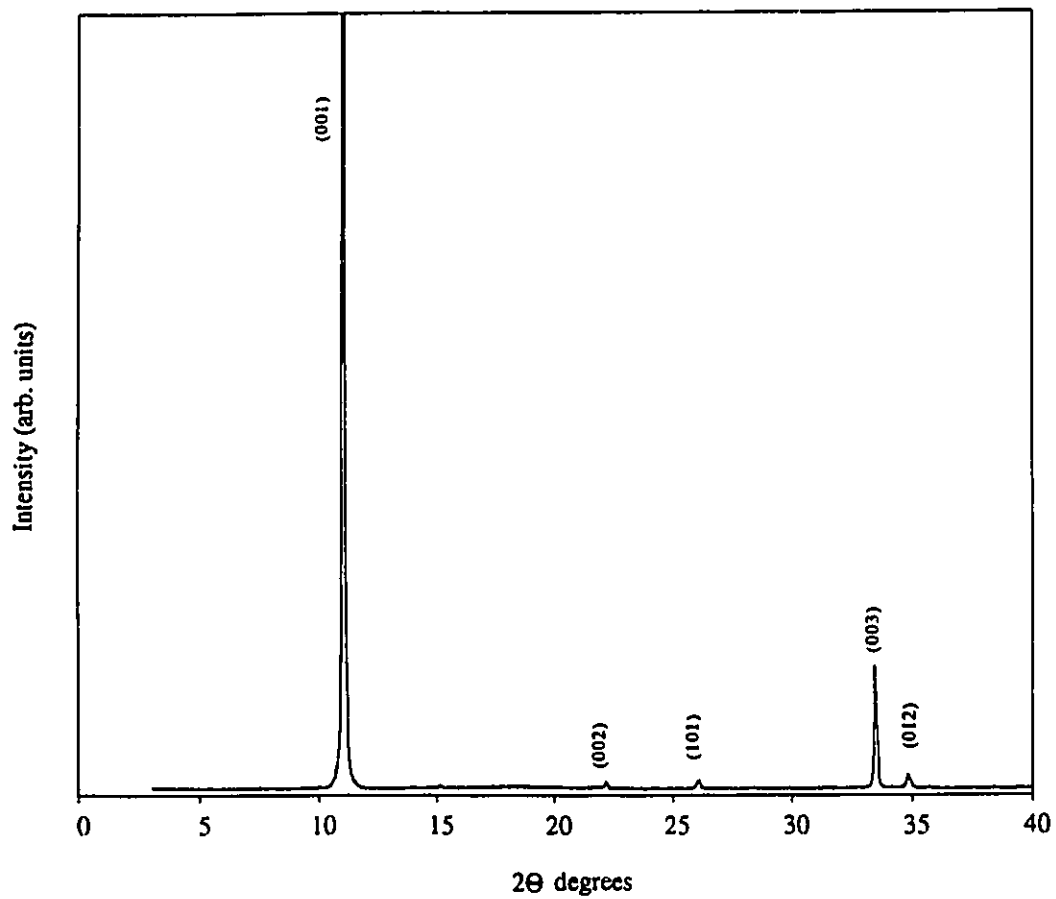


**Figure 8** Powder XRD spectrum of TiOCl

Table VI

Calculated and experimental powder patterns for TiOCl

Calculated		h k l	Experimental	
d-space (Å)	rel. intensity %		d-space (Å)	rel. intensity %
8.03	100	0 0 1	7.96 (8.01)*	100
4.01	2.0	0 0 2	4.00	0.2
3.42	69.0	1 0 1	3.41	0.3
3.11	1.0	0 1 1		
2.75	1.0	1 0 2		
2.67	0.0	0 0 3	2.67	2.9
2.58	60.0	0 1 2	2.57	0.4
2.52	0.0	1 1 0		
2.40	15.0	1 1 1		
2.18	1.0	1 0 3		

\* - Usually peak at the lower angle gives not precise d-spacing value. We used 002 and 003 peaks to calculate the real d-space.

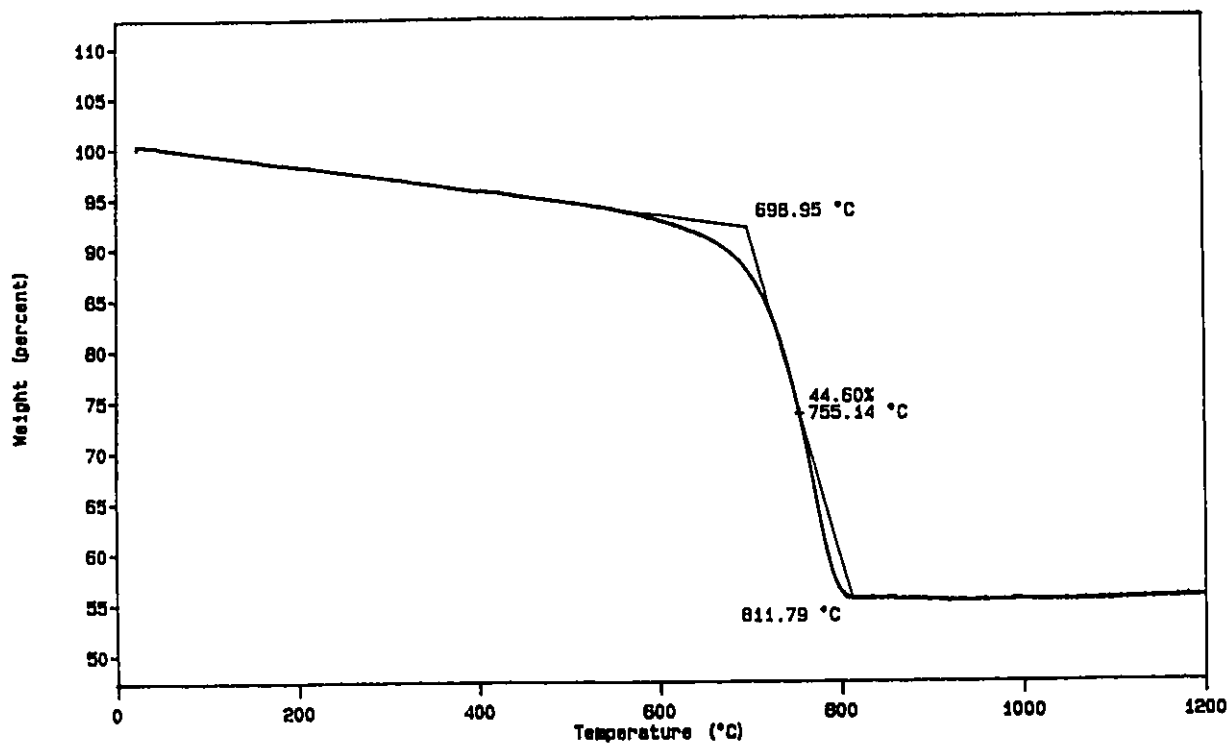


Figure 9 TGA curve of TiOCl

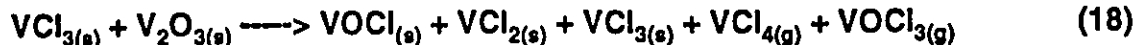
The thermal analysis curve (Figure 9) consists of only one weight loss at 755°C with a corresponding loss of 44.6% of the sample weight. This weight loss is consistent with the decomposition of  $\text{TiOCl}$  to  $\text{TiCl}_3$  and formation of  $\text{Ti}_2\text{O}_3$ , that was confirmed by PXRD.

XRF analysis gave the anticipated 1:1 ratio for Ti:Cl.

## 2. Synthesis of VOCl.

The solid state VOCl synthesis was first described by Schafer<sup>40</sup> and involved reaction of  $\text{VCl}_3$  and  $\text{V}_2\text{O}_3$  in a sealed quartz tube in a molar ratio 2:1. This procedure was applied in our laboratory but the product was of low quality in less than 50% yield. By varying the starting material ratio, and the range of the temperature gradient, it was determined that the ideal reaction conditions were close to 1.8  $\text{VCl}_3$  : 1.0  $\text{V}_2\text{O}_3$  ratio set along a 620° - 580°C gradient for 60 hours<sup>62</sup>.

The VOCl product obtained from the sealed tube reaction consisted mostly of dark brown VOCl powder located only in the hot end of the tube, and a small amount of large flat reddish - brown VOCl crystals located in the middle part of the sealed tube. Ehrlich and Siefert<sup>63</sup> have reported that the VOCl crystals could be a result of a vapour phase transport of volatile  $\text{VOCl}_2$ , which disproportionates to VOCl and  $\text{VOCl}_3$ . The balanced equation for the VOCl synthesis is not yet clear and the reaction can be described by the following general equation (18):



The major impurity in this reaction is green  $\text{VCl}_2$  crystals and powder. Any residual  $\text{VCl}_3$ ,  $\text{VCl}_4$ , and  $\text{VOCl}_3$  can be removed by washing the sample with dimethylformamide, ethanol and ether.

$\text{VOCl}$  crystals suitable for single crystal X-ray crystallography have not been obtained. Thus all characterisations were based on PXRD (Figure 10), TGA and XRF techniques. The powder pattern of  $\text{VOCl}$  is presented in Table VII. The interlayer spacing of our  $\text{VOCl}$  was 7.89 Å a value that differs by 0.04 Å from the reported one equal to 7.93 Å<sup>37</sup>.

The major problem involved in synthesis of  $\text{VOCl}$  is contamination of the product by  $\text{VCl}_2$ . This contamination mostly occurs during opening of the sealed tube when physical mixing of the products occur. Unfortunately our  $\text{VOCl}$  samples are sometimes contaminated with  $\text{VCl}_2$  impurity. Since  $\text{VCl}_2$  is very inert to the chemical reactions we carried out, its presence was monitored but did not appear to effect the reaction under investigation.

Thermal analysis showed two weight losses observed at 730°C (23% weight loss) and 880°C (15% weight loss) (Figure 11).

A V/Cl ratio of 1 was obtained by XRF for our  $\text{VOCl}$  samples.

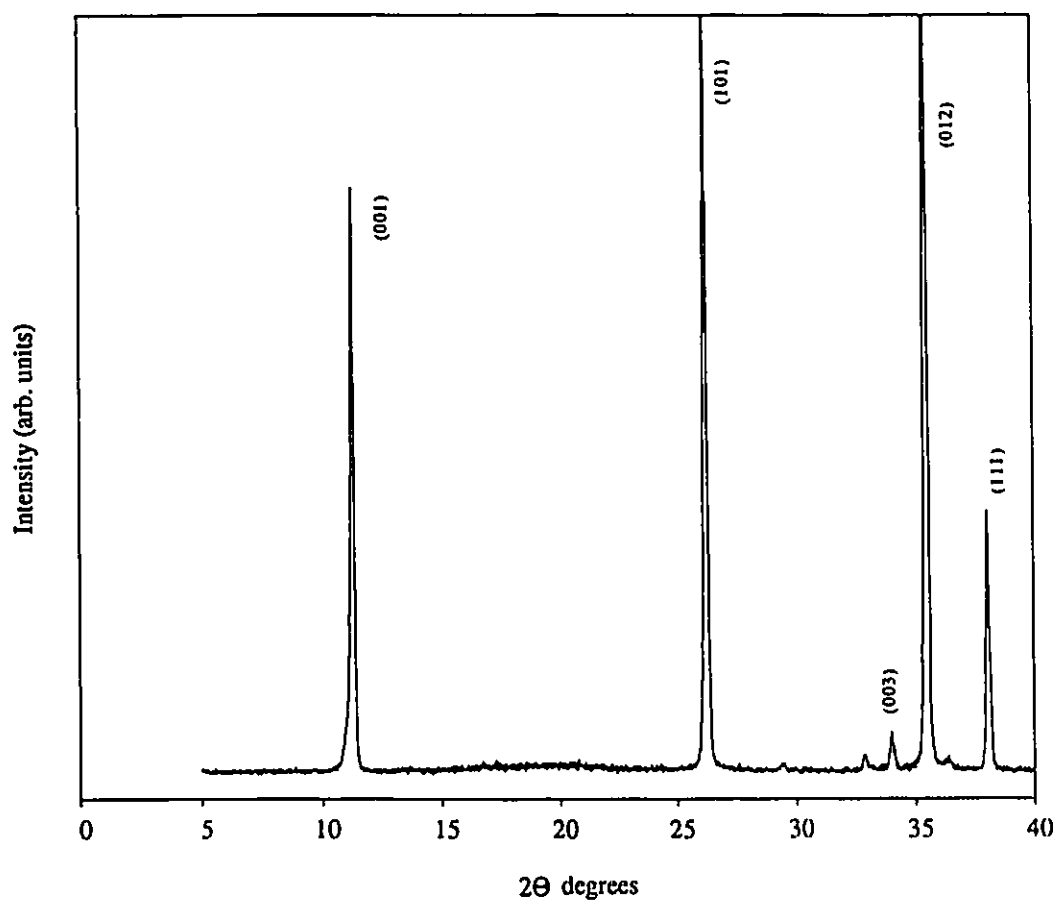


**Figure 10** Powder XRD spectrum of VOCl<sub>3</sub>

**Table VII**  
Powder pattern of VOCl

d-space (Å)	rel. intensity %	h k l	2 $\theta$ degrees
7.80 (7.89)*	100	0 0 1	11.33
3.38	10.9	1 0 1	26.29
2.63	2.1	0 0 3	34.05
2.52	13.8	0 1 2	35.51
2.36	2.5	1 1 1	38.07

\* - 003 peak was used to calculate d-space of VOCl

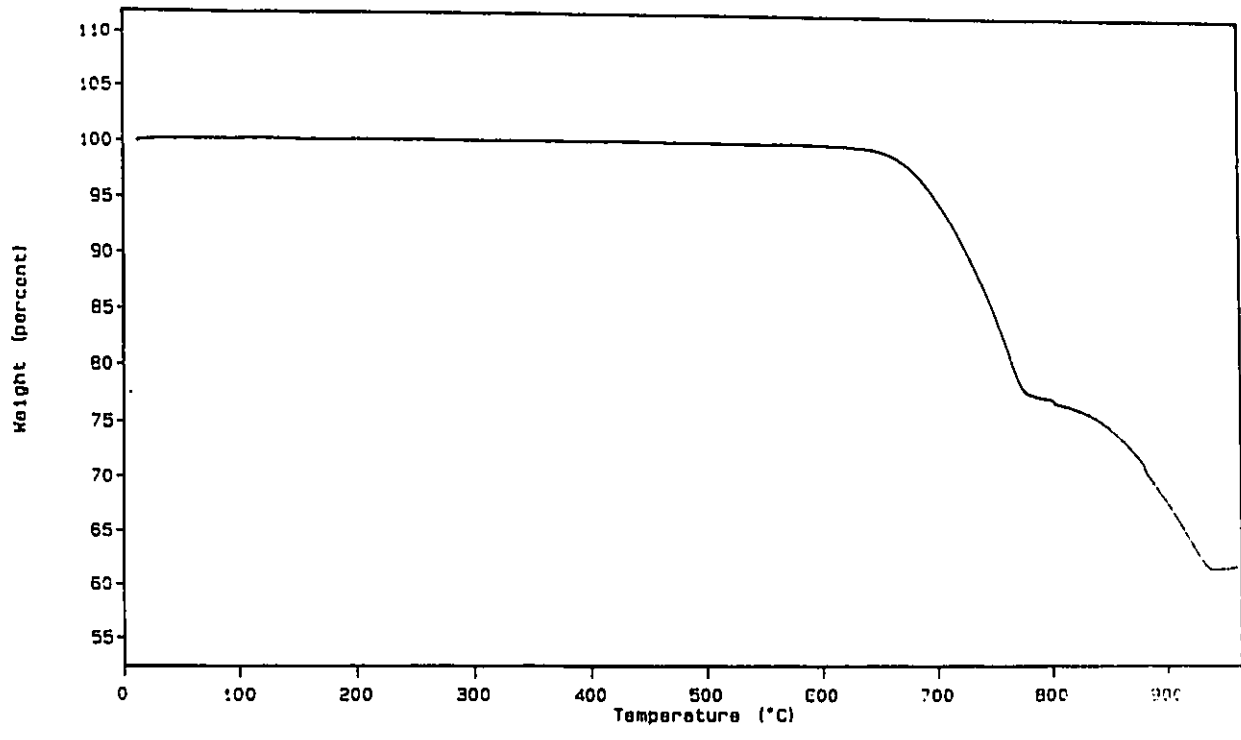


Figure 11 TGA of VOCl

### **Topochemical reactions of TiOCl and VOCl layered compounds.**

Although the existing literature gives substantial support to the idea that metal oxychlorides can undergo topochemical reactions, the features that control the intercalation process are complicated and not completely clear. It is quite clear that many intercalation reactions involving a variety of substrates and hosts other than MOX proceed via redox process. We have attempted to probe these features by a number of experiments involving quite wide range of substrates.

Substrates that have very different tendency to be oxidized were chosen as the guest molecules for intercalation reactions of TiOCl and VOCl hosts. In order to better understand the mechanism and driving forces of intercalation reaction of metal oxychlorides we chose guest molecules that possess reactive protons. The size of the guest molecules is also an important aspect in intercalation chemistry and we attempted to study the dependence of the layer expansion with the size of intercalated molecule. From these studies we hoped to give an idea about the orientation of the guest molecule inside the host.

In order to study the issues that control the intercalation process, we decided to perform the experiments with the following guest molecules:

1. Molecules displaying an oxidation potentials within a wide range, such as tertiary, secondary, primary, and aromatic amines; tertiary, secondary, and primary amides.
2. Molecules that contain reactive protons bound to nitrogen atoms (e.g. ethylenediamine, N,N'-dimethylethylenediamine, diethylenetriamine, N-methylformamide, and acetamide).

3. Molecules of different size and shape such as ethylenediamine, N,N,N',N'-tetramethylethylenediamine and pyridine.

The results of reactions with different substrates are discussed below.

## Reactions of TiOCl with amines.

Reactions of TiOCl with diamines, triamines and aromatic amines have never been reported in a literature. Various diamines and triamines are available with different redox properties, different numbers of active protons, and different molecular size. Diamines and triamines are flexible molecules, and contain two/three functional amino groups. These guest molecules can be oriented in a variety of ways inside the host thereby creating diverse layer expansions. Diamine and triamine molecules can be coordinated to two parallel TiOCl layers and form interlayer bridging, can lie parallel to the layers and be coordinated to the titanium ions within the same layer, or can be tilted with respect to the layers. Aromatic amines (e.g. pyridine) are planar molecules with their nitrogen lone pair more accessible which may play a role in the rate of intercalation. With this fact in mind, primary, secondary, and tertiary diamines, primary triamine and aromatic amine became guest molecules of our interest.

### 1. Reactions of TiOCl with N,N'-dimethylethylenediamine [CH<sub>3</sub>(H)N-CH<sub>2</sub>-CH<sub>2</sub>-N(H)CH<sub>3</sub>]

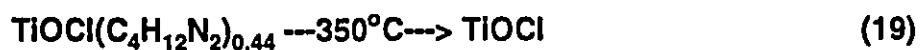
N,N'-dimethylethylenediamine contains two amine protons, one on each of the two nitrogen atoms. It was our interest to examine the influence of these protons on the intercalation process and establish possible participation in topochemical substitution reactions.

### 1.1 Reaction in a sealed tube at 80°C.

The first reaction to be studied took place in a sealed evacuated tube. Heating a mixture of TiOCl and DMEN in a sealed glass tube at 80°C for 2 days resulted in the formation of a dark blue product. Powder XRD spectrum of the dark blue solid (Figure 12) indicated the formation of a new intercalated compound with d-spacing 11.38Å and presence of unreacted starting material TiOCl with d-space 8.00Å. The powder pattern of the reaction product is presented in Table VIII.

A formulation of  $\text{TiOCl}(\text{C}_4\text{H}_{12}\text{N}_2)_{0.44}$  came from thermal analysis results. The TGA curve of the dark blue solid (Figure 13) consists of only one weight loss at 283°C (26.3% of the sample weight) that can be attributed to decomposition of the intercalated compound. The absence of the 755°C weight loss on the TGA curve indicates the small amount of unreacted TiOCl in the analysed sample (figure 9). In comparison to TGA, powder XRD is able to observe even a very small amount of TiOCl due to its very crystalline nature. According to our results, the amount of unreacted starting material is very small and could come from the walls of a sealed tube. During formulation calculations the presence of TiOCl was ignored.

The material remaining in a pan was confirmed to be TiOCl by PXRD. The thermal analysis result can be described by equation 19:



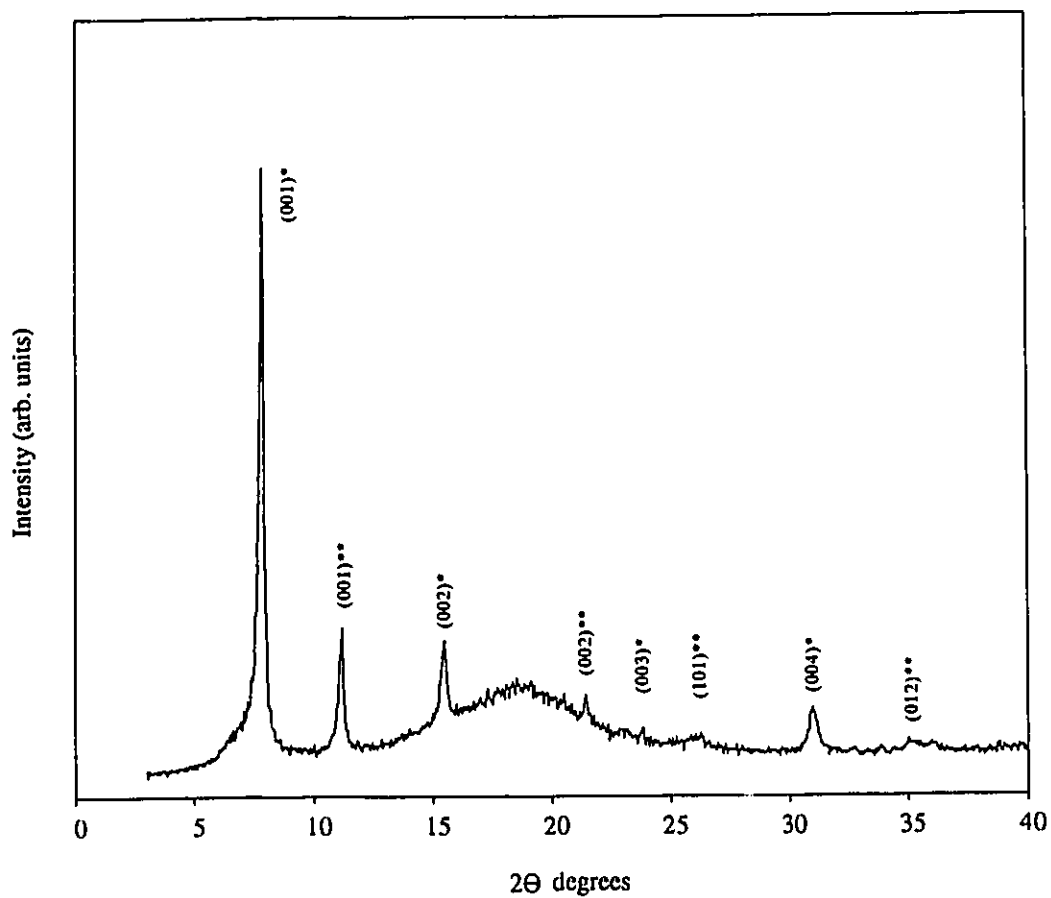


**Figure 12** PXRD spectrum of the product obtained during a sealed tube reaction of TiOCl with DMEN

Table VIII

Powder pattern of the product obtained during a sealed tube reaction of TiOCl with DMEN

d-space (Å)	rel. intensity %	h k l	2θ degrees	comments
11.25 (11.38) <sup>(a)</sup>	100	0 0 1	7.85	TiOCl(C <sub>4</sub> H <sub>12</sub> N <sub>2</sub> ) <sub>0.44</sub> *
7.91 (8.00) <sup>(b)</sup>	12.8	0 0 1	11.16	TiOCl**
5.71	6.9	0 0 2	15.50	*
4.00	1.4	0 0 2	21.44	**
3.73	0.5	0 0 3	23.79	*
3.41	0.4	1 0 1	26.10	**
2.88	2.0	0 0 4	30.99	*
2.55	0.4	0 1 2	35.08	**

\* - peaks related to a new intercalated compound TiOCl(C<sub>4</sub>H<sub>12</sub>N<sub>2</sub>)<sub>0.44</sub>

\*\* - peaks of TiOCl

(a) - d-space of an intercalated compound was calculated by using 002, 003, and 004 peaks

(b) - d-space of TiOCl was calculated by using 002 peak

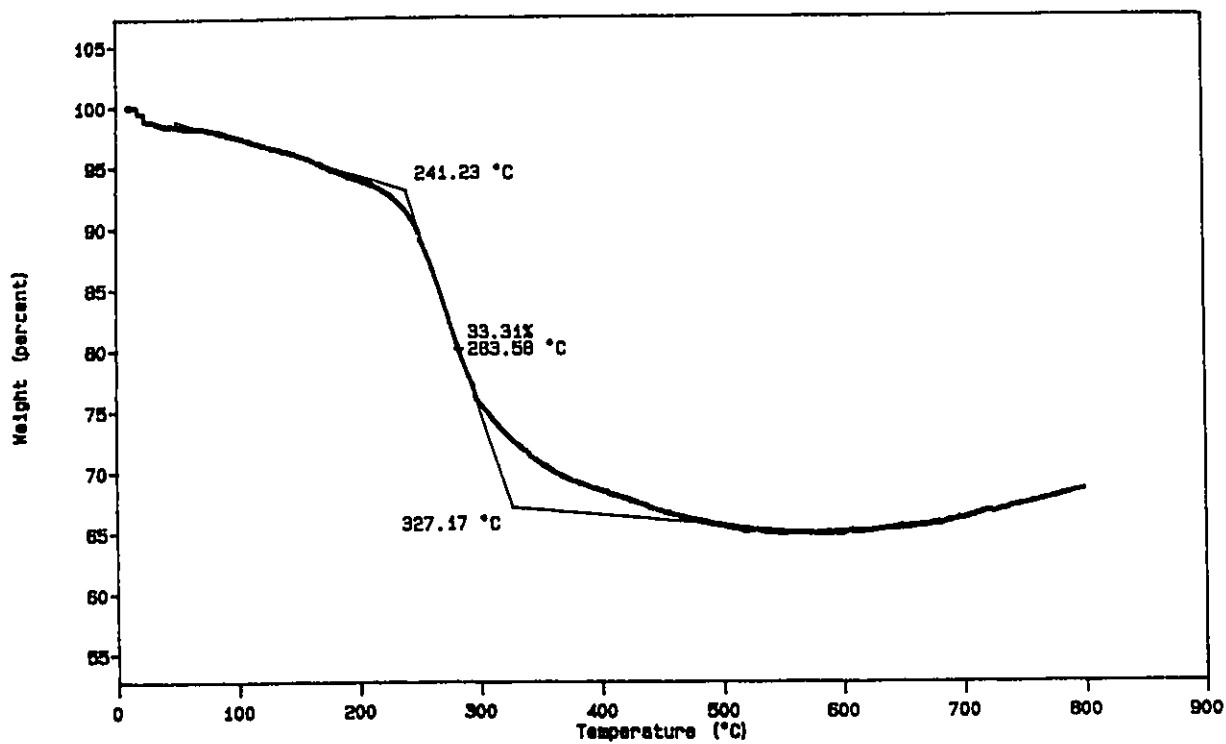


**Figure 13** TGA of the product obtained during a sealed tube reaction of  $\text{TiOCl}$  with DMEN

Based on the fact that intercalated DMEN molecules expanded the layers of the host by 3.38Å we can propose an orientation of DMEN molecules between the TiOCl layers. Based on estimating the length of 1.3Å for the C-C bond, and 1.47Å for the C-N bond for an extended DMEN molecule, we propose that this expansion value is most consistent with guest molecules tilted at angles at about 28° to the host layers.

### 1.2 Reaction in a Schlenk flask at 80°C.

In this case DMEN was vacuum transferred into a Schlenk flask containing TiOCl. The mixture of TiOCl and DMEN was heated at 80°C for 2 weeks. As soon as the colour of the solid changed from dark brown to dark blue-grey, and DMEN solution became cloudy, the reaction was stopped. The DMEN solution was removed under vacuum because the cloudy appearance of the solution could indicate the formation of the ammonium hydrochloride salt ( $[H(H)(CH_3)N-CH_2-CH_2-N(CH_3)(H)(H)H]^2+2Cl^-$ ) DMEN-salt which would be useful to examine by PXRD.

The product isolated from this reaction seemed to be a mixture of two different coloured solids: one dark blue-grey and the other white. The mixed product was characterised by PXRD (Figure 14). PXRD pattern of the reaction product is presented in Table IX.

The analysis of the PXRD pattern of the product obtained during this reaction of TiOCl with DMEN indicated four different compounds. One of them is unreacted TiOCl (d-space 8.01Å) while the other three compounds were formed during the reaction.

The first compound appears to be a new solid with d-space 11.60Å (layer expansion

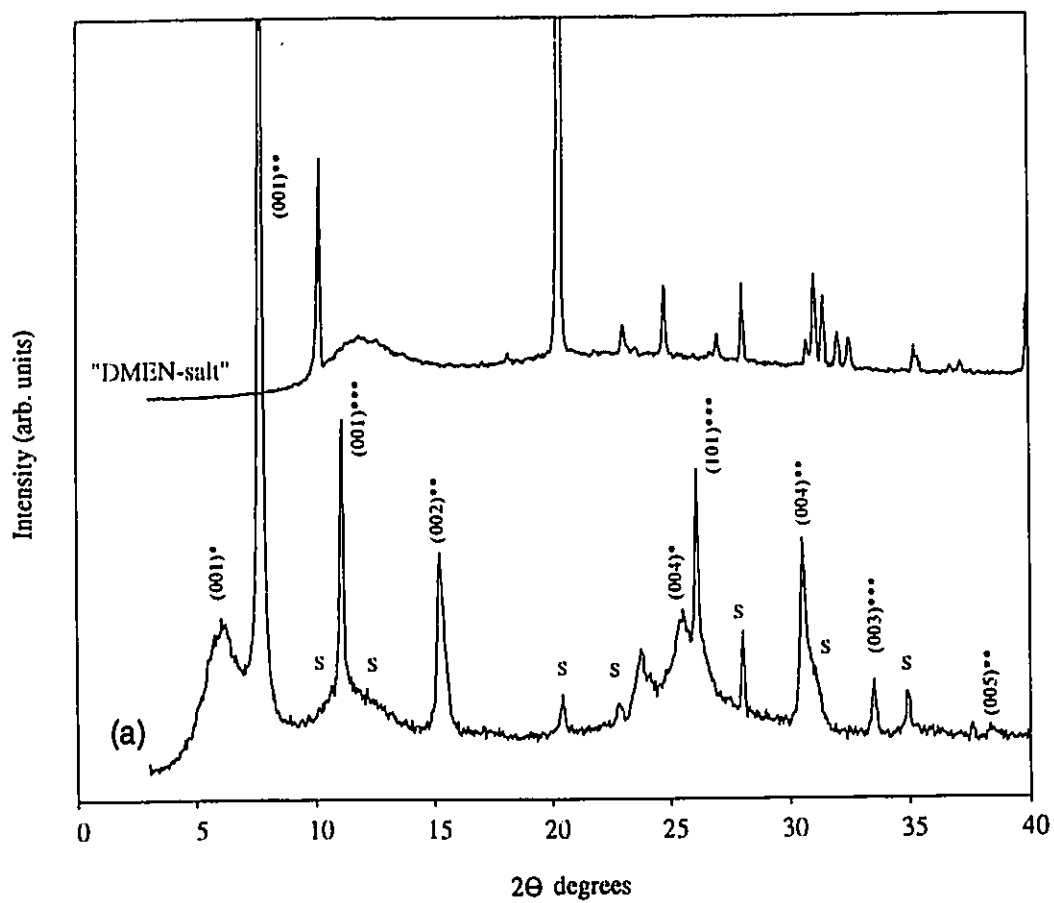


**Figure 14** (a) PXRD spectrum of the product obtained during a Schlenk flask reaction of  $\text{TiOCl}$  with DMEN.

(b) PXRD spectrum of the DMEN-salt  $[\text{H}(\text{H})(\text{CH}_3)\text{N}-\text{CH}_2-\text{CH}_2-\text{N}(\text{CH}_3)(\text{H})\text{H}]^{2+}2\text{Cl}^-$

Table IX

Powder pattern of the product obtained during a Schlenk flask reaction of TiOCl with DMEN

d-space	rel. intensity %	h k l	2 $\Theta$ degrees	comments
14.27	17.9	0 0 1	6.18	TiOCl <sub>x</sub> (C <sub>4</sub> H <sub>12-n</sub> N <sub>2</sub> ) <sub>y</sub> <sup>*</sup>
11.40 (11.60) <sup>(a)</sup>	100	0 0 1	7.74	TiOCl(C <sub>4</sub> H <sub>12</sub> N <sub>2</sub> ) <sub>x</sub> <sup>**</sup>
7.92 (8.01) <sup>(b)</sup>	23.6	0 0 1	11.16	TiOCl <sup>***</sup>
5.80	10.9	0 0 2	15.24	**
4.34	1.9		20.44	salt
3.89	1.2		22.82	salt
3.74	3.3		23.77	
3.48	4.5	0 0 4	25.57	*
3.40	9.5	1 0 1	26.14	***
3.17	3.3		28.04	salt
2.92	5.9	0 0 4	30.55	**
2.67	1.6	0 0 3	33.53	***

Table IX ( continue )

d-space (Å)	rel. intensity %	h k l	2 $\Theta$ degrees	comments
2.56	1.1		34.94	salt
2.34	0.2	0 0 5	38.41	**

\* - peaks related to the substituted product  $\text{TiOCl}_x(\text{C}_4\text{H}_{12-n}\text{N}_2)_y$  (  $n = 1$  or  $2$  )

\*\* - peaks related to the intercalated compound  $\text{TiOCl}(\text{C}_4\text{H}_{12}\text{N}_2)_x$

\*\*\* - peaks of  $\text{TiOCl}$

salt - peaks of the DMEN-salt  $[\text{H}(\text{H})(\text{CH}_3)\text{N}-\text{CH}_2-\text{CH}_2-\text{N}(\text{CH}_3)(\text{H})\text{H}]^{2+}2\text{Cl}^-$  (see Table XIII)

(a) - d-space was calculated by using 002 and 003 peaks

(b) - d-space was calculated by using 003 peak

is 3.59Å) which was observed in the previous reaction of TiOCl with DMEN in a sealed tube at 80°C and can be attributed to the intercalated product  $\text{TiOCl}(\text{C}_4\text{H}_{12}\text{N}_2)_{0.44}$ . In order to confirm that the second material was the DMEN-salt, the salt was independently synthesised and the XRD is shown in Figure 14 (see section 1.4). Based on the formation of the DMEN-salt we can propose that the third compound, with d-space 14.27Å (layered expansion 6.26Å), is a new organic derivative  $\text{TiOCl}_x(\text{C}_4\text{H}_{12-n}\text{N}_2)_y$  of the layered compound TiOCl derived through a substitution reaction.

This result clearly demonstrated that the reaction of TiOCl with DMEN lead to the formation of both intercalated and substituted compounds, and they can be easily formed under mild conditions. Formation of the substituted compound probably goes through the formation of intercalated one, and our interest was to observe the transformation of one compound into another upon heating.

To observe this transformation, the reaction product that consists of four compounds (Figure 14), was heated in a glass tube under nitrogen flow for 4 days. Heating of the solid was performed in the absence of solution and the established temperature was 80°C. No colour change of the solid was observed during heating. The change in the PXRD of the solid after heating (Figure 15) in comparison to PXRD of the solid before heating (Figure 14) indicated a reaction had occurred. The sharp peak at  $2\Theta = 7.74^\circ$ , due to the intercalated compound  $\text{TiOCl}(\text{C}_4\text{H}_{12}\text{N}_2)_{0.44}$ , (figure 14) disappeared with concurrent increase of the broad peak at  $2\Theta = 6.18^\circ$  (figure 14) assigned to the substituted compound  $\text{TiOCl}_x(\text{C}_4\text{H}_{12-n}\text{N}_2)_y$ . The new d-spacing of the substituted product corresponded to 14.57Å, and a layered expansion of 6.56Å. Powder XRD analysis of the

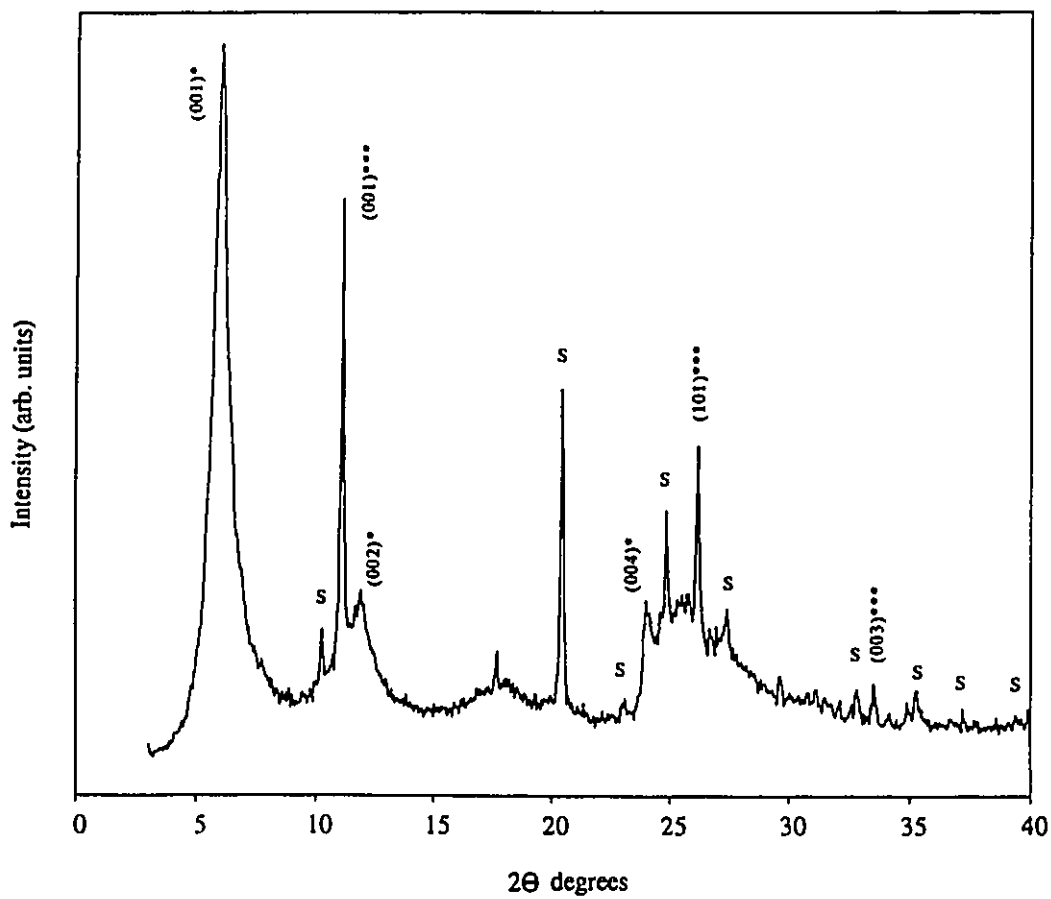


**Figure 15** PXRD spectrum of the product obtained during a Schlenk flask reaction of  $\text{TiOCl}$  with DMEN and heated for 4 days at  $80^\circ\text{C}$ .

Table X

Powder pattern of the product obtained during a Schlenk flask reaction of  $\text{TiOCl}$  with DMEN and heated at  $80^\circ\text{C}$  for 4 days.

d-space (Å)	rel. intensity %	h k l	2 $\theta$ degrees	comments
14.57 (14.57) <sup>(a)</sup>	100	0 0 1	6.06	$\text{TiOCl}_x(\text{C}_4\text{H}_{12-n}\text{N}_2)_y^*$
8.60	6.3		10.27	salt
7.91 (8.01) <sup>(b)</sup>	34.0	0 0 1	11.17	$\text{TiOCl}^{***}$
7.28	8.1	0 0 2	11.97	*
5.01	2.9		17.67	
4.33	15.6		20.45	salt
3.65	4.1	0 0 4	23.96	*
3.57	8.3		24.86	salt
3.40	10.3	1 0 1	26.18	***
3.25	4.0		27.40	salt
3.01	1.6		29.64	salt
2.87	1.1		31.10	salt

Table X ( continue )

d-space (Å)	rel. intensity %	h k l	2θ degrees	comments
2.78	0.5		32.05	salt
2.72	1.0		32.81	salt
2.67	1.2	0 0 3	33.51	***
2.54	1.0		35.27	salt

\* - peaks related to the substituted compound  $\text{TiOCl}_x(\text{C}_4\text{H}_{12-n}\text{N}_2)_y$

\*\*\* - peaks of  $\text{TiOCl}$

salt - peaks of the salt  $[\text{H}(\text{H})(\text{CH}_3)\text{N}-\text{CH}_2-\text{CH}_2-\text{N}(\text{CH}_3)(\text{H})\text{H}]^{2+}2\text{Cl}^-$  ( see Table XIII )

(a) - d-space was calculated by using 002 and 004 peaks

(b) - d-space was calculated by using 003 peak

product after heating clearly demonstrated the transformation of the intercalated product into the substituted one.

The powder pattern (Table X) of the product after heating also indicated the presence of DMEN-salt, which also became more crystalline relative to the starting material. The presence of the salt is also supported by infrared data. An absorption bands at 2449, 2360, 2160 and 850  $\text{cm}^{-1}$  appeared due to the salt formation and can be attributed to the N-H and N-C vibration modes of the salt.

Thermogravimetric analysis of the product after this heat treatment (Figure 16) showed three weight losses that can be attributed to the decomposition of the three compounds present in the product: substituted compound, DMEN-salt, and unreacted  $\text{TiOCl}$ . The first weight loss of 25% was observed at 310°C and can be assigned to the loss of the salt  $[\text{H}(\text{H})(\text{CH}_3)\text{N}-\text{CH}_2-\text{CH}_2-\text{N}(\text{CH}_3)(\text{H})\text{H}]^{2+}2\text{Cl}^-$ . The second weight loss occurred at 504°C (10%) and demonstrated the decomposition of the substituted compound  $\text{TiOCl}_x(\text{C}_4\text{H}_{12-n}\text{N}_2)_y$ . The third weight loss occurred at 700°C (10.87%) and indicated on the decomposition of unreacted  $\text{TiOCl}$ . Thermal analysis of intercalated and substituted compounds showed that the substituted compound decomposes at a higher temperature ( $T = 504^\circ\text{C}$ , figure 16) than the intercalated one ( $T = 283^\circ\text{C}$ , figure 13). This is likely due to formation of a bond between the inorganic layer and the organic molecule. Thus indicating that the DMEN molecules are directly bonded to the titanium metal centres in the  $\text{TiO}$  double layers via its own nitrogen atoms.

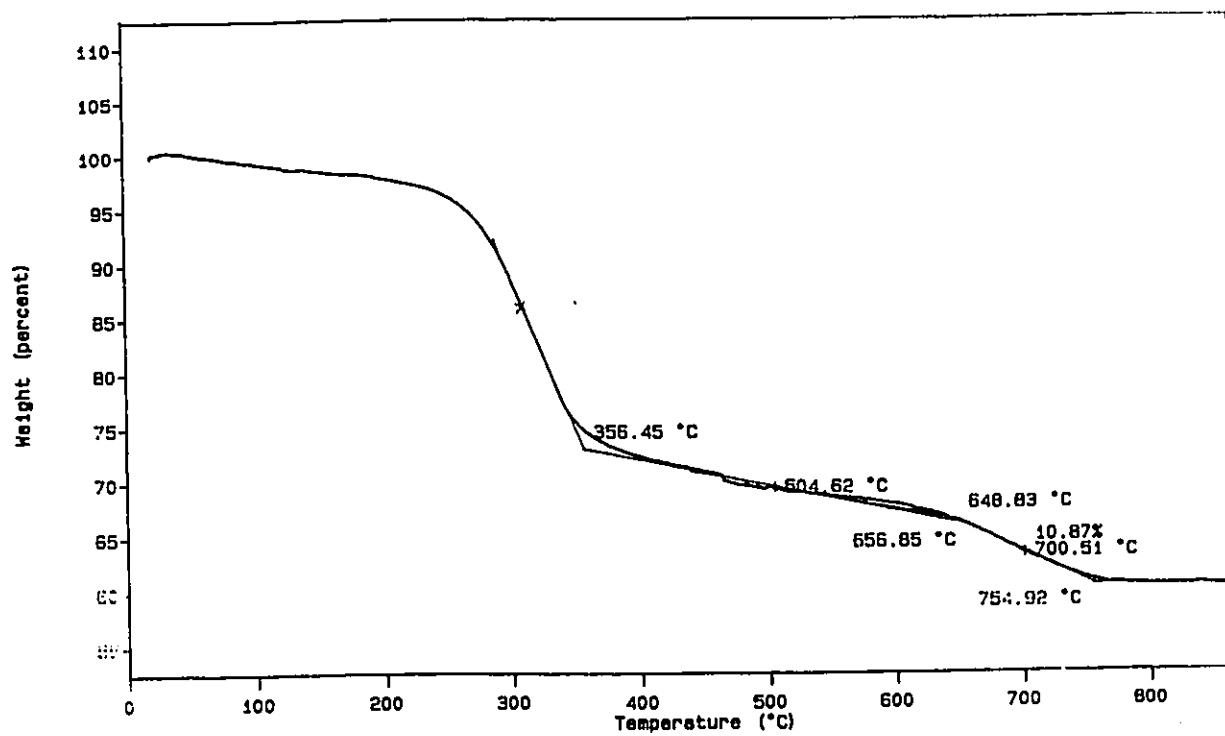


**Figure 16** TGA of the product obtained during a Schlenk flask reaction of  $\text{TiOCl}$  with DMEN and heated to  $80^\circ\text{C}$  for 4 days

### 1.3 DMEN-salt removal.

DMEN-salt, present in the product along with substituted compound and unreacted  $\text{TiOCl}$ , can be easily removed from the mixture by its sublimation or by washing the product with amine. The first method was chosen due to convenience of temperature control and cleaner operation. The product was heated to  $360^\circ\text{C}$  under  $\text{N}_2$  flow in the TGA apparatus. The final shiny grey product was obtained in the TGA pan.

This material was examined by PXRD (Figure 17). Powder XRD showed only the presence of unreacted  $\text{TiOCl}$  and a new compound with d-spacing equal  $10.12\text{\AA}$ . All of the DMEN-salt was removed from the sample. The powder pattern of the final shiny grey product is presented in Table XI.

The interlayer distance of the product before salt removal was  $14.57\text{\AA}$ . The d-spacing decreased to  $10.12\text{\AA}$  ( layered expansion is  $2.11\text{\AA}$  ) when the product was heated to  $360^\circ\text{C}$  using TGA. So, the result showed that after salt sublimation, the layers collapsed and the d-spacing of the shiny grey substituted compound became  $10.12\text{\AA}$ .

The IR spectrum of the final product showed an absorption bands at  $1718$  and  $1261\text{ cm}^{-1}$  that can be attributed to the N-H and C-N vibration modes of the amine. The IR spectrum exhibited an N-H vibration mode that indicate the participation of only one  $\text{H}(\text{CH}_3)_\text{N}$ - group in the substitution process.

Thermogravimetric analysis of the final shiny grey product (Figure 18) showed two decomposition steps. The first step was observed at  $506^\circ\text{C}$  (13.2%) and can be assigned as the decomposition of the substituted compound  $\text{TiOCl}_x(\text{C}_4\text{H}_{12-n}\text{N}_2)_y$ . The second decomposition step occurred at  $700^\circ\text{C}$  (12.0%) and indicated the decomposition of

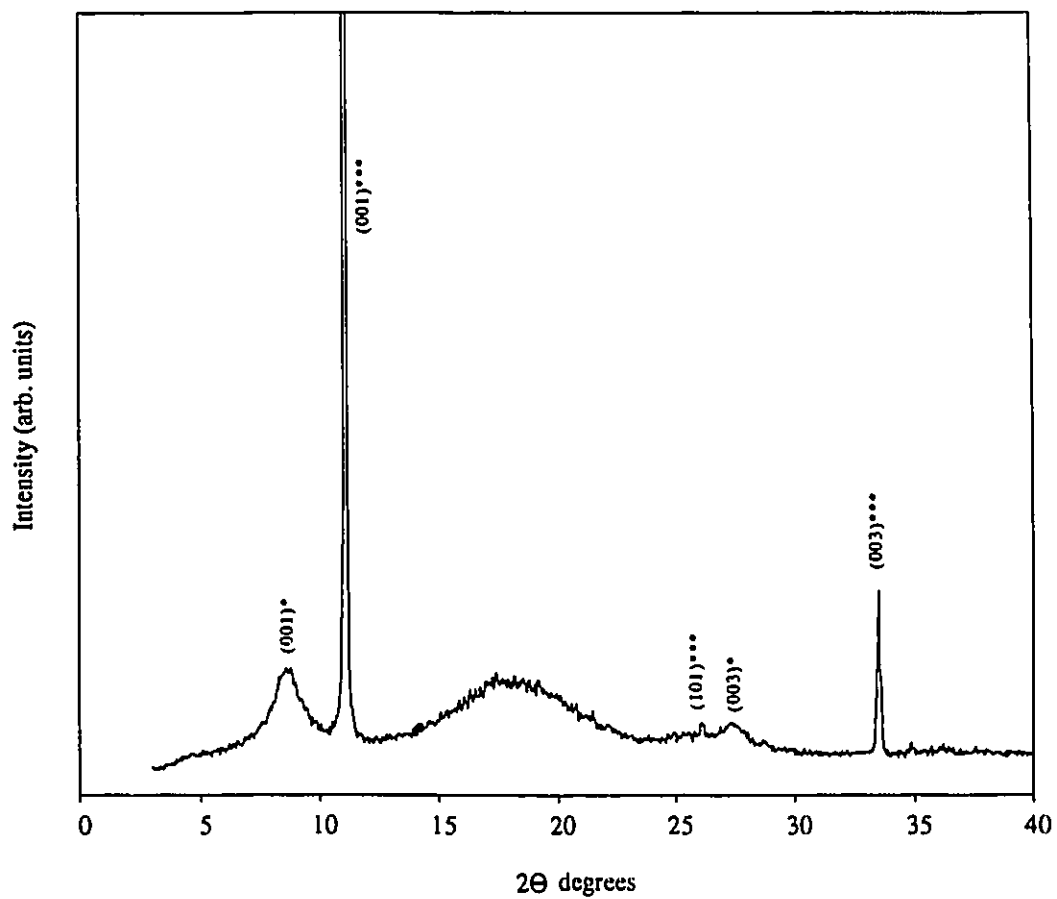


**Figure 17** PXR D of the final product of the reaction of TiOCl with DMEN

Table XI

Powder pattern of the final product of the reaction of TiOCl with DMEN

d-space (Å)	rel. intensity %	h k l	2 $\theta$ degrees	comments
10.12	7.9	0 0 1	8.73	TiOCl(C <sub>4</sub> H <sub>11</sub> N <sub>2</sub> ) <sub>y</sub> *
7.95 (8.01) <sup>(a)</sup>	100	0 0 1	11.11	TiOCl***
3.40	0.8	1 0 1	26.12	***
3.37	0.8	0 0 3	27.40	*
2.67	5.4	0 0 3	33.50	***

\* - peaks related to the substituted compound TiOCl<sub>x</sub>(C<sub>4</sub>H<sub>11</sub>N<sub>2</sub>)<sub>y</sub>

\*\*\* - peaks of TiOCl

(a) - d-space was calculated by using 003 peak

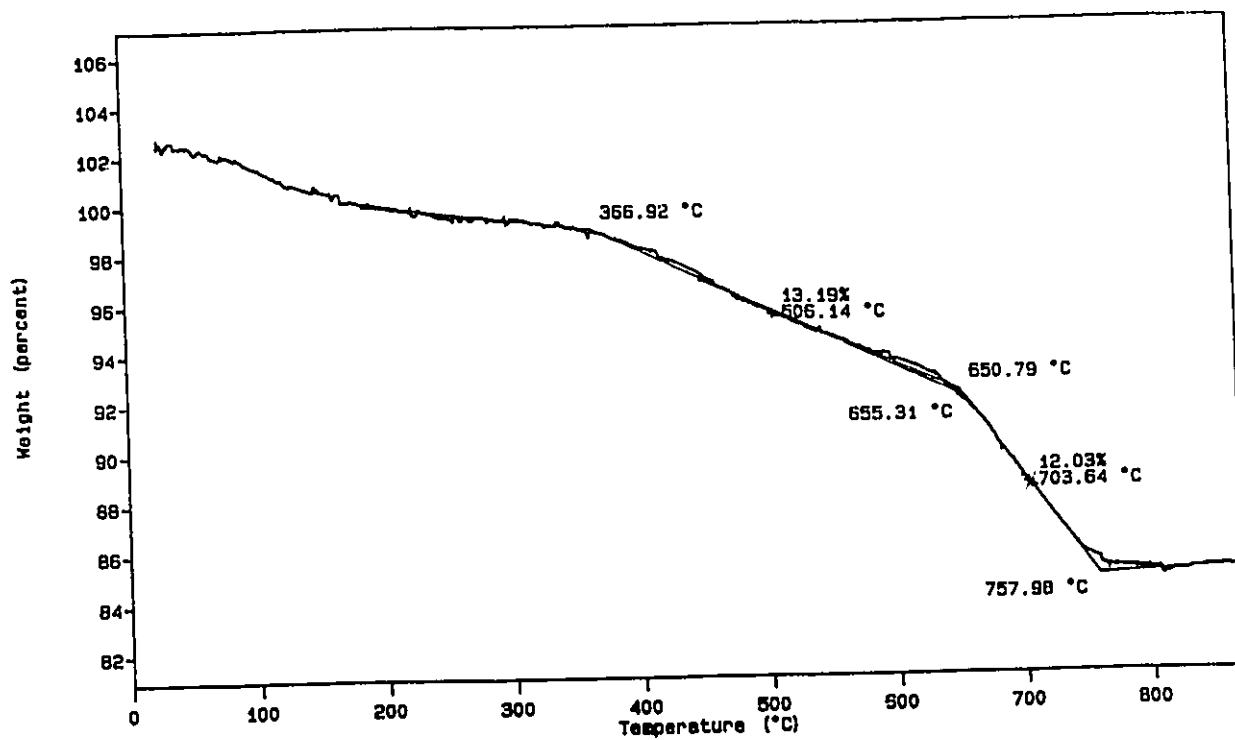


**Figure 18** TGA of the final product of the reaction of TiOCl with DMEN

unreacted TiOCl. The thermogravimetric analysis result is consistent with a previously obtained one (Figure 16) and shows that the final product is free of salt.

Chemical analysis of the final product gave the following experimental data: %C (3.09); %H (1.26); %N (0.76). X-ray fluorescence showed the ratio of Ti to Cl equal to 4.

Unfortunately, we were not able to determine the formulation of the final substituted product due to the presence of unreacted TiOCl. At the beginning we assumed that all chlorine ions detected by XRF (the ratio Ti:Cl equal to 4:1) could come with unreacted TiOCl (our final shiny grey product is a mixture of unreacted TiOCl and the substituted compound) but calculated formulation for the substituted product did not fit the elemental analysis data. The only conclusion which we can make so far is the following:

- the new substituted product has d-space 10.12Å (layered expansion is 2.11Å);
- the substituted product contain some chlorine ions resulting in the formulation  $\text{TiOCl}_x(\text{C}_4\text{H}_{11}\text{N}_2)_y$ ;
- only one proton adjacent to nitrogen atom participated in the substituted process.

Three model structures can be proposed for the substituted product: an interlayer bridging model, the intralayer bonding model, and the model where only one end of the organic molecule is bonded to the layer and molecules are tilted to the layers of the host. The first model is illustrated in Figure 19a. The estimated bond lengths used in these calculations are 1.5Å for the Ti-N bond, 1.47Å for the N-C bond and 1.3Å for the C-C bond when they are projected in the direction perpendicular to the layer. The interlayer distance for the first model is calculated to be below 8.02Å (d-space of TiOCl) even if the

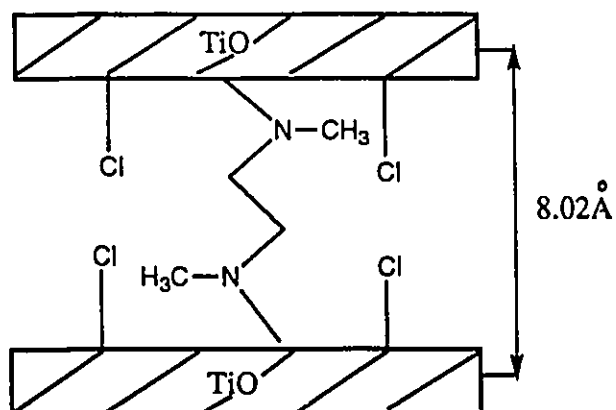


**Figure 19a** An interlayer bridging model for  $\text{TiOCl}_x(\text{C}_4\text{H}_{11}\text{N}_2)_y$

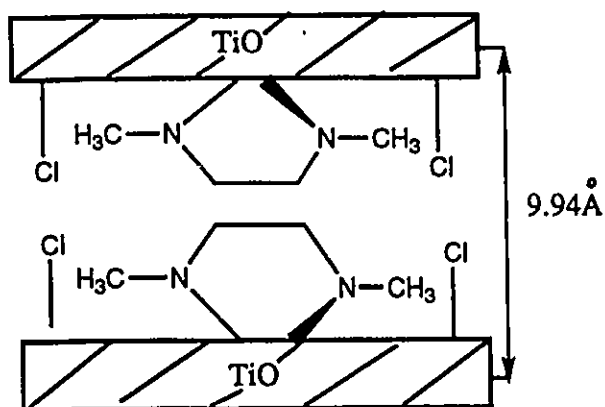


**Figure 19b** The intralayer bonding model for  $\text{TiOCl}_x(\text{C}_4\text{H}_{11}\text{N}_2)_y$

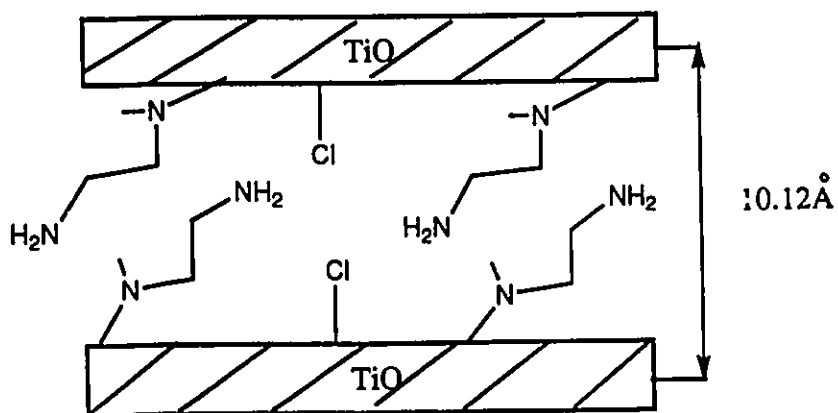


**Figure 19c** Model structure for  $\text{TiOCl}_x(\text{C}_4\text{H}_{11}\text{N}_2)_y$  represented by tilted guest molecules

molecules have the trans configuration in order to have the longest possible molecular length. The interlayer distance will be around  $10\text{\AA}$  if DMEN molecules coordinate to titanium ions within the same layer as shown in Figure 19b. The first model doesn't agree with the observed layer collapse. The second model involves participation of both protons adjacent to different nitrogen atoms in the substitution reaction and doesn't agree with IR data.

The third model (Figure 19c) is consistent with both the IR and layered expansion data. This model structure is also supported by the observed collapse of the layers during heating. The d-space of the product decreased from  $14.57\text{\AA}$  to  $10.12\text{\AA}$  when the DMEN-salt was removed by sublimation from the sample. The difference of  $4.45\text{\AA}$  could be due to DMEN-salt lying between layers of the host. After heating the sample to  $360^{\circ}\text{C}$  (salt removal), the interlayer space becomes less populated, the organic molecules become more oriented and strong interaction between DMEN molecules of upper and lower TiO double layers decreases the distance between layers.

A summary of reactions of TiOCl with N,N'-dimethylethylenediamine is presented in Table XII.

Table XII

Summary of reactions of TiOCl with N,N'-dimethylethylenediamine

Reaction conditions	d-space (Å)	layer exp. (Å)	product	comments
sealed tube 80°C, 2days	11.38	3.37	$\text{TiOCl}(\text{C}_4\text{H}_{12}\text{N}_2)_{0.44}$	intercalated prod. + TiOCl
Schl. flask 80°C, 14d	14.27	6.26	$\text{TiOCl}_x(\text{C}_4\text{H}_{12-n}\text{N}_2)_y$	subst. comp.
	11.60	3.59	$\text{TiOCl}(\text{C}_4\text{H}_{12}\text{N}_2)_{0.44}$	interc. comp TiOCl DMEN-salt ↓ 4d. heating
	14.57	6.56	$\text{TiOCl}_x(\text{C}_4\text{H}_{12-n}\text{N}_2)_y$	subst. comp. DMEN-salt TiOCl ↓ salt remov.
	10.12	2.11	$\text{TiOCl}_x(\text{C}_4\text{H}_{11}\text{N}_2)_y$	subst. product TiOCl unreact

#### 1.4 Synthesis of $[H(H)(CH_3)N-CH_2-CH_2-N(CH_3)(H)H]^2+2Cl^-$ ( DMEN-salt)

In order to confirm the DMEN-salt formation during topochemical substitution reaction of TiOCl with DMEN, the DMEN-salt was synthesised by adding HCl to DMEN. A white crystalline product was isolated and dried. The obtained DMEN-salt was characterised by PXRD (Figure 20). Powder pattern of the salt is presented in Table XIII. Thermogravimetric analysis showed only one weight loss at 327°C that corresponds to 100% of the sample weight.

The formulation  $[H(H)(CH_3)N-CH_2-CH_2-N(CH_3)(H)H]^2+2Cl^-$  is consistent with elemental analysis results (Table XIV).

**Table XIV**

EA results for  $[H(H)CH_3)N-CH_2-CH_2-N(CH_3)(H)H]^2+2Cl^-$

%	Calculated values	Experimental values
C	29.81	29.83
H	8.69	9.08
N	17.39	17.33

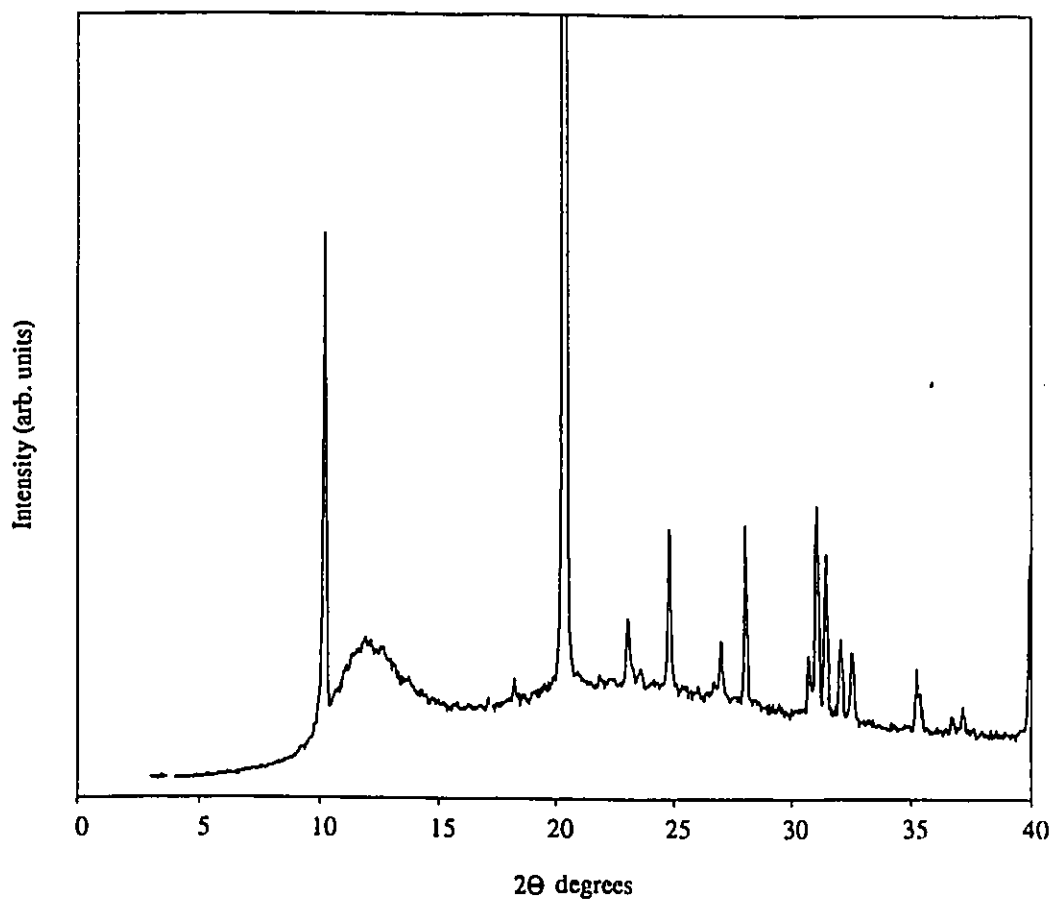


**Figure 20** PXRD of the DMEN-salt  $[H(H)(CH_3)N-CH_2-CH_2-N(CH_3)(H)H]^{2+}2Cl^-$

Table XIII

Powder pattern of the DMEN-salt  $[H(H)(CH_3)N-CH_2-CH_2-N(CH_3)(H)H]^2+2Cl^-$ 

d-value (Å)	relative intensity %	2 $\theta$ degrees
8.64	32.1	10.22
7.36	3.3	12.00
4.86	1.1	18.21
4.34	100	20.40
3.85	3.0	23.06
3.58	5.6	24.82
3.29	1.9	27.03
3.17	4.8	28.07
2.87	5.1	31.10
2.84	3.9	31.45
2.78	1.9	32.06
2.74	1.6	32.54
2.54	0.8	35.28
2.41	0.4	37.17

## Reactions of TiOCl with ethylenediamine [H<sub>2</sub>N-CH<sub>2</sub>-CH<sub>2</sub>-NH<sub>2</sub>]

Ethylenediamine molecules contain four active protons that can equally participate in topochemical substitution reaction. Different conditions were employed to reactions of TiOCl with EN.

### 2.1 Reactions of TiOCl with EN in a sealed tubes at 160° - 170°C.

A number of reactions of TiOCl with EN were done in sealed tubes for different length of time. The tubes containing TiOCl and EN were cooled in a liquid nitrogen, evacuated, sealed, and heated in the oven at 160° - 170°C for 2, 2.5 and 4 days. The dark grey/black products were isolated by removal of EN under vacuum and characterised by PXRD. PXRD gave only a broad featureless spectra indicating that the products formed were amorphous in nature. Based on the assumption that the reaction temperature was too high and had lead to the decomposition of EN and the products, we performed the next reactions under milder conditions.

### 2.2 Reaction in a Schlenk flask at 80°C.

Heating a mixture of TiOCl and EN in a Schlenk flask at 80°C for 5 days resulted in the formation of a dark blue-grey crystalline product. The EN solution was removed under vacuum and the product was characterised by PXRD (Figure 21). Powder pattern of the product is listed in Table XV. This pattern showed that all of the TiOCl was reacted

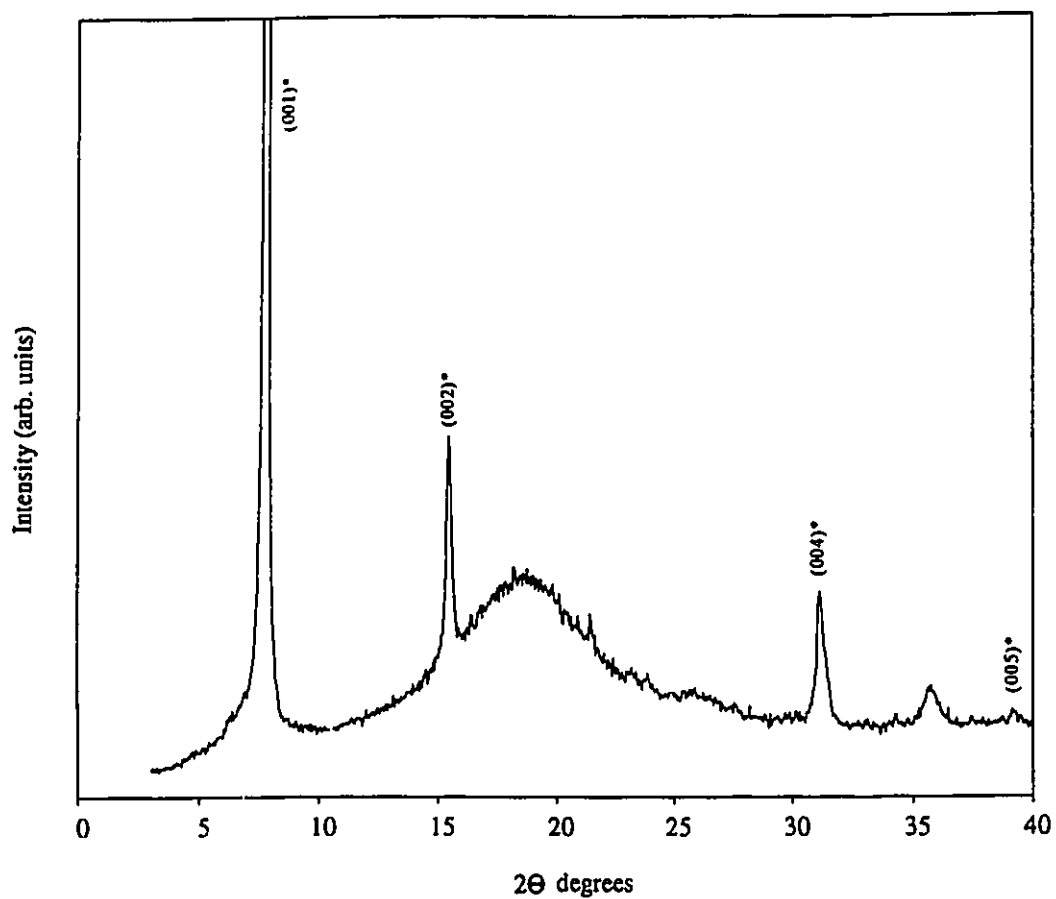


**Figure 21** PXRD spectrum of the product obtained during the reaction of  $\text{TiOCl}$  with EN in a Schlenk flask for 5 days at  $80^\circ\text{C}$

Table XV

Powder pattern of the product obtained during the reaction of TiOCl with EN in a Schlenk flask for 5 days at 80°C

d-space (Å)	rel. intensity %	h k l	2 $\theta$ degrees	comments
11.23 (11.42) <sup>(a)</sup>	100	0 0 1	7.86	TiOCl(C <sub>2</sub> H <sub>8</sub> N <sub>2</sub> ) <sub>x</sub> *
5.69	7.6	0 0 2	15.55	*
2.86	2.3	0 0 4	31.15	*
2.51	0.6		35.66	
2.29	0.2	0 0 5	39.22	*

\* - peaks related to the intercalated compound TiOCl(C<sub>2</sub>H<sub>8</sub>N<sub>2</sub>)<sub>x</sub>

(a) - d-space was calculated by using 002, 004, and 005 peaks

and the intercalated compound  $\text{TiOCl}(\text{C}_2\text{H}_8\text{N}_2)_x$  with d-space  $11.42\text{\AA}$  (layered expansion is  $3.41\text{\AA}$ ) was formed. The compound  $\text{TiOCl}(\text{C}_2\text{H}_8\text{N}_2)_x$  was characterised only by PXRD due to a very small reaction scale.

### 2.3 Reaction in a Schlenk flask at $75^\circ\text{C}$ for 9 hours.

The above reaction was repeated once more with the introduction of vigorous stirring. The reaction was performed in a Schlenk flask at  $75^\circ\text{C}$  for 9 hours. Approximately 7 hours after the reaction started, a colour change of the solid from dark brown to dark blue-grey was observed. After an additional 2 hours the reaction was stopped and the EN solution was removed under vacuum. The product appeared as a dark blue-grey crystalline solid that was analysed by PXRD (Figure 22). The powder pattern of a dark blue-grey product is presented in Table XVI.

PXRD analysis showed that the reaction of  $\text{TiOCl}$  with EN was very clean, all of the starting material had reacted and a new intercalated product was formed. A formulation of  $\text{TiOCl}(\text{C}_2\text{H}_8\text{N}_2)_{0.4}$  for the dark blue-grey product is consistent with chemical analysis results. EA results are presented in Table XVII. Consistent with the previous result, we observed a layer expansion of the host  $\text{TiOCl}$  by  $3.46\text{\AA}$  (d-space is  $11.47\text{\AA}$ ). Note also that the layer expansion value of  $\text{TiOCl}(\text{C}_2\text{H}_8\text{N}_2)_{0.4}$  is very similar to that of  $\text{TiOCl}(\text{C}_4\text{H}_{12}\text{N}_2)_{0.44}$  (Figure 12). On the base of obtained d-spacing value we can assume that the EN molecules are tilted relative to the host layers.

This reaction was remarkable and clearly demonstrated the influence of kinetic factors on the reaction rate. It was observed that in the case of heterogeneous systems kinetic

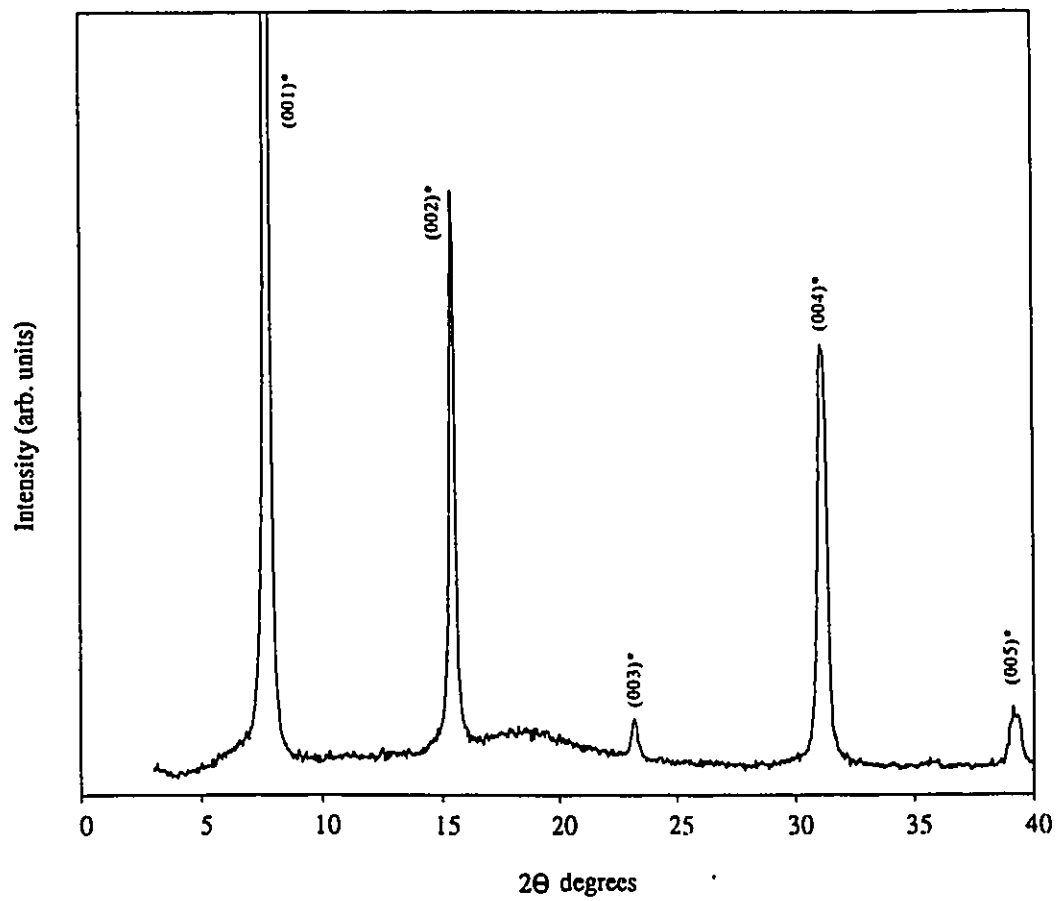


Figure 22 PXRD spectrum of  $\text{TiOCl}(\text{C}_2\text{H}_8\text{N}_2)_{0.4}$

Table XVI

Powder pattern of  $\text{TiOCl}(\text{C}_2\text{H}_8\text{N}_2)_{0.4}$ 

d-space (Å)	rel. intensity %	h k l	2 $\theta$ degrees	comments
11.39 (11.47) <sup>(a)</sup>	100	0 0 1	7.75	$\text{TiOCl}(\text{C}_2\text{H}_8\text{N}_2)_{0.4}$ *
5.72	14.0	0 0 2	15.46	*
3.82	0.6	0 0 3	23.21	*
2.87	5.0	0 0 4	31.05	*
2.30	0.5	0 0 5	39.10	*

\* - peaks related to the intercalated compound  $\text{TiOCl}(\text{C}_2\text{H}_8\text{N}_2)_{0.4}$

(a) - d-space was calculated by using 002, 003, 004, and 005 peaks

Table XVII

EA results for  $\text{TiOCl}(\text{C}_2\text{H}_8\text{N}_2)_{0.4}$ 

%	Calculated values	Experimental values
C	7.80	7.8
H	2.68	2.81
N	9.18	7.97

factors such as temperature, amount of starting materials, and especially speed of stirring that increase the surface area between two phases, are critical for the reaction rate.

Formation of the intercalated compound  $\text{TiOCl}(\text{C}_2\text{H}_8\text{N}_2)_{0.4}$  was confirmed by thermal analysis which showed the formation of starting material  $\text{TiOCl}$  during heating the intercalated compound to  $380^\circ\text{C}$  under nitrogen flow (equation 20). The formation of  $\text{TiOCl}$  was confirmed by PXRD.



#### 2.4 Reaction in a Schlenk flask at 75°C for 16 hours.

A mixture of TiOCl and EN was stirred vigorously for 16 hours at 75°C. In approximately 7 hours the colour of the solid had changed from dark brown to dark blue-grey. The reaction was allowed to continue for an additional 9 hours. Excess EN was removed by vacuum and the obtained dark blue-grey product was analysed by PXRD (Figure 23). The powder pattern of the dark blue-grey product is presented in Table XVIII. The PXRD spectrum demonstrated that in 16 hours two compounds with d-spaces 13.42Å and 11.31Å had already formed, in contrast to the 9 hour reaction where only one compound with d-space 11.47Å was observed by PXRD (Figure 22). The compound with d-space 11.31Å is assigned as the intercalated compound  $\text{TiOCl}(\text{C}_2\text{H}_8\text{N}_2)_x$  by the analogy with the previous reaction. The compound with d-space of 13.42Å could also be an intercalated compound but with different orientation of EN molecules inside layers or it could be a newly formed substituted compound. At this point we didn't have enough data to make a conclusion concerning the compound with d-space 13.42Å.

#### 2.5 Reaction in a Schlenk flask at 75°C for 4 days.

In an effort to identify the compound with d-space 13.42Å obtained during a 16 hours reaction of TiOCl with EN, we decided to continue the reaction with the dark blue-grey product.

The dark blue-grey product obtained during the previous reaction (reaction in a Schlenk flask at 75°C for 16 hours) was mixed together with EN solution in a Schlenk flask and heated for 3 additional days under vigorous stirring at 75°C. A colour of the solid stayed

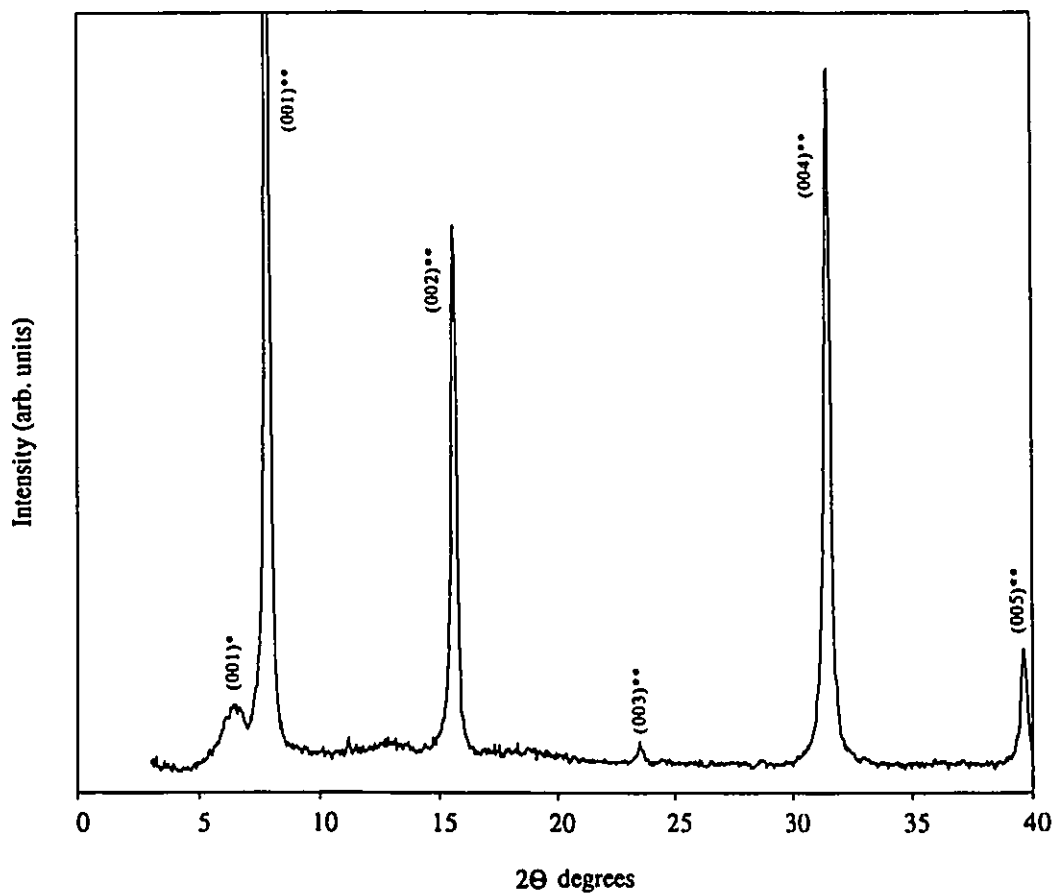


**Figure 23** PXRD spectrum of the product obtained from the reaction of  $\text{TiOCl}$  with EN in a Schlenk flask at  $75^\circ\text{C}$  for 16 hours.

Table XVIII

Powder pattern of the product obtained from the reaction of TiOCl with EN in a Schlenk flask at 75°C for 16 hours

d-space (Å)	rel. intensity %	h k l	2 $\theta$ degrees	comments
13.42	5.4	0 0 1	6.58	new compound*
11.31 (11.31) <sup>(a)</sup>	100	0 0 1	7.86	TiOCl(C <sub>2</sub> H <sub>8</sub> N <sub>2</sub> ) <sub>x</sub> **
5.65	25.4	0 0 2	15.67	**
3.77	0.5	0 0 3	23.54	**
2.83	17.2	0 0 4	31.53	**
2.27	2.2	0 0 5	39.65	**

\* - peaks related to a new formed compound

\*\* - peaks related to the intercalated compound TiOCl(C<sub>2</sub>H<sub>8</sub>N<sub>2</sub>)<sub>x</sub>

(a) - d-space was calculated by using 002, 003, 004, and 005 peaks

the same but the EN solution changed from colorless to foggy, and a white solid was observed on the walls of a Schlenk flask. The EN solution was removed by vacuum and the product appeared as a mixture of dark blue-grey and yellowish-white solids. This mixture was analysed by PXRD (Figure 24) which showed that the yellowish-white solid was the EN-salt  $[\text{H}_3\text{N}-\text{CH}_2-\text{CH}_2-\text{NH}_3]^{2+}2\text{Cl}^-$  by comparison with an authentic sample (see section 2.7), that could be formed only during the topochemical substitution reaction. Based on this fact we attribute the unidentified compound with d-space 13.42Å from the previous reaction (Figure 23) to a substituted compound,  $\text{TiOCl}_x(\text{C}_2\text{H}_{8-n}\text{N}_2)_y$  (where n is the number of protons participated in the substitution reaction).

The intercalated compound  $\text{TiOCl}(\text{C}_2\text{H}_8\text{N}_2)_x$  with d-space 11.31Å is still present in PXRD spectrum of this mixture. The powder pattern of the product obtained during the 4 day reaction of TiOCl with EN is presented in Table XIX.

#### 2.6 Reaction in a Schlenk flask at 75°C for 7.5 days.

The previous three reactions of TiOCl with EN demonstrated that the substituted compound can be formed through the formation of intercalated compound. The results indicate that it is simply a matter of heating the intercalated compound to cause substitution and salt formation. Thus far we have been unable to get only the substituted compound and our product is a mixture of both intercalated and substituted compounds (Figure 24). Therefore, we decided to continue the reaction with the dark blue-grey product that was obtained during the reaction in a Schlenk flask for 4 days at 75°C.

The dark blue-grey product obtained from the reaction in a Schlenk flask at 75°C for 4

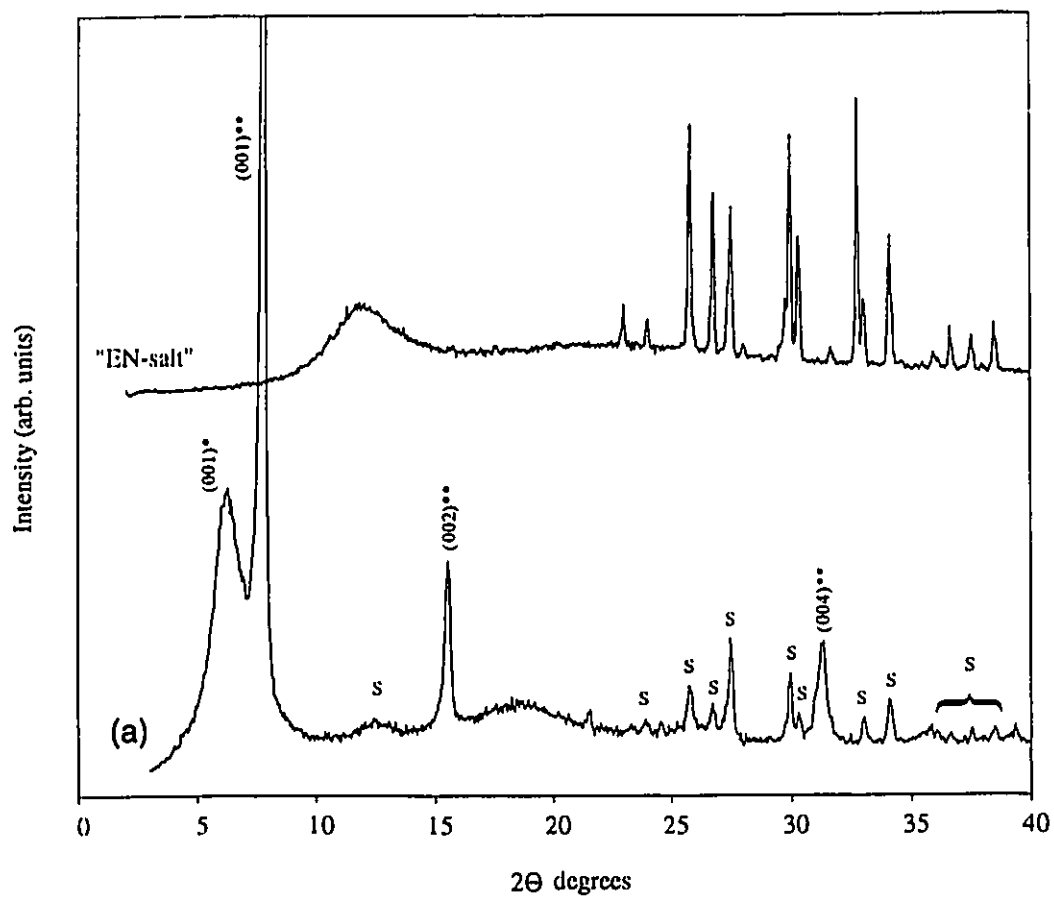


**Figure 24** (a) PXRD spectrum of the product obtained from the reaction of  $\text{TiOCl}$  with EN in a Schlenk flask at  $75^\circ\text{C}$  for 4 days.

(b) PXRD spectrum of the EN-salt  $[\text{H}_3\text{N}-\text{CH}_2-\text{CH}_2-\text{NH}_3]^{2+}2\text{Cl}^-$

Table XIX

Powder pattern of the product obtained from the reaction of TiOCl with EN in a Schlenk flask at 75°C for 4 days.

d-space (Å)	rel. intensity %	h k l	2θ degrees	comments
13.79	22.6	0 0 1	6.40	TiOCl <sub>x</sub> (C <sub>2</sub> H <sub>8-n</sub> N <sub>2</sub> ) <sub>y</sub> <sup>•</sup>
11.31	100	0 0 1	7.80	TiOCl(C <sub>2</sub> H <sub>8</sub> N <sub>2</sub> ) <sub>x</sub> <sup>**</sup>
5.65	6.5	0 0 2	15.55	**
3.71	0.2		23.93	salt
3.61	0.3		24.58	salt
3.45	1.1		25.78	salt
3.33	0.7		26.72	salt
3.24	2.1		27.48	salt
2.98	1.4		29.95	salt
2.94	0.5		30.34	salt
2.82	1.9	0 0 4	31.32	**
2.71	0.4		33.02	salt

Table XIX ( continue )

d-space (Å)	rel. intensity %	h k l	2θ degrees	comments
2.62	0.7		34.13	salt
2.50	0.2		35.76	salt
2.39	0.2		37.52	salt
2.33	0.2		38.51	salt
2.28	0.2		39.38	

\* - peaks related to the substituted compound  $\text{TiOCl}_x(\text{C}_2\text{H}_{8-n}\text{N}_2)_y$

\*\* - peaks related to the intercalated compound  $\text{TiOCl}(\text{C}_2\text{H}_8\text{N}_2)_x$

salt - peaks of the EN-salt  $[\text{H}_3\text{N}-\text{CH}_2-\text{CH}_2-\text{NH}_3]^{2+}2\text{Cl}^-$

days (the product is a mixture of intercalated compound, substituted one, and EN-salt (Figure 24)) was mixed with EN solution in a Schlenk flask. The mixture was heated for additional 3.5 days at 75°C under vigorous stirring. No changes in the colour of the solid were noticed, but the EN solution became cloudy. The EN was removed by vacuum and the isolated product was a mixture of dark blue-grey and yellowish-white solids. The mixture was examined by PXRD (Figure 25) which showed the absence of peaks related to the intercalated compound  $\text{TiOCl}(\text{C}_2\text{H}_8\text{N}_2)_x$ . The powder pattern of the obtained product is presented in Table XX and showed that the obtained dark blue-grey product of 7.5 days reaction is a mixture of substituted compound and EN-salt formed during the substitution process.

EN-salt can be easily removed from the product by washing with pure EN. The dark blue-grey product was washed with EN, dried with ether, heated at 80°C for 1 hour, and examined by PXRD (Figure 26). Powder XRD spectrum which is presented in Table XXI showed only the presence of peaks related to the substituted compound  $\text{TiOCl}_{0.5}(\text{C}_2\text{H}_7\text{N}_2)_{0.5}$ .

An IR spectrum of  $\text{TiOCl}_{0.5}(\text{C}_2\text{H}_7\text{N}_2)_{0.5}$  showed absorption bands at  $1716\text{ cm}^{-1}$  and  $1261\text{ cm}^{-1}$  that can be attributed to the N-H and C-N vibration modes of the amine. EA (Table XXII) and XRF are consistent with the formulation of the product as  $\text{TiOCl}_{0.5}(\text{C}_2\text{H}_7\text{N}_2)_{0.5}$ . XRF showed the ratio of Ti to Cl equal to 1.9.

The new organic derivative  $\text{TiOCl}_{0.5}(\text{C}_2\text{H}_7\text{N}_2)_{0.5}$  of TiOCl with d-space  $14.51\text{Å}$  (layered expansion is  $6.50\text{Å}$ ) was formed during a topochemical substitution reaction of TiOCl with EN, where half of the chlorine ions were substituted with EN molecules. It is

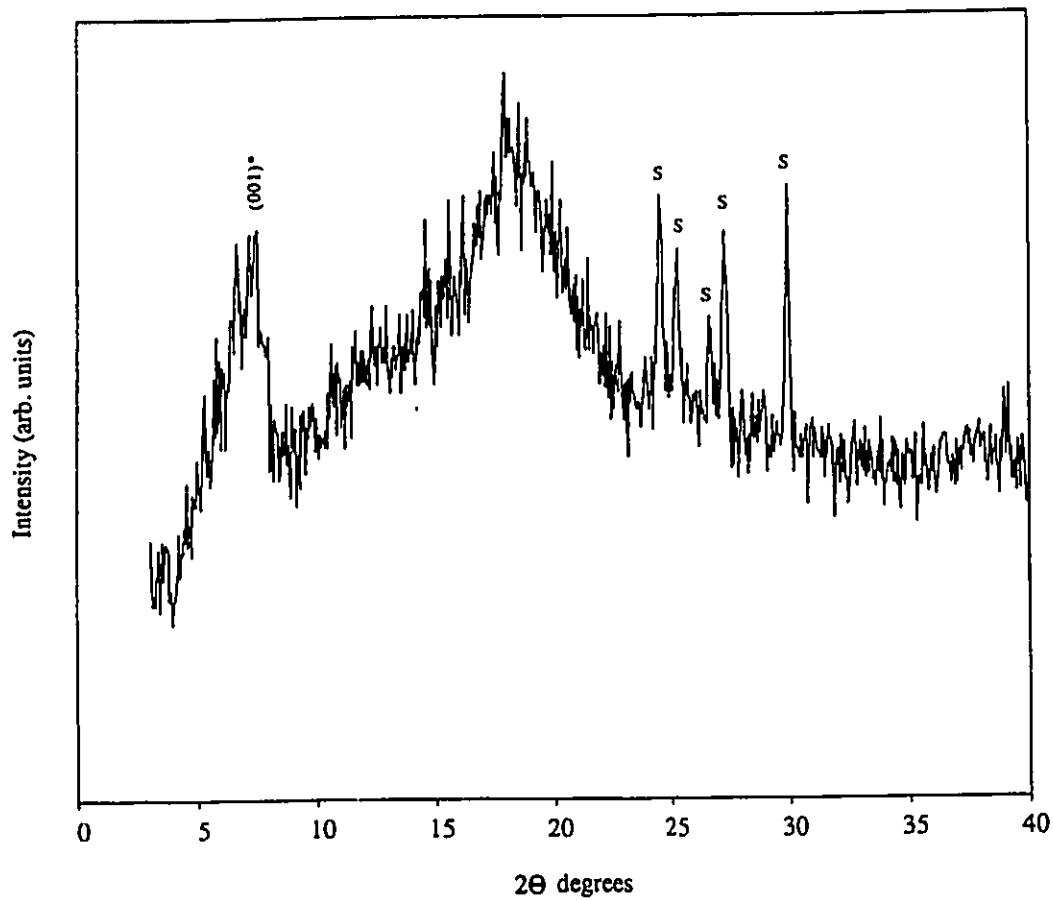


**Figure 25** PXRD spectrum of the product obtained from the reaction of  $\text{TiOCl}$  with EN at  $75^\circ\text{C}$  for 7.5 days.

Table XX

Powder pattern of the product obtained from the reaction of  $\text{TiOCl}$  with EN  
at  $75^\circ\text{C}$  for 7.5 days.

d-space (Å)	rel. intensity %	h k l	2 $\theta$ degrees	comments
13.16	100	0 0 1	6.71	$\text{TiOCl}_x(\text{C}_2\text{H}_{8-n}\text{N}_2)_y^*$
4.92	27.3		17.98	
3.62	22.2		24.56	salt
3.51	14.5		25.29	salt
3.33	7.0		26.69	salt
3.25	14.5		27.37	salt
2.98	21.6		29.95	salt

\* - peak related to the substituted compound  $\text{TiOCl}_x(\text{C}_2\text{H}_{8-n}\text{N}_2)_y$

salt - peaks of the EN-salt  $[\text{H}_3\text{N}-\text{CH}_2-\text{CH}_2-\text{NH}_3]^{2+}2\text{Cl}^-$

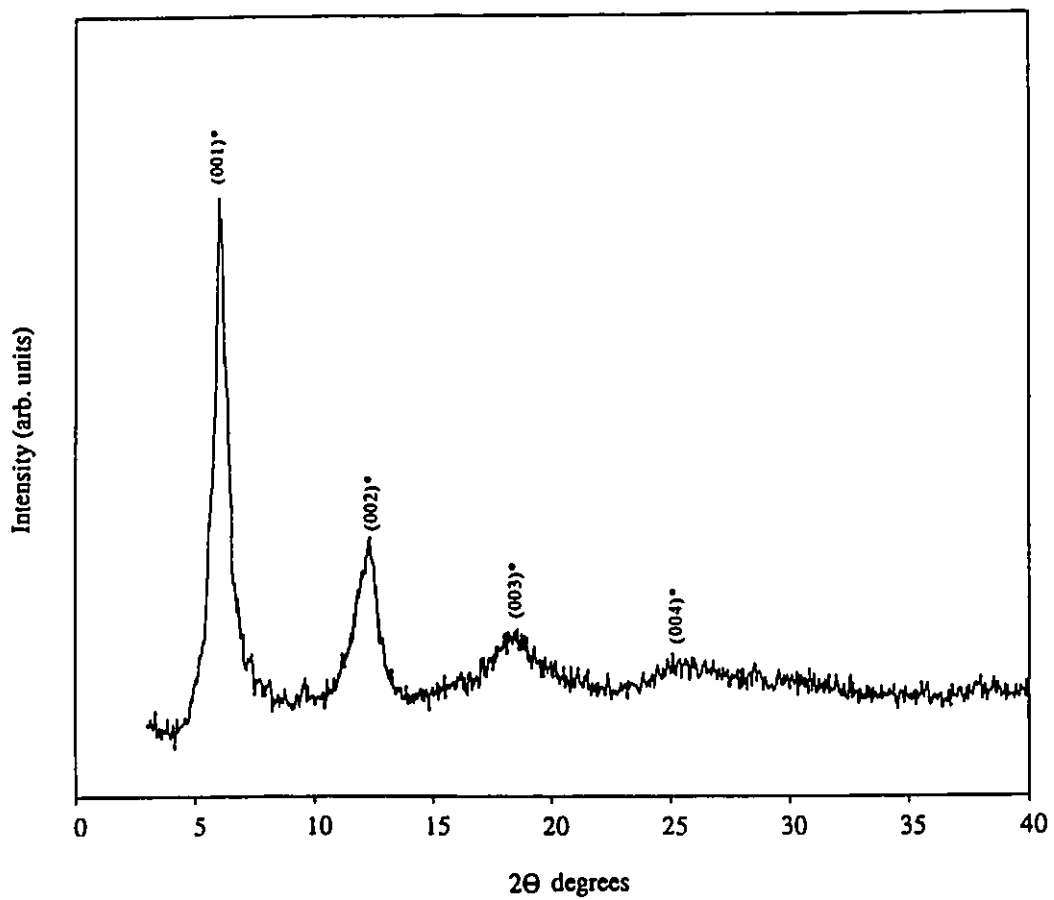


Figure 26 PXRD spectrum of  $\text{TiOCl}_{0.5}(\text{C}_2\text{H}_7\text{N}_2)_{0.5}$

Table XXI

Powder pattern of  $\text{TiOCl}_{0.5}(\text{C}_2\text{H}_7\text{N}_2)_{0.5}$ 

d-space (Å)	rel. intensity %	h k l	2θ degrees	comments
14.51	100	0 0 1	6.08	$\text{TiOCl}_{0.5}(\text{C}_2\text{H}_7\text{N}_2)_{0.5}$ *
7.18	16.2	0 0 2	12.30	*
4.84	2.1	0 0 3	18.13	*

\* - peaks related to the substituted compound  $\text{TiOCl}_{0.5}(\text{C}_2\text{H}_7\text{N}_2)_{0.5}$ 

Table XXII

EA data for  $\text{TiOCl}_{0.5}(\text{C}_2\text{H}_7\text{N}_2)_{0.5}$ 

%	Calculated values	Experimental values
C	10.6	10.24
H	3.5	3.52
N	12.4	10.14

very interesting to notice that after EN-salt removal, the layers of  $\text{TiOCl}_{0.5}(\text{C}_2\text{H}_7\text{N}_2)_{0.5}$  did not collapse, in contrast to  $\text{TiOCl}_x(\text{C}_4\text{H}_{11}\text{N}_2)_y$  where layered expansion after salt removal became just 2.11Å. This difference in d-spacing might be explained by different orientations of the organic molecules between the layers. Several structural models can be proposed for the EN - substitution product. We can estimate the interlayer distances in the models by using bond lengths of 2.39Å for Ti-Cl (bridged) bond; about 2.45Å for Ti-Cl (terminal) bond; 1.5Å for Ti-N bond; 1.47Å for N-C bond; 1.3Å for C-C bond; and Van der Waals radius of 1.8Å for a Cl ion, and 2Å for a  $\text{CH}_2$  group.

The first model is based upon formation of an interlayer bridging diamido illustrated in Figure 27a. The interlayer distance for the bridging model is estimated to be less than 8Å. A second model based upon intralayer bonding, with EN molecules coordinated to Ti ions within the same layer (Figure 27b), can have the terminal Cl ions of the parallel layer or another EN molecules opposing them. In both cases interlayer distance is calculated to be approximately 9 - 10Å. The first two models don't agree with the observed layer expansion value and chemical analysis results.

A third proposed model (Figure 27c) involves formation of hydrogen bonding between  $-\text{NH}_2$  groups of EN molecules and terminal Cl ions of the opposite layer. This model agrees with EA results but the estimated interlayer distance equal, to 12 - 13Å is less than the observed one.

In the last model (figure 27d) only one end of EN molecules is fixed by direct bonding to titanium metal centres in the TiO double layers via its own nitrogen atoms and the interlayer space of  $\text{TiOCl}_{0.5}(\text{C}_2\text{H}_7\text{N}_2)_{0.5}$  is quite populated by EN molecules. EN

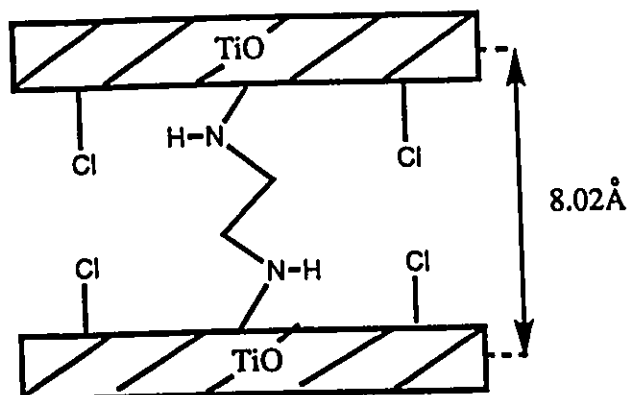


Figure 27a Interlayer bridging model for  $\text{TiOCl}_{0.5}(\text{C}_2\text{H}_7\text{N}_2)_{0.5}$

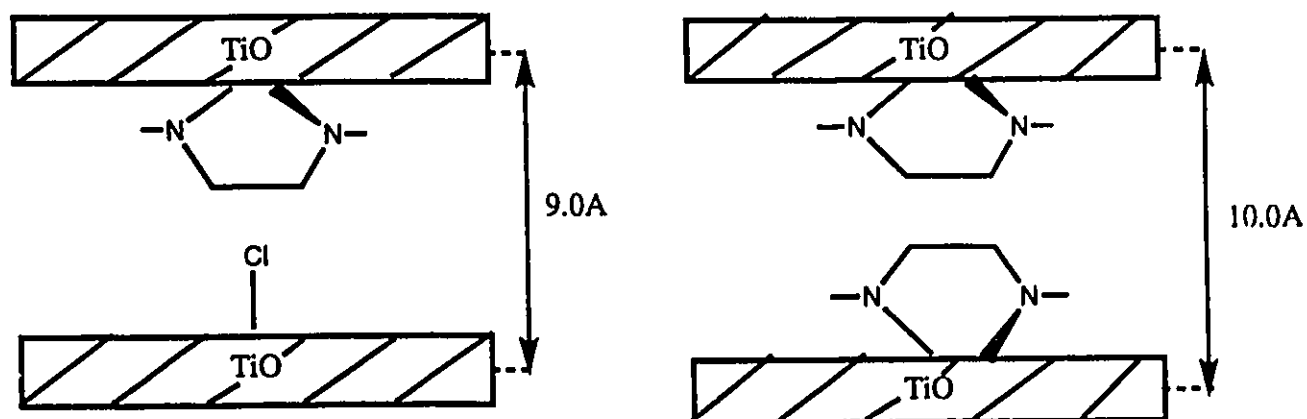


Figure 27b Intralayer bonding model for  $\text{TiOCl}_{0.5}(\text{C}_2\text{H}_7\text{N}_2)_{0.5}$

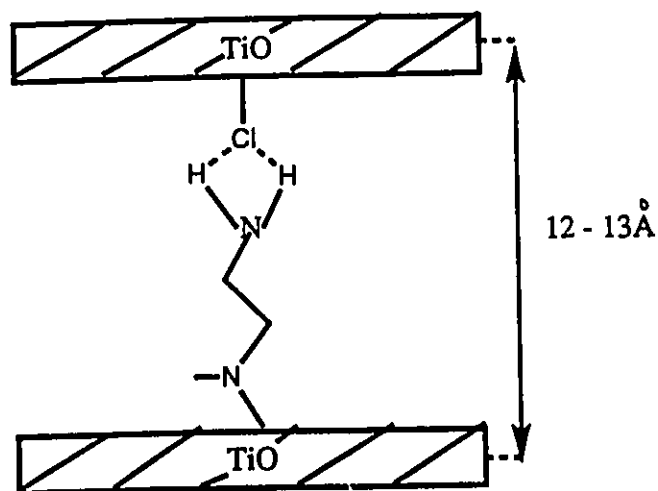


Figure 27c Model structure for  $\text{TiOCl}_{0.5}(\text{C}_2\text{H}_7\text{N}_2)_{0.5}$  represent hydrogen bonding

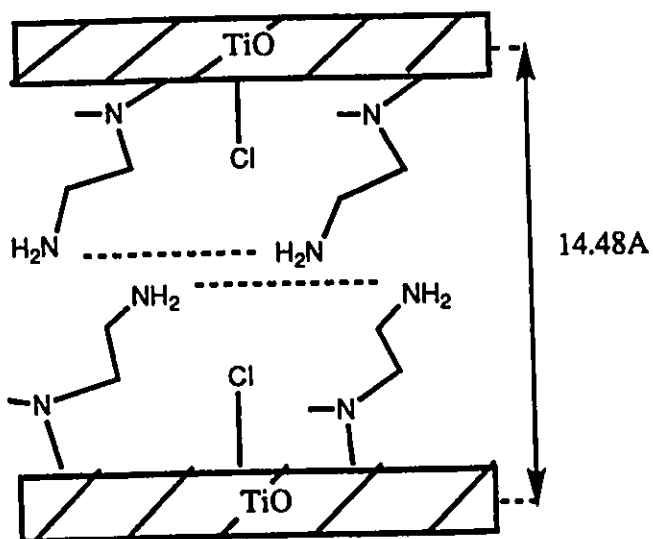


Figure 27d Model structure for  $\text{TiOCl}_{0.5}(\text{C}_2\text{H}_7\text{N}_2)_{0.5}$  where EN molecules form the second layer.

molecules belonging to the same TiO double layer interact strongly with each other, creating a second layer. The newly formed organic double layer interacts strongly with the upper and lower TiO double layers with a distance approximately equal to 14.48Å; a value which corresponds quite closely to the observed interlayer distance. Thus, the model that involves the formation of two organic layers by EN molecules seems the most probable.

A summary of reactions of TiOCl with EN is presented in Table XXIII.

Table XXIII

Summary of reactions of TiOCl with EN

Reaction conditions	d-space (Å)	layer exp. (Å)	product	comments
sealed tube 160-170°C, 2, 2.5, 4d				amorphous or decomposed product
Schl. flask 80°C, 5d	11.42	3.41	TiOCl(C <sub>2</sub> H <sub>8</sub> N <sub>2</sub> ) <sub>x</sub>	interc. comp.
Schl. flask 75°C, 9hours vig. stirring ↓	11.47	3.46	TiOCl(C <sub>2</sub> H <sub>8</sub> N <sub>2</sub> ) <sub>0.4</sub>	interc. comp.
Schl. flask 75°C, 16h vig. stirring ↓	13.42 11.31	5.41 3.30	TiOCl(C <sub>2</sub> H <sub>8</sub> N <sub>2</sub> ) <sub>x</sub>	intc. comp. unidentified compound

Table XXIII (continue)

Reaction conditions	d-space (Å)	layer exp. (Å)	product	comments
Schl. flask	13.80	5.79	$\text{TiOCl}_x(\text{C}_2\text{H}_{8-n}\text{N}_2)_y$	subst. comp.
75°C, 4d	11.31	3.30	$\text{TiOCl}(\text{C}_2\text{H}_8\text{N}_2)_x$	interc.comp.
vig. stirring				EN-salt
↓				
Schl. flask	13.16	5.15	$\text{TiOCl}_x(\text{C}_2\text{H}_{8-n}\text{N}_2)_y$	subst. comp.
75°C, 7.5d				EN-salt
vig. stirring				
↓ salt removal				
	14.51	6.50	$\text{TiOCl}_{0.5}(\text{C}_2\text{H}_7\text{N}_2)_{0.5}$	subst. prod.

### 2.7 Synthesis of $[H_3N-CH_2-CH_2-NH_3]^{2+}2Cl^-$ ( EN-salt )

To confirm formation of the EN-salt during the substitution reaction of TiOCl with EN, the salt was synthesised by adding HCl to EN solution. The yellowish-white solid was isolated, dried, and examined by PXRD (Figure 28) and TGA. Powder pattern of EN-salt is listed in Table XXIV.

Thermal analysis results showed one weight loss at 311.7°C that corresponds to 100% of the sample weight.

The formulation  $[H_3N-CH_2-CH_2-NH_3]^{2+}2Cl^-$  is consistent with the EA results (Table XXV).

**Table XXV**

EA data for  $[H_3N-CH_2-CH_2-NH_3]^{2+}2Cl^-$

%	Calculated values	Experimental values
C	18.0	19.35
H	7.52	7.81
N	21.05	21.08

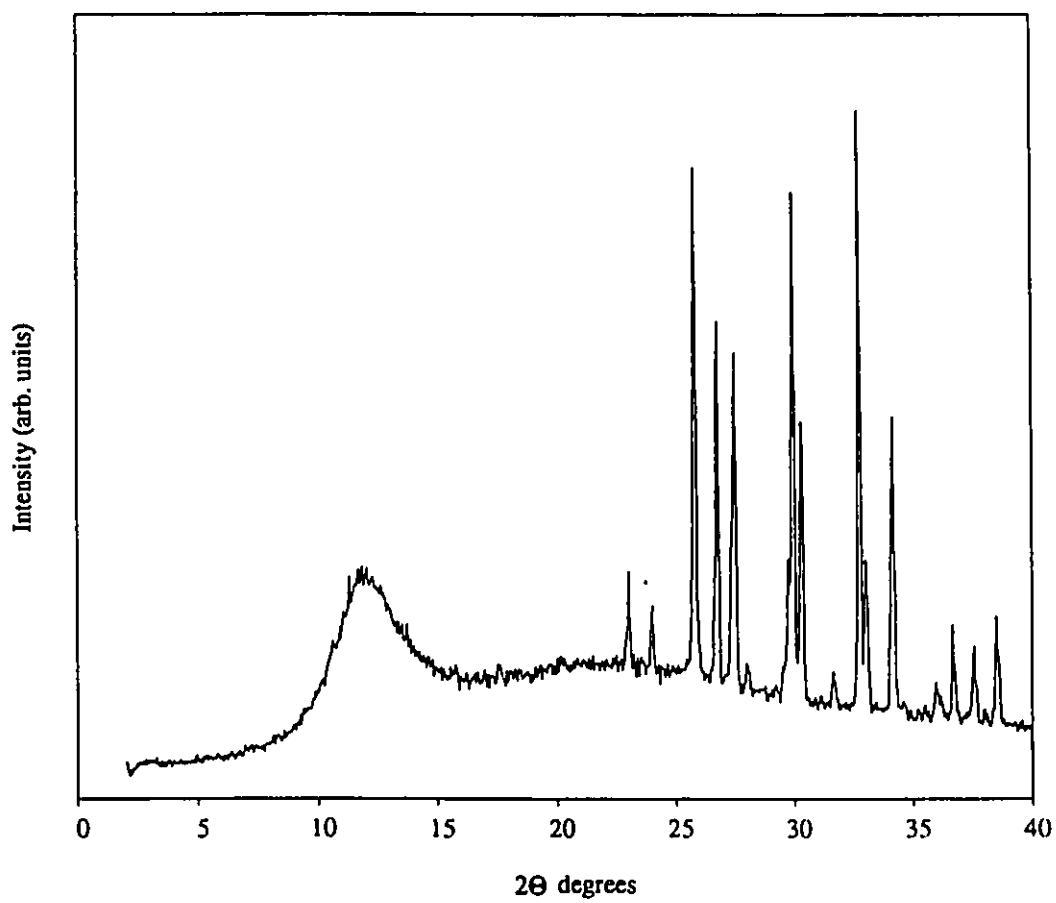


**Figure 28** PXRd spectrum of EN-salt  $[\text{H}_3\text{N}-\text{CH}_2-\text{CH}_2-\text{NH}_3]^{2+}2\text{Cl}^-$

Table XXIV

Powder pattern of EN-salt  $[\text{H}_3\text{N-CH}_2\text{-CH}_2\text{-NH}_3]^{2+}2\text{Cl}^-$ 

d-value (Å)	relative intensity %	2 $\theta$ degrees
7.50	30.9	11.77
3.86	20.6	22.99
3.70	14.7	23.98
3.45	100	25.79
3.33	70.3	26.73
3.24	62.7	27.48
3.18	5.1	28.02
2.97	81.3	29.97
2.94	45.2	30.33
2.82	5.2	31.66
2.73	91.9	32.75
2.70	20.7	33.05

Table XXIV ( continue )

d-value (Å)	relative intensity %	2 $\theta$ degrees
2.62	43.7	34.15
2.49	4.9	35.95
2.44	9.6	36.69
2.39	10.2	37.55
2.33	10.4	38.54

### 3. Reaction of TiOCl with diethylenetriamine [H<sub>2</sub>N-CH<sub>2</sub>-CH<sub>2</sub>-N(H)-CH<sub>2</sub>-CH<sub>2</sub>-NH<sub>2</sub>]

TiOCl and diethylenetriamine were mixed together in a Schlenk flask. The mixture was heated for 5 days at 90°C under vigorous stirring. Diethylenetriamine was removed by filtration when the colour of the solid had changed from dark brown to dark grey. The dark grey product was washed with THF to remove an excess of diethylenetriamine. The reaction product was examined by PXRD (Figure 29) and showed the formation of a new compound with d-space 12.06Å (layered expansion is 4.05Å). The powder pattern of the dark grey product is presented in Table XXVI. Since no salt formation was observed during the reaction we can assume that the dark grey product is the intercalated compound TiOCl(C<sub>4</sub>H<sub>13</sub>N<sub>3</sub>)<sub>x</sub>.

It is easy to confirm that the product of this reaction is an intercalated compound just by heating it to its de-intercalation temperature. The remaining compound should be starting material TiOCl. Therefore, the dark grey product was heated to 360°C under nitrogen flow in a glass tube and the resulting compound was analysed by PXRD. The PXRD spectrum of intercalated compound TiOCl(C<sub>4</sub>H<sub>13</sub>N<sub>3</sub>)<sub>x</sub> after heating to 360°C was identical to that of TiOCl. This thermal reaction can be described by equation (21).



This result indicates that the reaction of TiOCl with diethylenetriamine yields a new intercalated compound TiOCl(C<sub>4</sub>H<sub>13</sub>N<sub>3</sub>)<sub>x</sub>.

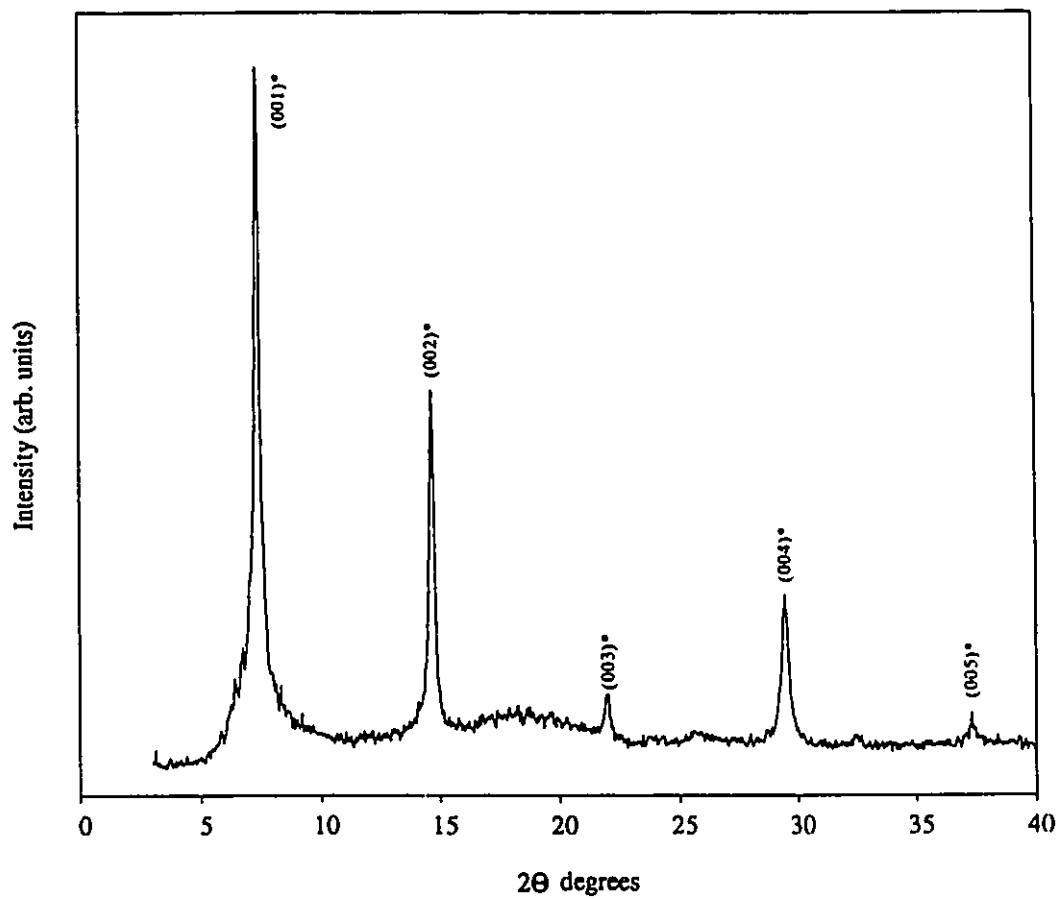


Figure 29 PXRD spectrum of  $\text{TiOCl}(\text{C}_4\text{H}_{13}\text{N}_3)_{0.15}$

Table XXVI

Powder pattern of  $\text{TiOCl}(\text{C}_4\text{H}_{13}\text{N}_3)_{0.15}$ 

d-space (Å)	rel. intensity %	h k l	2 $\theta$ degrees	comments
12.01 (12.06) <sup>(a)</sup>	100	0 0 1	7.35	$\text{TiOCl}(\text{C}_4\text{H}_{13}\text{N}_3)_{0.15}$ *
6.02	25.0	0 0 2	14.70	*
4.03	2.0	0 0 3	22.00	*
3.03	5.6	0 0 4	29.46	*
2.41	0.9	0 0 5	37.31	*

\* - peaks related to the intercalated compound  $\text{TiOCl}(\text{C}_4\text{H}_{13}\text{N}_3)_{0.15}$

(a) - d-value was calculated by using 002, 003, and 005 peaks

The degree of intercalation,  $x$ , can be calculated from microanalysis data which are consistent with the formulation  $\text{TiOCl}(\text{C}_4\text{H}_{13}\text{N}_3)_{0.15}$  (Table XXVII).

Table XXVII

EA data for  $\text{TiOCl}(\text{C}_4\text{H}_{13}\text{N}_3)_{0.15}$

%	Calculated values	Experimental values
C	6.30	6.31
H	1.96	2.14
N	5.50	5.29

An IR spectrum of  $\text{TiOCl}(\text{C}_4\text{H}_{13}\text{N}_3)_{0.15}$  showed an absorption bands at 1718 and  $800\text{ cm}^{-1}$  that can be assigned to vibration modes of N-H bond, and an absorption band at  $1081\text{ cm}^{-1}$  that indicate on vibration modes of C-N bond.

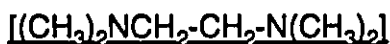
This intercalated compound has an interlayer distance of  $12.06\text{Å}$  that corresponds to the layered expansion of  $4.05\text{Å}$ . The only model we believe is consistent with this observation is where the diethylenetriamine molecules lie almost parallel ( or with a small angle ) to TiOCl layers.

We attempted to synthesise the substituted compound by heating  $\text{TiOCl}(\text{C}_4\text{H}_{13}\text{N}_2)_{0.15}$  in diethylenetriamine solution, but our efforts were not very succesful. The product after heating was analysed by PXRD which did indicate diethylenetriamine-

salt formation as well as formation of several compounds, however, they couldn't be identified.

The formation of several compounds is not surprising based on the fact that diethylenetriamine molecules have five reactive protons and three amino groups available to participate in the substitution process. A wide number of structural models are possible for diethylenetriamine organic derivative of TiOCl.

#### 4. Reactions of TiOCl with N,N,N',N'-tetramethylethylenediamine



The reactivity of TiOCl with TMEDA was examined under a variety of conditions.

The first attempt was carried inside a teflon lined acid digestion bomb. The bomb was heated at 100°C for 1.5 days. The colorless TMEDA solution was then removed by filtration and the product appeared as a brown crystalline solid. The solid was examined by PXRD. The PXRD spectrum of the solid looked exactly the same as that of the starting material, indicating that no reaction between TiOCl and TMEDA had taken place.

We decided to repeat the reaction at higher temperature with TiOCl and TMEDA in a sealed evacuated heavy walled glass tube. After heating at 170°C for 4.5 days no changes in the appearance of the solution or the solid were noticed and the reaction mixture was allowed to stay in the sealed tube for 18 months at room temperature. The brown crystalline product was isolated by filtration and analysed by PXRD (Figure 30).

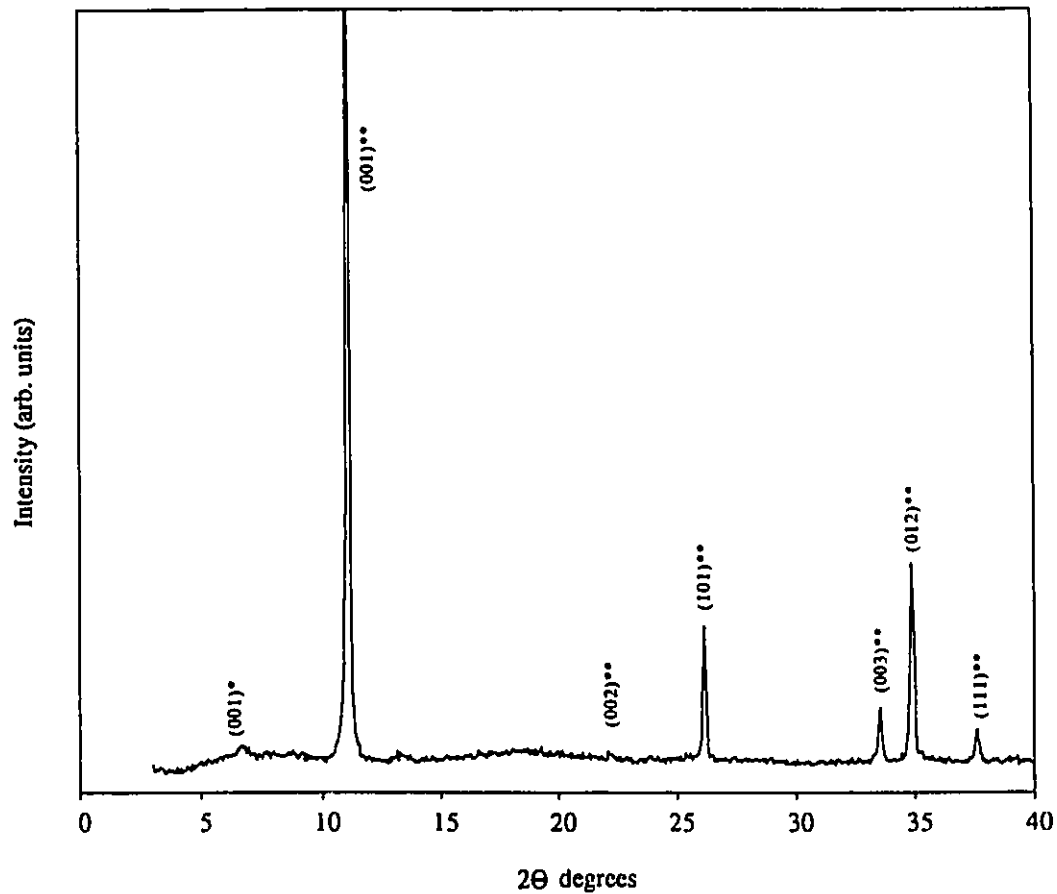


**Figure 30** PXRD spectrum of the product obtained from the sealed tube reaction of TiOCl with TMEDA.

Table XXVIII

Powder pattern of the product obtained during a sealed tube reaction of  $\text{TiOCl}$  with  
TMEDA

d-space (Å)	rel. intensity %	h k l	2 $\theta$ degrees	comments
13.18	1.9	0 0 1	6.70	new product*
7.93	100	0 0 1	11.14	$\text{TiOCl}$ **
3.99	0.3	0 0 2	22.25	**
3.40	5.1	1 0 1	26.15	**
2.67	1.7	0 0 3	33.53	**
2.56	5.8	0 1 2	34.88	**
2.39	0.9	1 1 1	37.59	**

\* - peak of the reaction product

\*\* - peaks related to the starting material  $\text{TiOCl}$

The powder pattern of the reaction product is presented in Table XXVIII.

Again, the PXRD spectrum is very similar to that of TiOCl. The only difference is a small broad peak with d-space 13.18Å. The relative intensity of this peak is very small and only slightly above the noise level. These results indicate that the reaction of TiOCl with tertiary amine TMEDA did not occur.

## 5. Reactions of TiOCl with pyridine (C<sub>5</sub>H<sub>5</sub>N)

### 5.1 Reaction in a sealed tube at 250°C.

The reaction of TiOCl with pyridine was carried out in an evacuated, sealed, heavy walled glass tube at 250°C for 2 days. Pyridine was then removed by vacuum, and the isolated grey crystalline material was characterised by PXRD (Figure 31). The PXRD spectrum showed the formation of an intercalated compound TiOCl(py)<sub>x</sub> as well as unreacted TiOCl. The powder pattern of the grey product is presented in Table XXIX. According to the PXRD spectrum, the new intercalated compound TiOCl(py)<sub>x</sub> has d-space equal to 11.93Å which corresponds to a layer expansion of 3.92Å. Intercalation of pyridine into TiOCl host layers has been confirmed by thermal analysis. The TGA curve (Figure 32) of the grey product heated to 300°C consists of two weight losses. The first weight loss was observed at 70°C (4% of the original mass) and is assigned to the loss of surface pyridine. The second weight loss occurred between 150°C and 300°C (9% of the original mass) and corresponds to the loss of intercalated pyridine. The compound

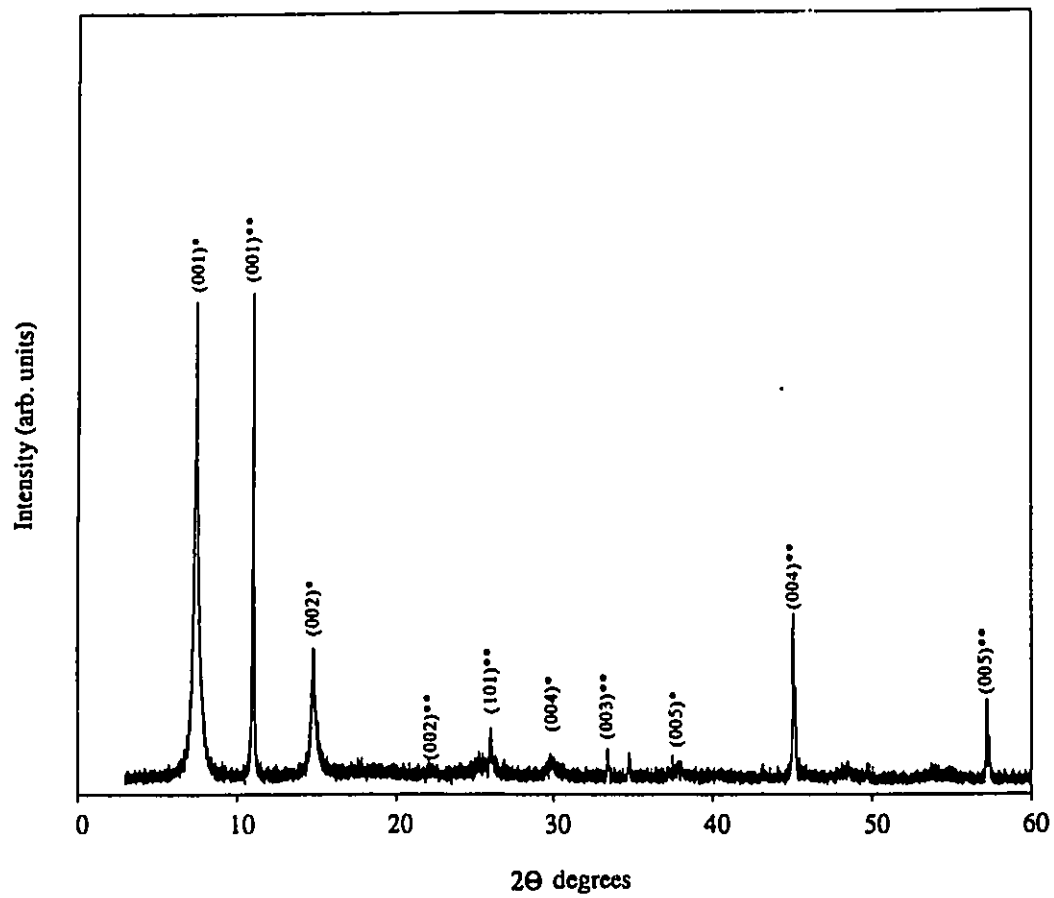


**Figure 31** PXR D of the grey product obtained from the sealed tube reaction of  $\text{TiOCl}$  with pyridine

Table XXIX

Powder pattern of the grey product obtained from the sealed tube reaction of TiOCl with pyridine.

d-space (Å)	rel. intensity %	h k l	2θ degrees	comments
11.85 (11.93) <sup>(a)</sup>	100	0 0 1	7.45	TiOCl(py) <sub>0.11</sub> *
7.99	66.0	0 0 1	11.06	TiOCl**
5.96	12.8	0 0 2	14.85	*
4.00	0.3	0 0 2	22.19	**
3.41	2.0	1 0 1	26.07	**
2.98	0.7	0 0 4	29.89	*
2.67	1.1	0 0 3	33.43	**
2.57	0.8	0 1 2	34.81	**
2.39	0.3	0 0 5	37.52	*
2.01	5.6	0 0 4	45.08	**
1.61	1.9	0 0 5	57.20	**

\* - peaks related to the intercalated compound TiOCl(py)<sub>0.11</sub>

\*\* - peaks of TiOCl

(a) - d-space was calculated by using 002, 004, and 005 peaks

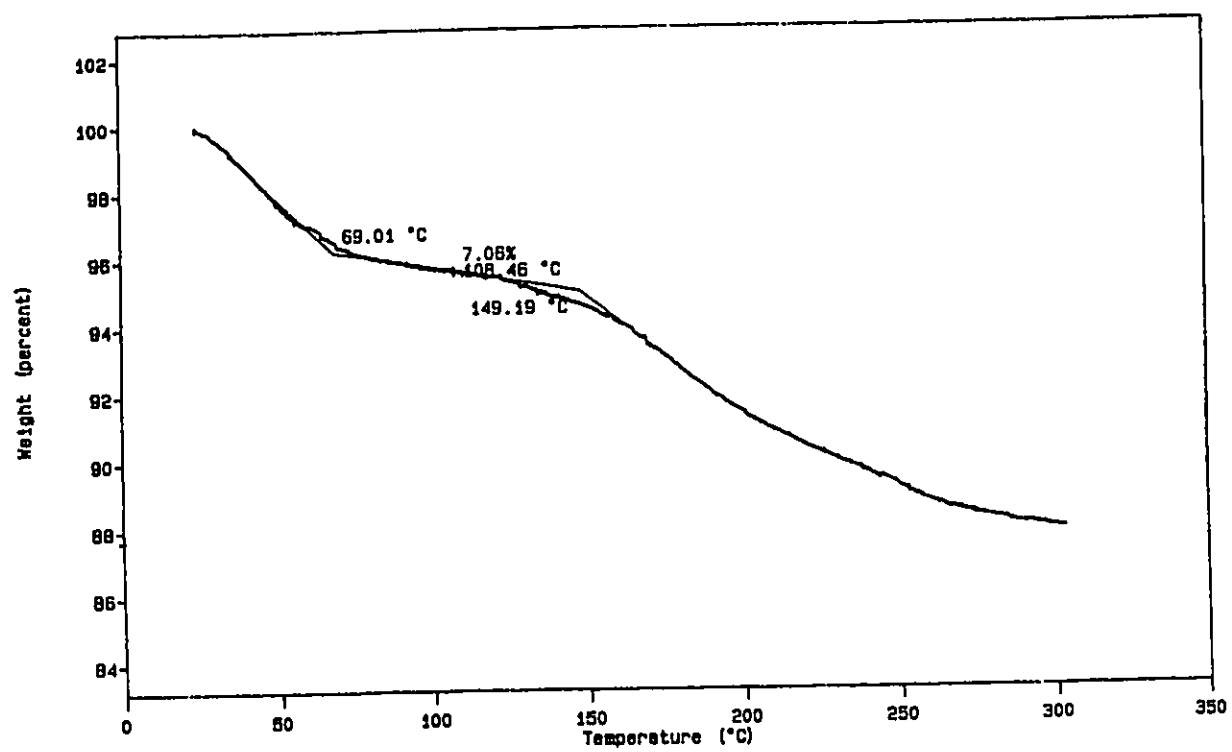


**Figure 32** TGA of the grey product obtained from the sealed tube reaction of  $\text{TiOCl}$  with pyridine

remaining in the pan after the TGA run was confirmed to be TiOCl by PXRD (equation 22).



Based on the TGA analysis we assign a formulation of  $\text{TiOCl(py)}_{0.11}$  to the intercalated product. Chemical analysis (Table XXX) gave a result for a slightly different formulation of  $\text{TiOCl(py)}_{0.2}$ . This may be due to the presence of surface pyridine that had not been removed from the sample before EA run.

## 5.2 Reaction in a Schlenk flask at 80°C.

TiOCl and pyridine were mixed together in a Schlenk flask and vigorously stirred for 2 weeks at 80°C. A dark grey crystalline solid was isolated by filtration and analysed by PXRD (Figure 33). The PXRD pattern showed the formation of a new compound with d-space 12.72Å as well as unreacted TiOCl. The powder pattern of the dark grey product is listed in Table XXXI.

The formulation  $\text{TiOCl(py)}_{0.38}$  is consistent with EA results (Table XXXII). This sample was heated to 80°C for 15 minutes before the EA run in order to remove the surface pyridine. The intercalation of pyridine into TiOCl was confirmed by heating a sample of  $\text{TiOCl(py)}_{0.38}$  in a glass tube under nitrogen flow to 300°C (equation 23). The compound remaining in a tube was examined by PXRD and confirmed to be TiOCl.

**Table XXX**  
EA data for  $\text{TiOCl}(\text{py})_{0.2}$

%	Calculated values	Experimental values
C	10.4	10.1
H	0.8	1.05
N	2.4	2.0

**Table XXXII**  
EA data for  $\text{TiOCl}(\text{py})_{0.38}$

%	Calculated values	Experimental values
C	17.61	17.53
H	1.46	2.28
N	4.1	4.50

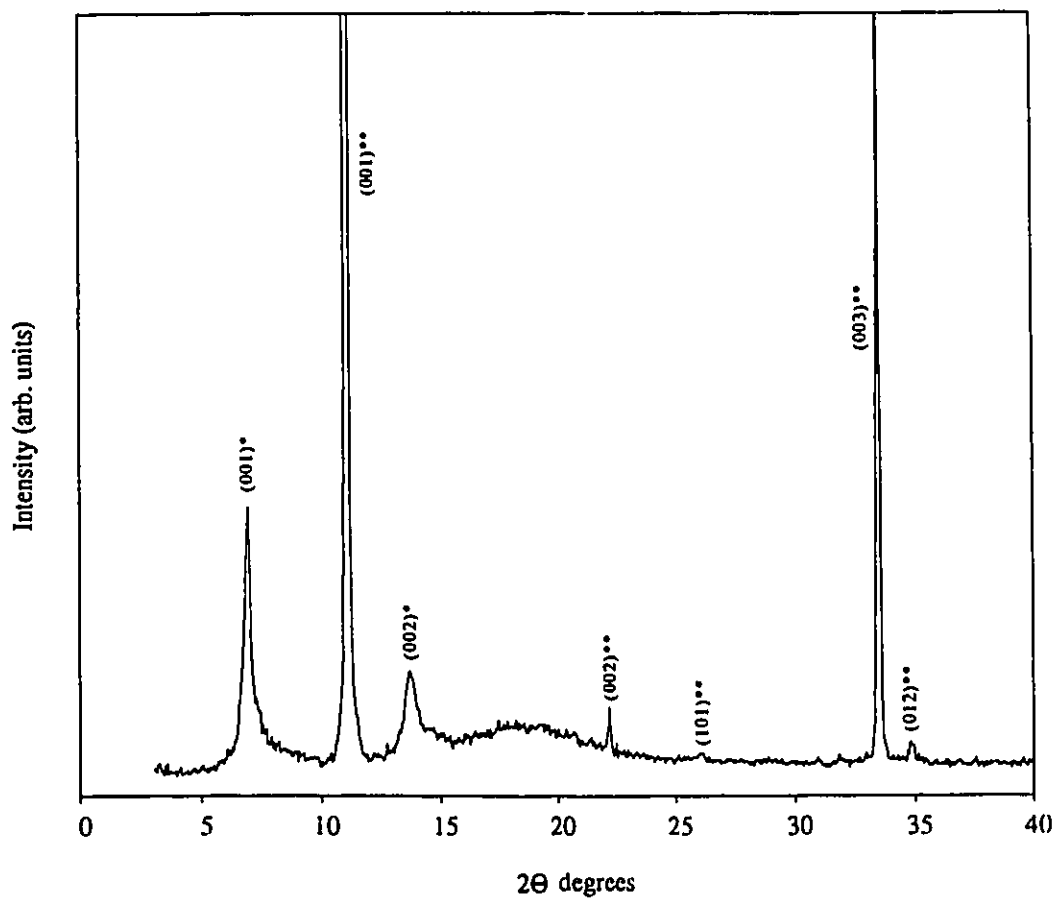


**Figure 33** PXRD of the product obtained from the Schlenk flask reaction of  $\text{TiOCl}$  with pyridine

Table XXXI

Powder pattern of the product obtained from the Schlenk flask reaction of TiOCl with pyridine

d-space (Å)	rel. intensity %	h k l	2θ degrees	comments
12.72	8.03	0 0 1	6.94	TiOCl(py) <sub>0.38</sub> *
7.95 (8.01) <sup>(a)</sup>	100	0 0 1	11.12	TiOCl**
6.45	1.2	0 0 2	13.71	*
4.00	0.4	0 0 2	22.20	**
2.67	5.4	0 0 3	33.50	**
2.57	0.1	0 1 2	34.88	**

\* - peaks related to the intercalated compound TiOCl(py)<sub>0.38</sub>

\*\* - peaks of TiOCl

(a) - d-space of TiOCl was calculated by using 002 and 003 peaks



The new intercalated compound  $\text{TiOCl(py)}_{0.38}$  was found to have d-space of 12.72Å which corresponds to layered expansion of 4.71Å.

A summary of reactions of TiOCl with pyridine is presented in Table XXXIII. The results of both reactions of TiOCl with pyridine indicated that with pyridine the stoichiometry can be variable. In a sealed tube at 250°C TiOCl reacts with pyridine to give  $\text{TiOCl(py)}_{0.11}$  whereas in a Schlenk flask under vigorous stirring at 80°C it gives  $\text{TiOCl(py)}_{0.38}$ . This result is very interesting and demonstrates that the rate of intercalation reaction is strongly dependent on the area of contact surface between the two phases (solid TiOCl and liquid pyridine).

The layer expansion values for the two pyridine intercalated compounds, 3.92Å and 4.71Å are not consistent with Koizumi's<sup>57</sup> uniform model in which the pyridine molecules lie in the van der Waals gap with their aromatic rings perpendicular to the host layers and their nitrogen lone pairs bonding to the layers. Rather these values are consistent with a model (Figure 34) where pyridine molecules are tilted to the layers of the host TiOCl. This tilting of the pyridine molecules relative to the TiO double layers may be consistent with a model in which the pyridine is coordinated to the Ti centres. The proposed coordination of the pyridine molecules to the metal centres could be the major force which holds the organic molecules inside the layers. In this model, the bridging chlorine ions would become terminal and the length of Ti-Cl bonds will increase. In this situation only small and selected molecules can be accommodated by the host layers. Pyridine molecules

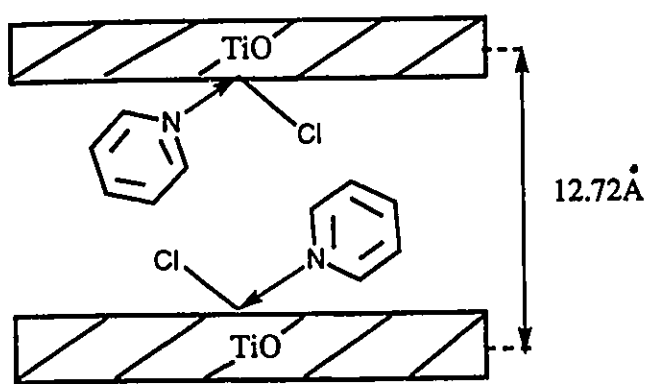


**Figure 34** Structural model for pyridine intercalated compounds.

prefer a tilted orientation inside TiOCl layers in order to avoid the contact with terminal chlorine ions and each other.

In contrast to pyridine molecules, TMEDA molecules are bulky, which may present a kinetic barrier to intercalation into TiOCl. The planar pyridine molecule with its lone pair more accessible may allow easier and faster the intercalation reaction to occur.

**Table XXXIII**

Summary of reactions of TiOCl with pyridine

Reaction conditions	d-space (Å)	layer exp. (Å)	product	comments
sealed tube 250°C, 2d	11.93	3.93	TiOCl(py) <sub>0.11</sub>	interc. comp. TiOCl
Schl. flask 80°C, 2weeks vig. stirring	12.72	4.71	TiOCl(py) <sub>0.38</sub>	interc. comp. TiOCl

### **A proposed mechanism for topochemical reactions of TiOCl with amines**

With the accumulation of experimental data that has been described, it is appropriate to address the mechanism and driving forces involved in the intercalation of amines into TiOCl. As was mentioned at the introduction of this section, except for solvolysis and ion exchange intercalation reactions, redox processes are often invoked to explain the results of intercalations for a variety of host materials. Among the intercalation reactions of metal oxychlorides, FeOCl has been the major host lattice that has been studied. The literature present data consistent with the idea that redox reactions can be a driving force for intercalation of FeOCl with various substrate molecules. Reduction of Fe<sup>III</sup> to Fe<sup>II</sup> during intercalation reaction is not particularly surprising due to the fact that this couple is characterised by a relatively low value of redox potential. The same can not be said about the Ti<sup>III</sup>/Ti<sup>II</sup> couple. Our study of topochemical reactions of TiOCl with several amines such as TMEDA, DMEN, EN, diethylenetriamine and py had as one of its goals, the desire to clarify the role of redox reactions in the intercalation of TiOCl. If these guest species are arranged in order of their ability to be oxidized, the first one will be TMEDA due to the fact that it contains four methyl groups which play the role of electron donors. At the end of this order we can place the molecules with a higher redox potential (vs SCE) such as EN, diethylenetriamine, and py. The results of the present work showed that the reaction of TiOCl with TMEDA doesn't occur even during a long reaction time. In contrast, intercalation reactions of TiOCl with those molecules that are harder to oxidize, takes place relatively smoothly and within several hours. These

intercalation of amines into TiOCl host lattice doesn't proceed by a redox mechanism.

This leaves the question of what is the driving force of intercalation of amines into TiOCl?

The results clearly show that only amines that have an active protons adjacent to nitrogen atom (the exception is pyridine ) can be intercalated into our layered host, TiOCl, and they indicate that subsequent substitution reactions with accompanying salt formation can occur. For the reactions under study, formation of intercalated compounds is quite a fast process in comparison to other heterogeneous reactions, and it is difficult to catch a moment when the intercalation has been completed but the subsequent substitution reaction has not yet taken place. In many cases, the intercalation reaction was followed immediately by a substitution reaction during heating either in the presence or absence of the amine.

We can propose the following mechanism for the intercalation and substitution reactions of amines with TiOCl that is a combination of three processes that are described by diagram I.

The first process is the **coordination** of a guest amine via its nitrogen lone electron pair to  $Ti^{3+}$  metal centres (Lewis Acid - Base interaction). We believe that coordination of amine is a key stage for intercalation reactions. The newly formed intercalated system can now undergo some degree of **electron transfer** from the guest to the host. This corresponds to the metal centres of the layers being reduced while the guest molecules are being partially oxidized. These reduced metal centres now have two different routes for chemical reaction (see diagram I) :

1. The Brønsted acidity of the guest species is increased by the partial oxidation

- thus allowing the chlorine ions of the host to become involved in a **chemical reaction** with a guest molecules forming HCl, and further reaction with amine to form the salt. This chemical reaction leads to the formation of a substituted compound where chlorine ions of the host are substituted by amine molecules. Amine molecules are covalently bonded to titanium metal centres of TiO double layers. This reaction corresponds to reoxidation of the reduced metal centres and the substituted system is characterised by stable energetic state.
2. The other route can take place only in the case when the guest amines don't have active protons. In this situation the degree of electron transfer is small which leads to simple coordination of the amine to  $Ti^{3+}$  metal centres of TiOCl host lattice.

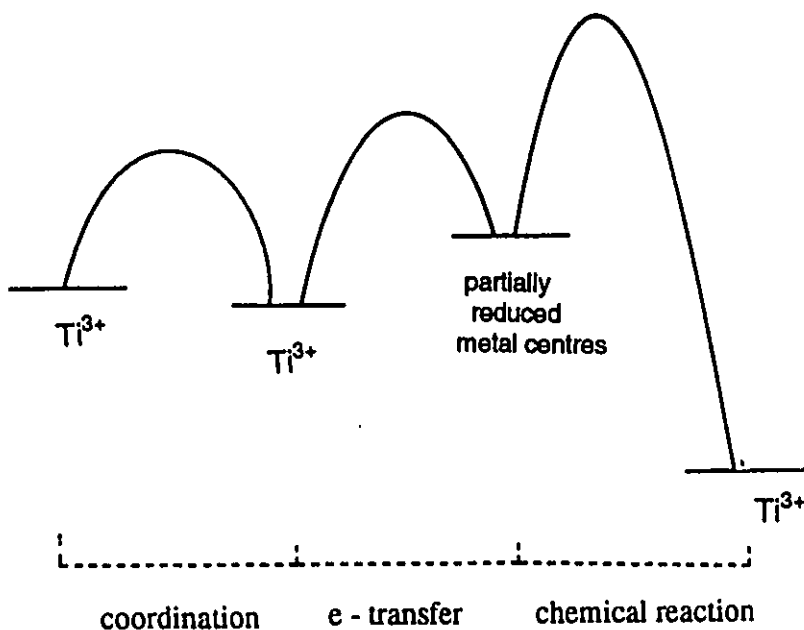
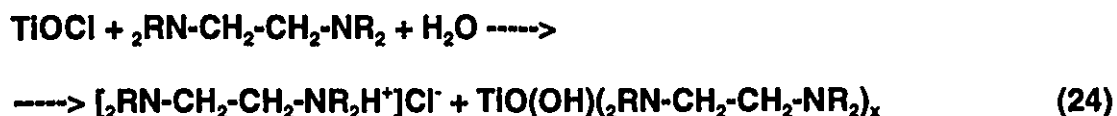


**Diagram I** Proposed mechanism for the topochemical reactions of TiOCl with amines.

The coordination of two amines with different size and shape, TMEDA and py, have been studied. Theoretically, both of these molecules may intercalate between the TiOCl layers and be coordinated via their nitrogen atoms to titanium metal centres. Coordination of py molecules resulted in the formation of a stable intercalated compound due the small size of the molecules that could be easily accomodated by the host layers. In contrast, we didn't observe intercalation of TMEDA molecules and we suppose that the main reason for this is kinetics. Due to the fact that TMEDA is a more sterically demanding molecule than pyridine, they may just need more time to be intercalated into TiOCl.

All topochemical reactions of TiOCl reported in this thesis were performed using dry amines and taking precautions to exclude moisture. Although TiOCl is reported to be stable to moisture and appears to be so in our hands, it is critical that water be excluded from these reactions in order to eliminate the complications arising from reactions such as equation 24:



R = H, Me

Traces of water could provide a source of protons which could lead to the formation of amine intercalated compound as well as amine-salt formation. In addition to our precautions, a number of experiments prove that reaction (24) does not take place in our system and salt formation arises from the active protons of the amine:

- During the reaction of TiOCl with TMEDA and pyridine no ammonium salt formation was observed. Traces of water present in amine could lead to the formation of TMEDA-salt (  $[\text{Me}_2\text{N-CH}_2\text{-CH}_2\text{-NMe}_2\text{H}^+]\text{Cl}^-$  ) as well as py-salt (  $\text{C}_5\text{H}_5\text{NH}^+\text{Cl}^-$  ) ;
- The formation of amine intercalated compounds such as  $\text{TiOCl}(\text{C}_2\text{H}_8\text{N}_2)_{0.4}$ ;  $\text{TiOCl}(\text{C}_4\text{H}_{12}\text{N}_2)_{0.44}$ ;  $\text{TiOCl}(\text{C}_4\text{H}_{13}\text{N}_3)_{0.15}$ , and  $\text{TiOCl}(\text{py})_{0.11, 0.38}$  was confirmed by thermal deintercalation which showed the regeneration of starting material TiOCl. Formation of TiOCl is not possible during heating of  $\text{TiO}(\text{OH})(\text{amine})_x$ .

## Reactions of TiOCl and VOCl with amides

We would suspect that the mechanism for amide intercalation into layered inorganic solids should be different from those of amines. The main reason for this is their structural distinction.

We have assume, that the intercalation of amines into TiOCl host lattice is at least partially based on coordination of amines to the titanium centres in the TiO double layers via there nitrogen atoms. In contrast to amines, nitrogen lone pair in amides are not available for coordination to a metal centre due to the interraction with the carbonyl group and creation an amide resonance structure. This means, that an important role in intercalation process may be played by alkyl groups adjacent to nitrogen and carbon atoms. The intercalation behavior of amides may provide information on whathow or not this intercalation reaction is a redox process. Various amides, displaying oxidation potentials within wide range, are readily available.

Finally, amides are planar molecules and their intercalation into the host layers may help to provide an information on orientation in the interlamellar space.

### Reaction of TiOCl with N,N-dimethylacetamide [ $\text{CH}_3\text{C}(\text{O})\text{N}(\text{CH}_3)_2$ ]

The reaction between TiOCl and N,N-dimethylacetamide was carried out in evacuated, sealed glass tube, that was heated to 60°C for 10 days. Excess DMA was

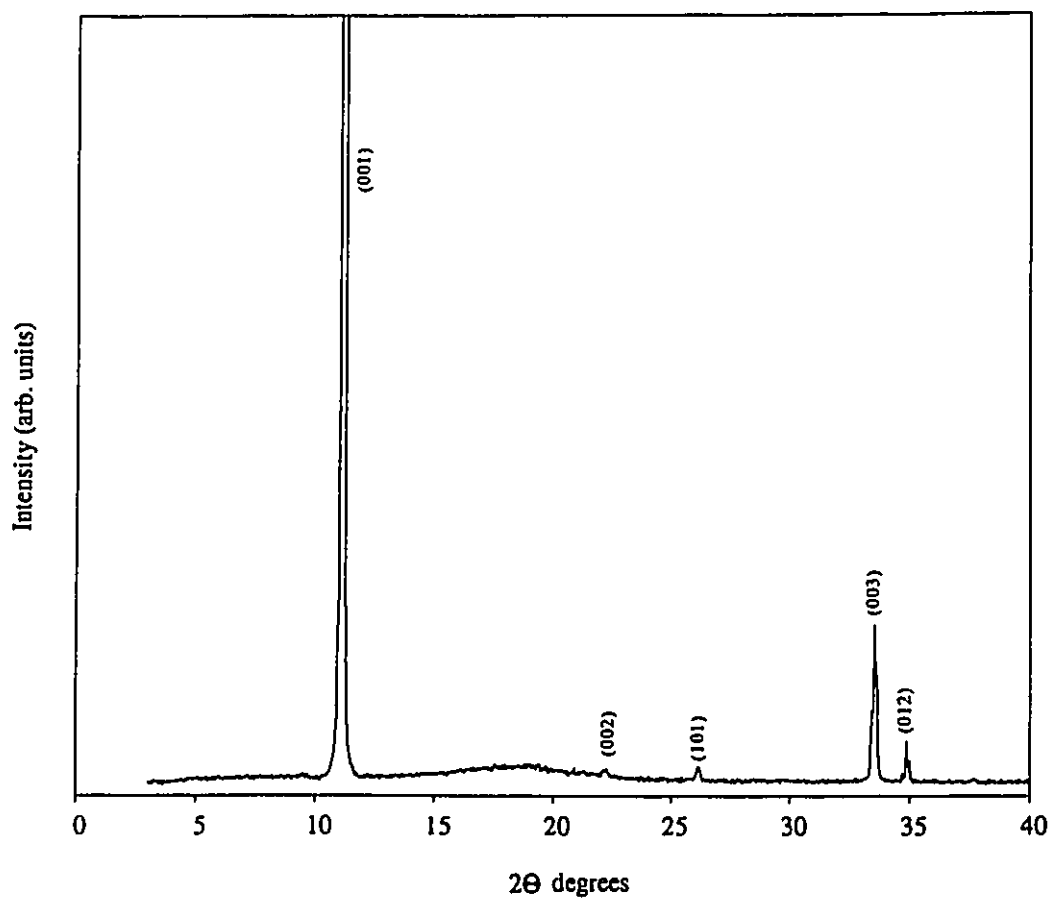


**Figure 35** PXRD of the product obtained from the reaction of  $\text{TiOCl}$  with DMA

Table XXXIV

Powder pattern of the product obtained from the reaction of TiOCl with DMA

d-space (Å)	rel. intensity	h k l	2 $\theta$ degrees	comments
7.91 (8.01) <sup>(a)</sup>	100	0 0 1	11.18	TiOCl <sup>†</sup>
3.99	0.2	0 0 2	22.24	*
3.40	0.3	1 0 1	26.17	*
2.67	2.6	0 0 3	33.57	*
2.57	0.4	0 1 2	24.90	*

\* - peaks related to TiOCl

(a) - d-space was calculated by using 003 peak

removed by filtration and the isolated brown solid was dried under vacuum. The powder pattern of the brown product is presented in Figure 35 and Table XXXIV.

The PXRD spectrum of the brown product obtained during the reaction of TiOCl with DMA is identical to that of TiOCl; it seems that a reaction did not take place. The IR spectrum did not show any absorption bands indicating the presence of DMA.

#### Reaction of TiOCl with dimethylformamide [ HC(O)N(CH<sub>3</sub>)<sub>2</sub> ]

The reaction of TiOCl with dimethylformamide was carried out in a Schlenk flask at 80°C for 1 week under vigorous stirring. Excess DMF was removed by filtration, and the isolated brown solid was dried under vacuum and analysed by PXRD (Figure 36). The powder pattern of the brown product is presented in Table XXXV.

The PXRD spectrum showed the formation of an extremely low intensity new peak of an intercalated material TiOCl(DMF)<sub>x</sub>. The IR spectrum of a brown reaction product did not show characteristic bands for DMF (vibration modes of C=O bond at 1650 cm<sup>-1</sup>).

Based on these results we conclude that under these reaction conditions only a very small amount of DMF molecules was able to intercalate inside host TiOCl layers.

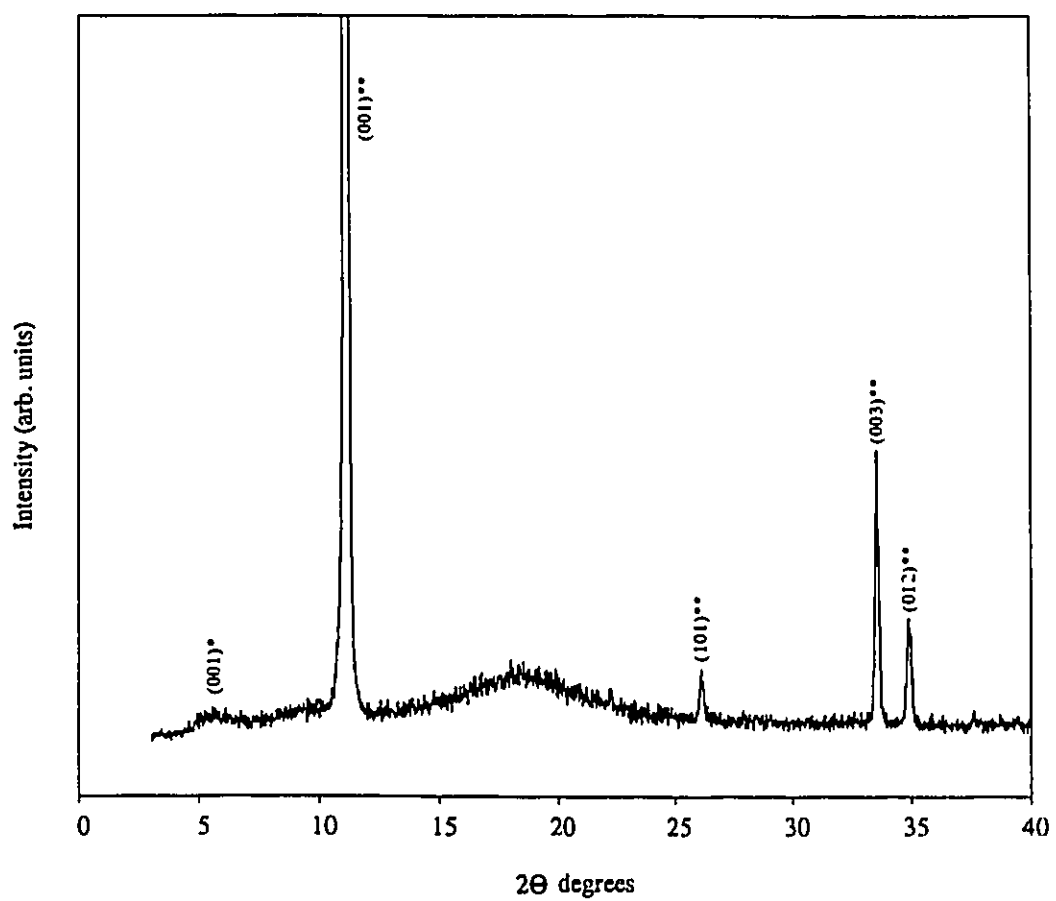


**Figure 36** PXRD of the product obtained from the reaction of TiOCl with DMF

Table XXXV

Powder pattern of the product obtained from the reaction of TiOCl with DMF

d-space (Å)	rel. intensity %	h k l	2 $\theta$ degrees	comments
16.01	0.5	0 0 1	5.51	TiOCl(DMF) <sub>x</sub> *
7.88 (8.01) <sup>(a)</sup>	100	0 0 1	11.21	TiOCl**
3.99	0.2	0 0 2	22.26	**
3.40	0.4	1 0 1	26.18	**
2.67	2.2	0 0 3	33.55	**
2.57	0.8	0 1 2	34.86	**

\* - peak of a new compound TiOCl(DMF)<sub>x</sub>

\*\* - peaks of TiOCl

(a) - d-space was calculated by using 003 peak

Reaction of TiOCl with N - methylformamide [ HC(O)N(H)CH<sub>3</sub> ]

The reaction between TiOCl and N - methylformamide was carried out in a sealed evacuated glass tube which was heated to 100 - 110°C for 8 days. The NMF solution remained colorless through the reaction, however, the solid changed colour from dark brown to dark blue-grey. The NMF solution was removed by filtration, and the dark blue-grey solid was dried under vacuum.

The PXRD spectrum of the reaction product (Figure 37) showed the formation of a new intercalation product  $\text{TiOCl}(\text{HC}(\text{O})\text{N}(\text{H})\text{CH}_3)_x$  with d-space 15.35Å (layered expansion 7.39Å) as well as the presence of unreacted TiOCl. The powder pattern of the dark blue-grey product is presented in Table XXXVI.

The formation of an intercalated compound  $\text{TiOCl}(\text{HC}(\text{O})\text{N}(\text{H})\text{CH}_3)_x$  was further confirmed by XRF which showed the same Ti/Cl ratio as in the starting material TiOCl. We assign a formulation  $\text{TiOCl}(\text{HC}(\text{O})\text{N}(\text{H})\text{CH}_3)_{0.95}$  for this compound based on EA results ( Table XXXVII ).

An IR spectrum of  $\text{TiOCl}(\text{NMF})_{0.95}$  showed absorption bands at 3300, 1670, 1570, and 721  $\text{cm}^{-1}$ . The signals at 3300  $\text{cm}^{-1}$  and 1570  $\text{cm}^{-1}$  corresponds to vibration modes of N-H bond. The absorption band at 1670  $\text{cm}^{-1}$  can be assigned to a vibration modes of C=O bond, and the signal at 721  $\text{cm}^{-1}$  corresponds to vibration modes of Ti-Cl bond.

Table XXXVII

EA results for  $\text{TiOCl}(\text{HC}(\text{O})\text{N}(\text{H})\text{CH}_3)_{0.95}$ 

%	Calculated values	Experimental values
C	14.67	14.53
H	3.05	3.34
N	8.5	9.5

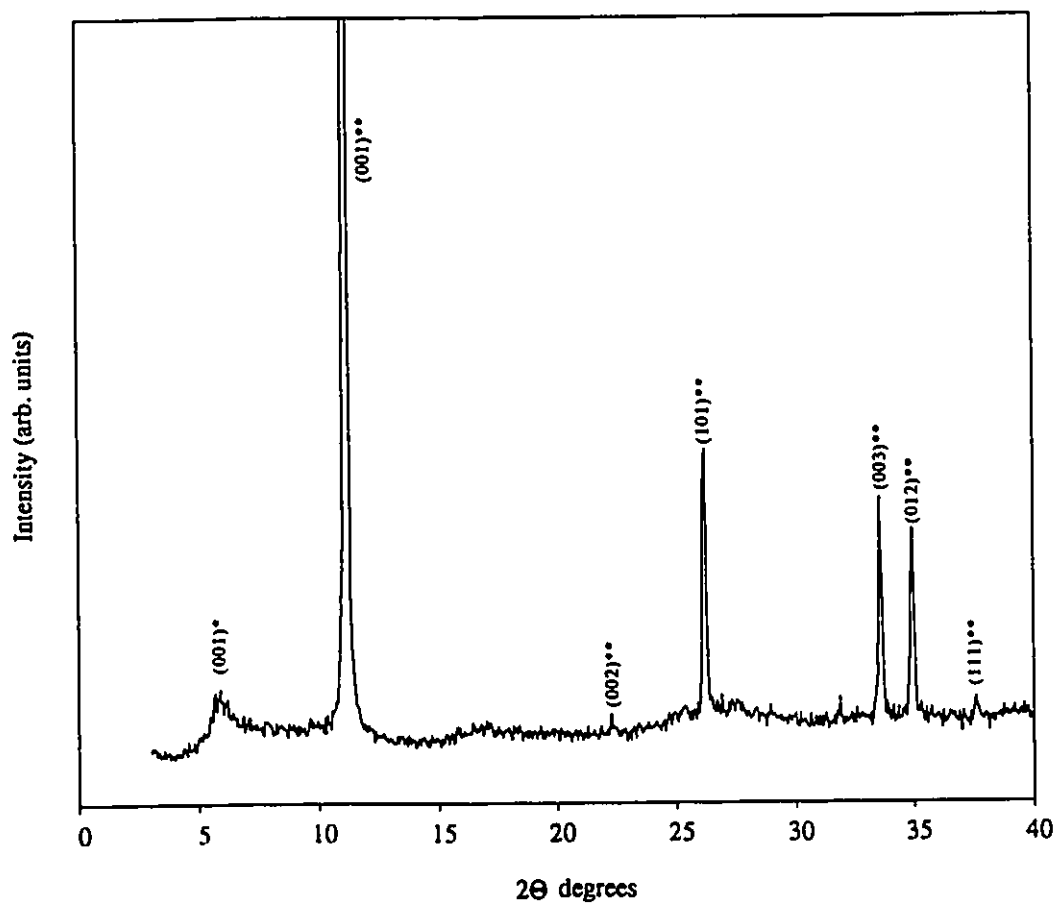
Figure 37 PXRD of the product obtained from the reaction of  $\text{TiOCl}$  with NMF

Table XXXVI

Powder pattern of the product obtained from the reaction of TiOCl with NMF

d-space (Å)	rel. intensity %	h k l	2 $\theta$ degrees	comments
15.35	2.7	0 0 1	5.75	TiOCl(NMF) <sub>0.95</sub> *
7.87 (7.96) <sup>(a)</sup>	100	0 0 1	11.23	TiOCl**
3.97	0.2	0 0 2	22.33	**
3.39	4.2	1 0 1	26.21	**
2.66	2.3	0 0 3	33.63	**
2.56	2.0	0 1 2	34.97	**
2.39	0.2	1 1 1	37.61	**

\* - peak of the intercalated compound TiOCl(NMF)<sub>0.95</sub>

\*\* - peaks related to TiOCl

(a) - d-space was calculated by using 002 and 003 peaks

Reaction of TiOCl with acetamide [(CH<sub>3</sub>)C(O)NH<sub>2</sub>]

The reaction of TiOCl and acetamide was carried out in an evacuated, sealed glass tube, which was heated for 9 days at 100 - 110°C (the melting point of acetamide is 81°C). Unreacted acetamide was removed by washing the product with ethanol. The final dark brown/purple product was dried under vacuum and analysed by PXRD (Figure 38). The PXRD pattern of the dark brown/purple product is presented in Table XXXVIII.

The PXRD spectrum showed the presence of unreacted TiOCl and formation of a new compound that appeared in the spectrum as a broad peak with two maxima at  $2\theta = 7.59^\circ$  and  $6.21^\circ$ . We can assume that this broad peak consists of two peaks that correspond to the formation of two different compounds. The presence of two active protons adjacent to nitrogen atom in acetamide molecule can be involved into substitution process. It is possible that one of the newly formed compounds is the product of substitution reaction between TiOCl and acetamide, and another one is intercalated compound. EA results (Table XXXVII) call our assumption in question because the amount of acetamide molecules that sit inside TiOCl layers is extremely small (TiOCl(acetamide)<sub>0.03</sub>) and possible that substitution reaction did not occur.

The IR spectrum of the dark brown/purple product TiOCl[(CH<sub>3</sub>)C(O)NH<sub>2</sub>]<sub>0.03</sub> only showed an absorption signal at 721 cm<sup>-1</sup> which corresponds to vibration modes of Ti-Cl bond. No absorption bands indicating the presence of acetamide were observed.

Table XXXIX

EA results for  $\text{TiOCl}[(\text{CH}_3)\text{C}(\text{O})\text{NH}_2]_{0.03}$ 

%	Calculated values	Experimental values
C	0.71	0.80
H	0.14	0.12
N	0.41	0.38

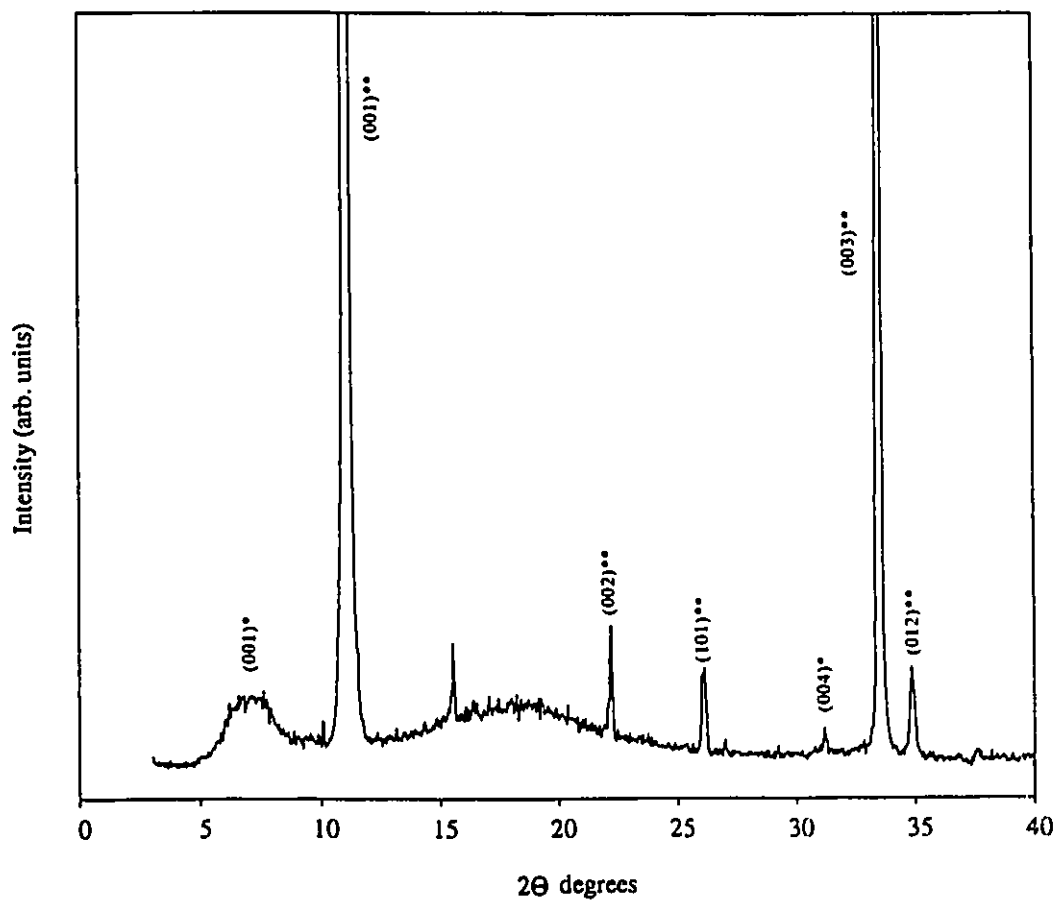
Figure 38 PXRD of the product obtained from the reaction of  $\text{TiOCl}$  with acetamide

Table XXXVIII

Powder pattern of the product obtained from the reaction of TiOCl with acetamide

d-space (Å)	rel. intensity %	h k l	2 $\theta$ degrees	comments
14.21	0.3	0 0 1	6.21	TiOCl(AC) <sub>0.03</sub> *
11.63	0.3	0 0 1	7.59	TiOCl(AC) <sub>0.03</sub> *
7.92 (8.00) <sup>(a)</sup>	100	0 0 1	11.15	TiOCl**
5.69	0.3		15.55	TiCl <sub>3</sub>
3.99	0.3	0 0 2	22.23	**
3.41	0.1	1 0 1	26.11	**
2.86	0.0	0 0 4	31.20	*
2.67	3.9	0 0 3	33.55	**
2.57	0.1	0 1 2	34.86	**

\* - peaks of intercalated compound TiOCl(acetamide)<sub>0.03</sub>

\*\* - peaks of TiOCl

(a) - d-space was calculated by using 002 and 003 peaks

The PXRD results showed that the interlayer expansions in the case of amides intercalation into TiOCl host is much bigger than the expected one ( see calculated layered expansions in Table XL, where we assumed that C=O axis of amide is perpendicular to the layers). The only explanation which can be given so far comes from very broad appearance of the 001 peaks of the intercalation compounds. When the peak is broad, it is very difficult to find its maximum and d-space values are not accurately determined.

**Table XL**

Summary of reactions of TiOCl with amides

Amides	reaction conditions	d-space (Å)	layered exp. (Å)	calculated layered exp. (Å)	product
DMA	sealed tube 60°C, 10d	8.01	--	4.73	TiOCl
DMF	Schl. flask 80°C, 7d	16.01	8.0	4.73	TiOCl(DMF) <sub>x</sub>
NMF	sealed tube 110°C, 8d	15.35	7.39	4.13	TiOCl(NMF) <sub>0.95</sub>
AC	sealed tube 110°C, 9d	14.21 11.63	6.21 3.63	4.13	TiOCl(AC) <sub>0.03</sub>

Reaction of VOCl with N,N-dimethylacetamide

The reaction of VOCl and N,N-dimethylacetamide was carried out in a Schlenk flask. The mixture was heated for 10 days at 80°C. Excess DMF was then removed by filtration and the dark brown product was characterised by PXRD (Figure 39). The powder pattern of the dark brown product is presented in Table XLI.

An IR spectrum of the isolated solid did not show any characteristic absorption bands for DMA. On the basis of PXRD and IR results we conclude that no reaction occurred between VOCl and DMA.

**Table XLI**

Powder pattern of the product obtained from the reaction of VOCl with DMA

d-space (Å)	rel. intensity %	h k l	2 $\theta$ degrees	comments
7.87 (7.89) <sup>(a)</sup>	100	0 0 1	11.23	VOCl <sup>†</sup>
3.39	0.4	1 0 1	26.22	*
2.63	2.2	0 0 3	34.00	*
2.53	0.7	0 1 2	35.47	*

\* - peaks related to VOCl

(a) - d-space was calculated using 003 peak

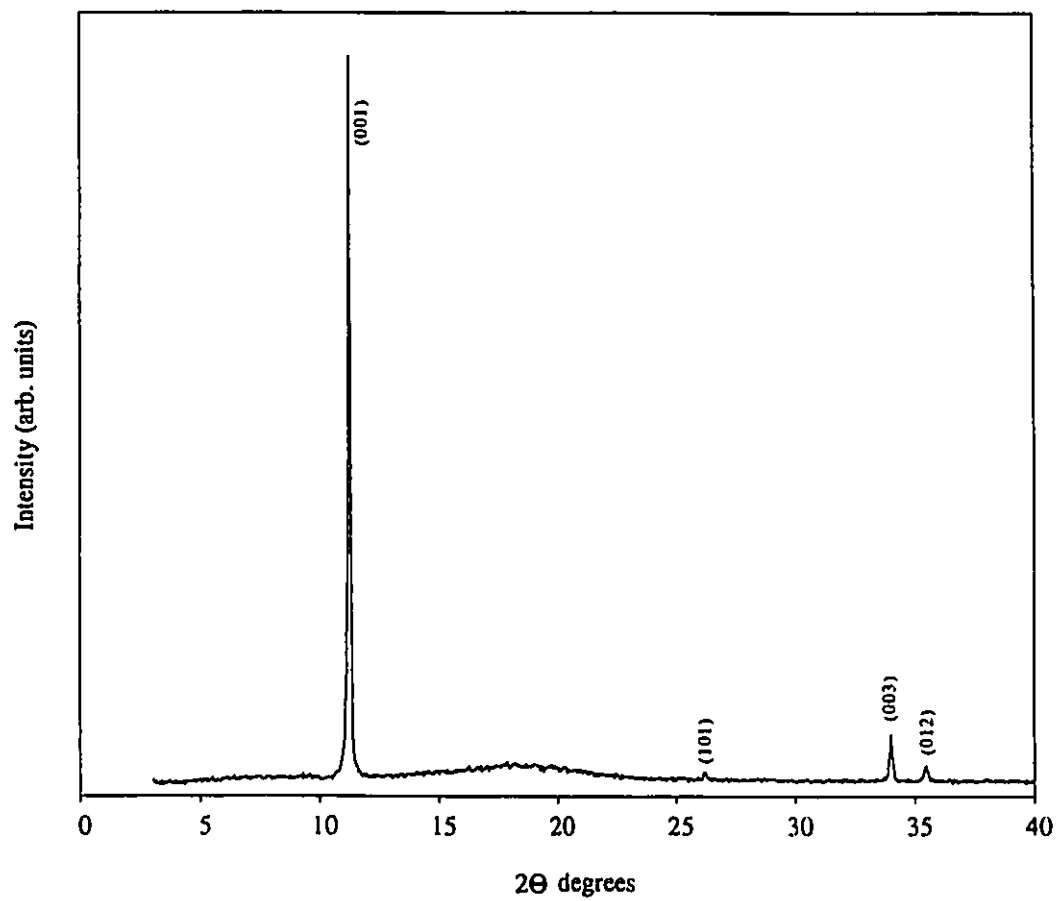


**Figure 39** PXRD of the product obtained from the reaction of VOCl with DMA

Reaction of VOCl with N - methylformamide [HC(O)N(CH<sub>3</sub>)H]

The reaction of VOCl and NMF was carried out in an evacuated, sealed heavy walled glass tube heated to 100° - 110°C for 8 days. Excess NMF was removed by vacuum and a dark brown product was isolated.

The PXRD spectrum (Figure 40) showed that all VOCl have reacted, and a new compound with d-space 13.24Å was formed. The powder pattern of a product is presented in Table XLII.

**Table XLII**

Powder pattern of the product of the reaction of VOCl and NMF

d-space (Å)	rel. intensity %	h k l	2 $\Theta$ degrees	comments
12.84 (13.24) <sup>(a)</sup>	100	0 0 1	6.87	VOCL(NMF) <sub>1.0</sub> *
6.49	21.2	0 0 2	13.61	*
3.31	6.2	0 0 4	25.57	*
2.70	1.9	0 0 5	33.08	*

\* - peaks related to the intercalated compound VOCL(HC(O)N(CH<sub>3</sub>)H)<sub>1.0</sub>

(a) - d-space was calculated by using 002, 004, and 005 peaks

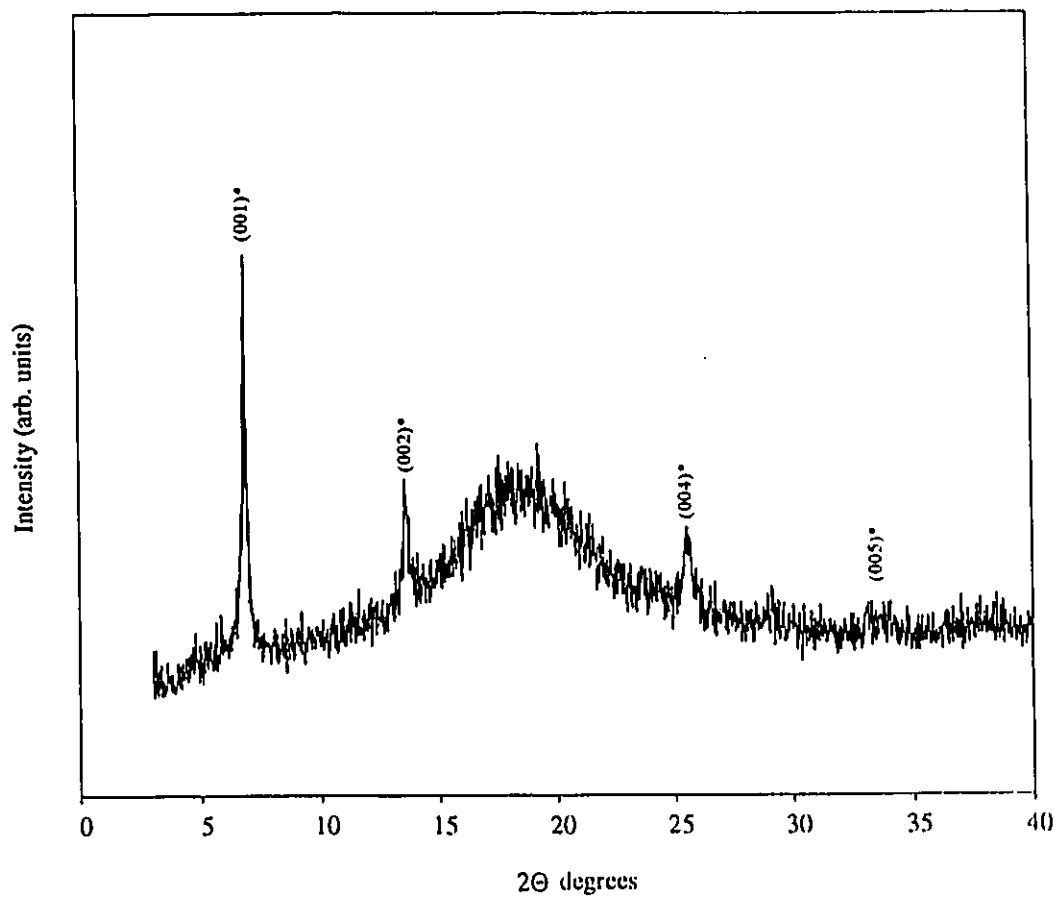


**Figure 40** PXRD spectrum of VOCl(NMF)<sub>1.0</sub>

If a substitution reaction had occurred we would have expected formation of the ammonium salt of NMF, however, no salt formation was observed during the reaction. We attempted to synthesise NMF-salt by adding HCl to NMF. A very small amount of the white solid was formed on the walls of a beaker used for the salt synthesis. But as soon as the solid was taken from a beaker for the analysis, it immediately became a liquid. Our dark brown product after isolation from the excess NMF, looked dry and we concluded that the salt has not been formed during the reaction. We assume that the new compound is the product of intercalation reaction. On the basis of EA results (Table XLIII) we propose the formulation  $\text{VOCl}(\text{HC}(\text{O})\text{N}(\text{CH}_3)\text{H})_{1.0}$ .

Table XLIII

EA data for  $\text{VOCl}(\text{HC}(\text{O})\text{N}(\text{CH}_3)\text{H})_{1.0}$ 

%	Calculated values	Experimental values
C	14.86	14.56
H	3.09	3.28
N	8.6	7.12

An IR spectrum of  $\text{VOCl}(\text{HC}(\text{O})\text{N}(\text{CH}_3)\text{H})_{1.0}$  showed absorption bands at 1714, 1658, and 723  $\text{cm}^{-1}$ . The absorption band at 1714  $\text{cm}^{-1}$  can be assigned to the vibration modes of C=O bond. The signal at 1658  $\text{cm}^{-1}$  corresponds to a vibration modes of N-H

N-H bonds, and the absorption at  $723\text{ cm}^{-1}$  indicates a vibration modes of V-Cl bond.

#### Reaction of VOCl with acetamide $[(\text{CH}_3)\text{C}(\text{O})\text{NH}_2]$

VOCl and acetamide were combined in a heavy walled glass tube which was evacuated, sealed, and heated to  $100^\circ - 110^\circ\text{C}$  for 9 days. The dark brown product was washed with ethanol in order to remove unreacted acetamide, and analysed by PXRD (Figure 41).

The PXRD spectrum showed the disappearance of diffraction peaks for VOCl, and the appearance of reflections for two new compounds with d-space  $11.77\text{\AA}$  and  $8.57\text{\AA}$ . The PXRD pattern of a dark brown product is presented in Table XLIV.

Due to the presence of reactive protons bound to the nitrogen atom in the acetamide molecule, it may be that one of the newly formed compounds is a product of substitution reaction, while another one is the intercalated compound. Interlayer expansion in the case of substituted compound should be smaller than in the case of intercalated compound, therefore the peak at  $2\Theta = 10.31^\circ$  can be attributed to the possibly formed substituted product. The compound with d-space  $11.77\text{\AA}$  is assigned as the intercalated compound. EA results (Table XLV) gave us an idea of the ratio between VOCl and NMF which is equal to 4. But we don't know the ratio between intercalated and substituted compound, and that is why we can't propose formulations for the newly formed products.

The IR spectrum of the dark brown product showed an absorption bands at  $1670$ ,  $1640$ , and  $723\text{ cm}^{-1}$ . The absorption band at  $1670\text{ cm}^{-1}$  can be assigned to the vibration modes of C=O bond. A signal at  $1640\text{ cm}^{-1}$  is characteristic of the vibration modes of N-H

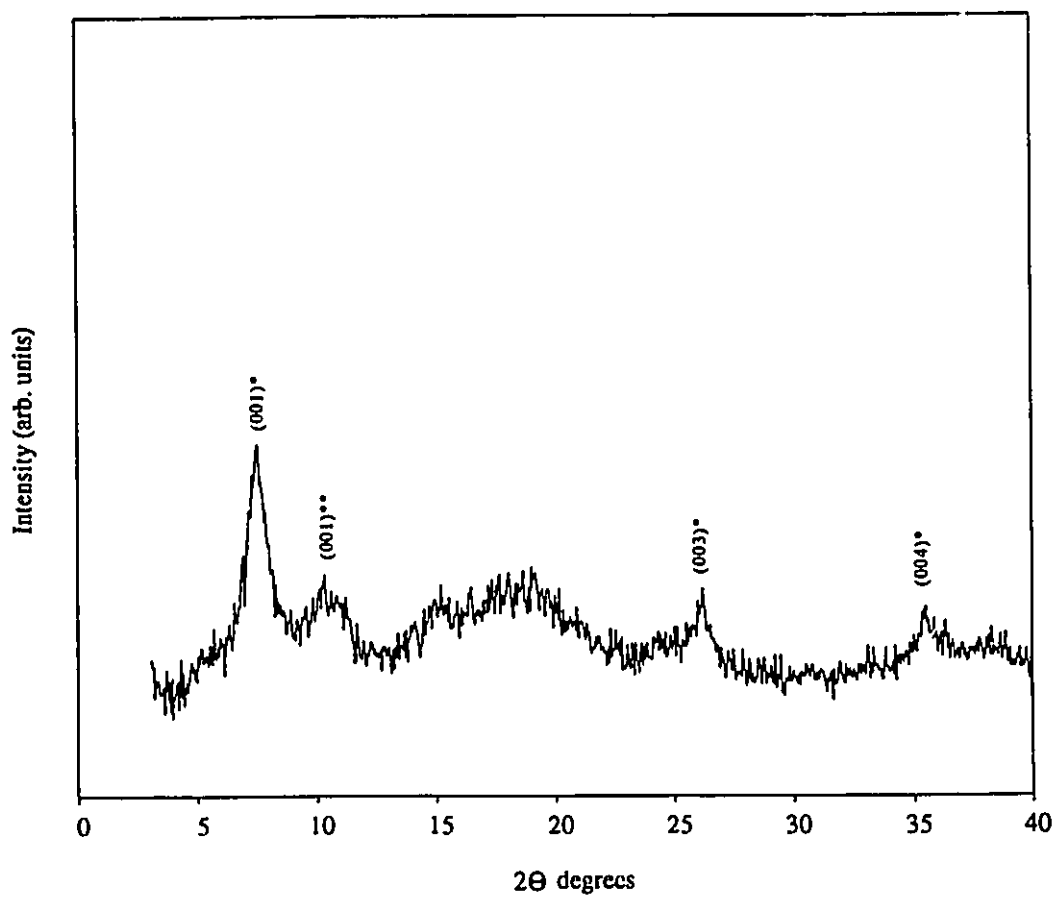


**Figure 41** PXRD spectrum of the product obtained from the reaction of VOCl with acetamide

Table XLIV

Powder pattern of the product obtained from the reaction of VOCl with acetamide

d-space (Å)	rel. intensity %	h k l	2θ degrees	comments
11.77	100	0 0 1	7.50	VOCl(AC) <sub>x</sub> *
8.57	21.50	0 0 1	10.31	VOCl <sub>x</sub> (AC) <sub>y</sub> **
3.94	6.6	0 0 3	26.19	*
2.95	4.3	0 0 4	35.44	*

\* - peaks related to the intercalated compound VOCl(CH<sub>3</sub>C(O)NH<sub>2</sub>)<sub>x</sub>

\*\* - peak of a possibly substituted product VOCl<sub>x</sub>(CH<sub>3</sub>C(O)NH<sub>2</sub>)<sub>y</sub>

Table XLV

EA results for VOCL / (CH<sub>3</sub>C(O)NH<sub>2</sub>)<sub>0.25</sub>

%	Calculated values	Experimental values
C	5.1	4.91
H	1.07	1.20
N	2.9	

bond, and the signal at  $723\text{ cm}^{-1}$  corresponds to the vibration modes of V-Cl bond.

Summary of reactions of VOCl with amides is listed in Table XLVI.

**Table XLVI**

Summary of reactions of VOCl with amides

Amides	reaction conditions	d-space (Å)	layered exp. (Å)	calculated layered exp (Å)	product
DMA	Schl.flask 80°C, 10d	7.89	--	4.73	VOCl
DMF <sup>62</sup>	Reflux for 7d	13.22	5.33	4.73	VOCl(DMF) <sub>0.18</sub>
NMF	sealed tube 110°C, 8d	13.24	5.35	4.13	VOCl(NMF) <sub>1.0</sub>
AC	sealed tube 110°C, 9d	11.77	3.88	4.13	VOCl(AC) <sub>x</sub>
		8.57	0.68		VOCl <sub>x</sub> (AC) <sub>y</sub>

### **A proposed mechanism for intercalation reactions of TiOCl and VOCl with amides.**

The results obtained for the reactions between TiOCl and VOCl, and guest amides clearly demonstrated that the intercalation of amide molecules into layered materials do not proceed via a redox mechanism. Among the amides that were used in this study, the easiest molecule to oxidise is DMA, yet DMA did not react with either TiOCl or VOCl. The molecules that have higher redox potentials than that of DMA were intercalated in both TiOCl and VOCl host materials.

From this study it appears that the necessary condition for amides intercalation is the presence of protons adjacent to carbon or nitrogen atoms in amide molecule. Perhaps these protons form hydrogen bonds with chloride ions of the host which, hold the guest molecules inside layers.

It is very interesting to compare the intercalation results using NMF with those of acetamide . Both NMF and acetamide molecules contain two protons. In the case of NMF, these protons belong to different atoms - carbon and nitrogen, while in acetamide the two protons are both bound to nitrogen. It may be that NMF molecules have a stronger interaction with the TiOCl and VOCl layers due to formation of hydrogen bonds with Cl ions of two opposite MO double layers. This interlayer bridging model is presented in Figure 42a,b. In contrast, the protons of the acetamide molecule may be bonded to the same Cl ions with only one end of the molecule becoming fixed as schematically shown in Figure 42c,d. In the case of the TiOCl host material, only a small amount of acetamide is intercalated into the interlamellar space, while VOCl contains almost 10 times this amount.

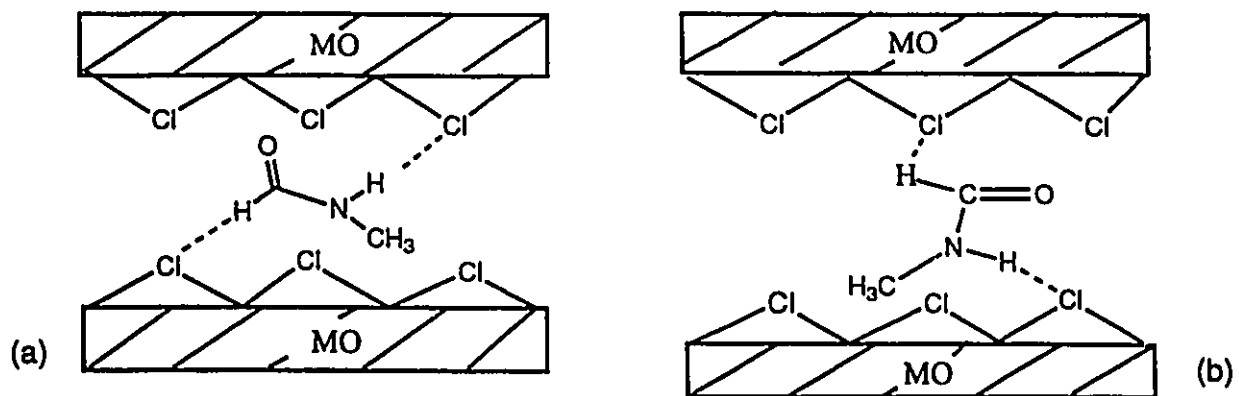


Figure 42a,b Interlayer bridging model for NMF intercalation into  $\text{TiOCl}$  and  $\text{VOCl}$

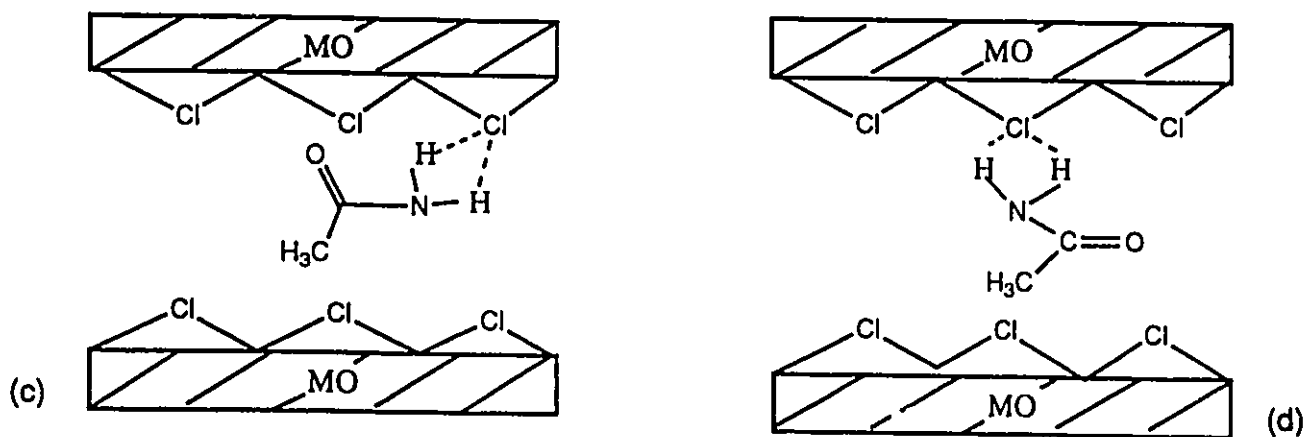


Figure 42c,d Structural model for acetamide intercalation into  $\text{TiOCl}$  and  $\text{VOCl}$

We propose that this difference arises from the level of interaction between layers in two host layered materials VOCl and TiOCl. It appears that the interaction between VOCl layers is less strong than those between TiOCl layers. Therefore, amide molecules enter this host more easily and interact with the VOCl layers by means of hydrogen bonding with Cl ions of the host. The interlayer forces between TiOCl layers may be stronger which present a kinetic barrier to the inclusion of guest molecules.

The obtained layer expansion values for NMF and acetamide intercalation into VOCl and TiOCl host materials are consistent with the proposed models. This model can accommodate two possible orientations of the amide molecules inside the MOX layers. One with the C=O axis of the amide perpendicular (Figure 42a,b) and the other having this axis parallel (Figure 42c,d) to the layers. Both orientations of amide molecules give approximately the same layer expansion values (with the difference within 1 Å).

## CONCLUSIONS

1. Intercalation of both amines and amides into TiOCl and VOCl lattices does not appear to be a redox process.
2. A key step for intercalation of amines into TiOCl host material is coordination via nitrogen lone electron pair to  $Ti^{3+}$  metal centres.
3. Intercalation of amines is followed by substitution reaction immediately during heating either in the presence or absence of the amine solution.
4. The mechanism proposed for intercalation and substitution reactions is a combination of three processes: coordination, e-transfer, and chemical reaction.
5. A driving force for the substitution reactions is ammonium hydrochloride salt formation.
6. The driving force for intercalation of amides into TiOCl and VOCl is the formation of hydrogen bonding between amides protons and Cl ions of the host lattice.
7. Intercalation of amides takes place much easier into VOCl host lattice than into TiOCl due to a less strong interaction between host layers.

## References

1. Kanatzidis M.G., Marks T.S., *Inorg. Chem.*, 1987, 26, 6.
2. Votinsky J., Kalousova J., Benes L., *J. of Inclusion Phenomena and Molecular Recognition in Chemistry*, 1992, 14, 19.
3. (a) Bartlett N., McQuillan B.W., in "Intercalation Chemistry" (Whittingham S.M., Jacobson A.J., ed.), Academic press, inc., New-York, 1982, 30.  
(b) Schöllhorn R., in "Intercalation chemistry" (Whittingham S.M., Jacobson A.J., ed.), Academic press, inc., New-York, 1982, 315
4. Lerf A., Lalik E., Kolodziejcki W., Klinowski J., *J. Phys. Chem.*, 1992, 96, 7389.
5. Bradley S., Kydd R., *Catal. Lett.*, 1991, 8, 185.
6. Gonzales F., Pesquera C., Benito I., Maendioroz S., *J. Chem. Soc., Chem. Commun.*, 1991, 587.
7. Bissessur R., DeGroot D., Schindler J., Kannewurf C., Kanadzidis M., *J. Chem. Soc., Chem. Commun.*, 1993, 687.
8. Ruiz - Hitzky E., *Adv. Mater.*, 1993, 5, 334.
9. Whittingham S.M., *Prog. Solid State Chem.*, 1978, 12, 41.
10. Kanatzidis M.G., Bissessur R., DeGroot D.C., Schindler J.L., Kannewurf C.R., *Chem. Mat.*, 1993, 5, 595.
11. Lemmon J.P., Lerner M.M., *Chem. Mat.*, 1994, 6, 207.
12. Divigalpitiya W.M., Frindt R.F., Morrison S.R., *J. Mater. Res.*, 1991, 6, 1103.
13. Schöllhorn R., *Angew. Chem. Int. Ed. Engl.*, 1980, 19, 983.

14. Rudorff W., *Chimia*, 1965, 19, 489.
15. Ong E.W., Eckert J., *Chem. Mat.*, 1994, 6, 1946.
16. Schöllhorn R., Zagefka H-D., *Angew. Chem. Int. Ed. Engl.*, 1977, 16, 199.
17. Clement R., Lomas L., Audiere P., *Chem. Mater.*, 1990, 2, 641.
18. (a) Clement R., *J. Chem. Soc., Chem. Commun.*, 1980, 647.  
(b) Clement R., Garnier O., Jegoudez J., *Inorg. Chem.*, 1986, 25, 1404.
19. Joy P.A., Vasudevan S., *J. Am. Chem. Soc.*, 1992, 114, 7792.
20. Schöllhorn R., Zagefka H-D., Butz T., Lerf A., *Mater. Res. Bull.*, 1979, 14, 369.
21. Glueck D.S., Brough A.R., Mountford P., Green M., *Inorg. Chem.*, 1993, 32, 1893.
22. Alberti G., Constantino U., in "Intercalation Chemistry" (Whittingham S.M., Jacobson A.J., ed.), Academic press, inc, New-York, 1982, 157.
23. Menendez A., Bárcena M., Jaimez E., Garcia J., Rodrigues J., *Chem. Mater.*, 1993, 5, 1078.
24. Oleinik S., Aylmore L.A., Posner A.M., Quirk J.P., *J. Phys. Chem.*, 1968, 72, 241.
25. Olejnik S., Posner A.M., Quirk J.P., *Clay Miner.*, 1970, 8, 421.
26. Olejnik S., Posner A.M., Quirk J.P., *Clays Clay Miner.*, 1971, 19, 83.
27. Ledoux R.L., White J.L., *Proc. Int. Clay Conf.*, 1966, 1, 361.
28. Weiss A., Thielepape W., Orth H., *Proc. Int. Clay Conf.*, 1966, 1, 277.
29. Halbert T.R., in "Intercalation Chemistry" (Whittingham S.M., Jacobson A.J., ed.), Acad. press, inc., New-York, 1982, 375.
30. (a) Hagenmuller P., Rouxel J., David J., Colin A., Le Neindre B., *Z. Anorg. Allg. Chem.*, 1963, 1, 323.

- (b) Herdy A., Hardy A-M., *C. R. Hebd. Seances Acad. Sci.*, 1963, 256, 3477.
31. (a) Schafer H., Goser C., Bayer L., *Z. Anorg. Allg. Chem.*, 1950, 263, 87.  
(b) Schafer H., Wittig E., Wilborn W., *Z. Anorg. Chem.*, 1958, 297, 48.
32. Hagenmuller P., Hardy A-M., *C. R. Hebd. Seances Acad. Sci.*, 1963, 256, 1784.
33. Hagenmuller P., Rouxel J., Le Neindre B., *C. R. Hebd. Seances Acad. Sci.*, 1961, 252, 282.
34. Hagenmuller P., Rouxel J., David J., Colin A., *C. R. Hebd. Seances Acad. Sci.*, 1961, 253, 667.
35. Goldsztaub S., *C. R. Hebd. Seances Acad. Sci.*, 1934, 198, 667.
36. Lind M.D., *Acta Crystallogr., Sect.B*, 1970, 26, 1058.
37. Haase A., Brauer G., *Acta Crystallogr., Sect.B*, 1975, 31, 2521.
38. Schafer H., Wartenpfehl F., Weise E., *Z. Anorg. Allg. Chem.*, 1958, 295, 268.
39. Von Schnering H.G., Collin M., Hassscheider M., *Z. Anorg. Allg. Chem.*, 1972, 387, 137.
40. Schafer H., Wartenpfehl F., *J. Less-Common Met.*, 1961, 3, 29.
41. Levayer C., Rouxel J., *C. R. Hebd. Seances Acad. Sci., Ser.C*, 1969, 268, 167.
42. Halbert T.R., Scanlon J.C., *Mater. Bull.*, 1979, 14, 415.
43. Kanatzidis M.G., Marks T.S., *Inorg. Chem.*, 1987, 26, 783.
44. Armand M., Coic I., Palvadeau P., Rouxel J., *J. Power Sources*, 1978, 3, 137.
45. Bringley J.F., Fabre J-M., Averill B.A., *J. Amer. Chem. Soc.*, 1990, 112, 4577.
46. Wu C-G., Marcy H.O., DeGroot D., Schindler J., Kannewurf C., Leung W., Benz M., Le Goff E., Kanatzidis M., *J. Synthetic Metals*, 1991, 41-43, 797.

47. (a) Kanatzidis M.G., Wu C-G., Marcy H.O., **J. Adv. Mater.**, 1990, 2, 364.  
(b) Kanatzidis M.G., Marcy H.O., **J. Solid State Ionics**, 1989, 32/33, 594.
48. Kanatzidis M.G., tonge L.M., Marks T.S., **J. Am. Chem. Soc.**, 1987, 109, 3797.
49. Dines M.B., **Science**, 1975, 188, 210.
50. Davies W.B., Green M.L.H., Jacobson A.J., **J. C. S. Chem. Comm.**, 1976, 781.
51. Halbert T.R., Johnston D.C., **Physica B**, 1980, 99, 128.
52. Halbert T.R., Scanlon J., **Mat. Res. Bull.**, 1979, 14, 415.
53. Schäfer - Stahl H., Abele R., **Angew. Chem. Int. Ed. Engl.**, 1980, 6, 477.
54. Hagenmuller P., Portier J., Barbe B., Bouclier P., **Z. Anorg. Allg. Chem.**, 1967, 355, 209.
55. Choy J.-H., Un J.-W., Kang J.-K., **J. Solid State Chem.**, 1988, 77, 60.
56. Choy J.-H., Kim H., **Bull. Korean Chem Soc.**, 1986, 1, 84.
57. Kikkawa S., Kanamaru F., Koizumi M., **J. Solid State Chem.**, 1980, 31, 249.
58. Clough S., Palvadeau P., Venien J.P., **J. Phys. C: Solid State Phys.**, 1982, 15, 641.
59. Son S., Kikkawa S., Kanamaru F., Koizumi M., **Inorg. Chem.**, 1980, 19, 262.
60. Kikkawa S., Kanamaru F., Koizumi M., **Inorg. Chem.**, 1980, 19, 259.
61. Vorob'ev N., Pechkovskii V., Kobetz L., **Zh. Neorg. Khim.**, 1974, 19, 3.
62. Patel B., BSc thesis "Topochemical reactions of VOCl and TiOCl", Ottawa University, 1994.
63. Ehrlich P., Siefert H.-J., **Z. Anorg. Allg. Chem.**, 1959, 301, 282.